6-1978

Structural Analysis of the Great Smoky Thrust Sheet Along the Little Tennessee River

John E. Livingston
University of Tennessee - Knoxville

To the Graduate Council:

I am submitting herewith a thesis written by John E. Livingston entitled "Structural Analysis of the Great Smoky Thrust Sheet Along the Little Tennessee River." I have examined the final electronic copy of this thesis for form and content and recommend that it be accepted in partial fulfillment of the requirements for the degree of Master of Science, with a major in Geology.

D. H. Roeder, Major Professor

We have read this thesis and recommend its acceptance:

Garrett Briggs, Kula Misra

Accepted for the Council:
Carolyn R. Hodges

Vice Provost and Dean of the Graduate School

(Original signatures are on file with official student records.)

To the Graduate Council:

I am submitting herewith a thesis written by John E. Livingston entitled "Structural Analysis of the Great Smoky Thrust Sheet Along the Little Tennessee River, Tennessee." I recommend that it be accepted in partial fulfillment of the requirements for the degree of Master of Science, with a major in Geology.

D. H. Roeder
Major Professor

We have read this thesis and recommend its acceptance:

Accepted for the Council:

Vice Chancellor
Graduate Studies and Research

STRUCTURAL ANALYSIS OF THE GREAT SMOKY THRUST SHEET ALONG THE LITTLE TENNESSEE RIVER, TENNESSEE

A Thesis
Presented for the
Master of Science
Degree
The University of Tennessee, Knoxville

John E. Livingston

June 1978

ACKNOWLEDGMENTS

The author wishes to thank Dr. D. H. Roeder, who suggested the field area and served as thesis chairman. His guidance and instruction is appreciated. Dr. Garret Briggs and Dr. Kula Misra are to be thanked for serving on the thesis committee and providing help on clarifying and editing the thesis. The Donald Jones Fund provided a grant which helped to defray field work costs. The author is grateful to the Aluminum Company of America for granting permission to work on their property in the Little Tennessee River area. My wife, Sandra, provided invaluable assistance at all stages in the preparation of this thesis study and was a joy to work with.

ABSTRACT

This study involves a structural analysis of a portion of the Great Smoky thrust sheet in the Great Smoky Mountains of Tennessee. Four groups of folds and related structures have been identified in this area. The earliest folds include second-order mesoscopic F1 folds with a slaty cleavage axial plane foliation (S1). These folds occur on the limbs of first-order macroscopic F1 folds which are discordant to the Great Smoky fault. In several places, the F1 folds are overprinted by mesoscopic F2 folds which are characterized by crenulation cleavage axial plane foliation (S2). F2 folds include tight to isoclinal folds with boudinage on fold limbs oriented subparallel to S2 and small, angular zigzag folds. Evidence indicates that some degree of transposition of foliations was involved in the formation of S2. Macroscopic F3 folds involve the folding of the slaty cleavage (S1) and are probably related to the deformation of the Great Smoky fault surface, which resulted in its present undulatory nature. Mesoscopic F4 structures consist of kink bands and related thrust faults.

At least two major episodes of deformation can be recognized in the Taconic fold belt of the Blue Ridge province. The first episode involved the formation of "similar-type" folds with a slaty cleavage axial plane

foliation, regional metamorphism, and thrusting on the Greenbrier fault. These structural features are believed to be representative of the Taconic orogeny (430-470 m.y. ago). A second period of deformation involved the formation of folds with a crenulation or slip cleavage axial plane foliation, emplacement of the Great Smoky and Blue Ridge thrust sheets and the creation of the Gatlinburg fault system. These events have been dated as Late Paleozoic (Mississippian or Pennsylvanian).

Structural elements in the area of this report can be differentiated into two major episodes of deformation. They can be integrated into the regional deformational history of the Blue Ridge in the following way. F1 folds with a slaty cleavage axial plane foliation (S1) are correlated with the early period of deformation and regional metamorphism of Taconic age. F2 folds probably belong to the second period of deformation and are related to the Late Paleozoic thrust faulting. F3 and F4 postdate the Great Smoky fault.

TABLE OF CONTENTS

LIST OF TABLES

LIST OF FIGURES

FIGURE PAGE

FIGURE PAGE

LIST OF PLATES

CHAPTER I

INTRODUCTION

The area of investigation in this study lies on the western edge of the Blue Ridge province of the Great Smoky Mountains (page 4). A geologic map of the field area is shown on page 13. Blue Ridge Cambrian and Precambrian rocks have been thrust over Valley and Ridge province rocks by the Great Smoky fault. This thrust fault outcrops along the northwest face of Chilhowee Mountain. Here it dips gently to the southeast. The Great Smoky fault rises farther to the southeast and reappears at numerous windows within the Great Smoky Mountains such as Calderwood window (see page 13), Cades Cove, Wear Cove, and Tuckaleechee Cove. This undulatory nature of the Great Smoky fault thrust sheet suggests that deformation of the fault surface occurred at a later date. In another interpretation, King (1964) suggests that the present shape of the thrust sheet resulted from the configuration of the initial fracture in the Paleozoic strata, and not from later deformation of the fault surface.

Overriding rocks of the Cambrian Chilhowee Group and Precambrian Ocoee Series have been separated into slices by other major thrust faults. Some of these faults, such as the Miller Cove fault, are believed to be splays from

the Great Smoky fault (Neuman and Nelson, 1965). Other faults, including the Rabbit Creek fault and the Greenbriar fault, are believed to predate the Great Smoky faulting and may or may not involve renewed thrusting at the time of the Great Smoky fault emplacement.

The Ordovician rocks exposed northwest of the Great Smoky fault trace on Chilhowee Mountain and in the windows show no evidence of the regional metamorphism which affected much of the Ocoee Series. Structures in the highly deformed Ocoee Series are also not reflected in these Ordovician rocks. Such evidence suggests that transport on the Great Smoky fault occurred after the regional metamorphism of the Ocoee Series. In the central Great Smoky Mountains, the Greenbrier fault has been folded and faulted and does not offset the metamorphic facies boundaries which transect the fault (King, 1964, Carpenter, 1970). Evidently the main deformation of the Greenbrier fault occurred before the regional metamorphism, believed to be Taconic (Late Ordovician) (King, 1964).

Rocks within the field area show a complex relationship of structures formed by polyphase thrusting and folding. Superposition of structural elements can be seen on scales from mesoscopic to macroscopic. Distinct groups of folds and related structures can be determined and overprinting relationships between some of the groups can be observed.

A kinematic sequence of folding has been formulated for folds within this field area on the basis of this overprinting evidence. By comparing this sequence of structural events with known tectonic events and the regional depositional history of the southern Appalachians, an attempt will be made to formulate a relative chronology for the structural evolution of this area of the Great Smoky Mountains.

A. Location

In this study, mapping was undertaken in the upper plate of the Great Smoky fault in the vicinity of the Little Tennessee River in Tennessee. The field area, Figure 1, includes the Tallassee quadrangle and parts of Calderwood, Blockhouse, and Tapoco quadrangles. Structural mapping was concentrated on the relatively continuous exposures along Route 129, on the Foothills Parkway between the Little Tennessee River and Look Rock, and on the Happy Valley Road over Chilhowee Mountain. The rocks in the field area are highly folded and are affected by well-developed slaty cleavage and numerous thrust faults.

B. Previous Work

The general geology of the western portion of the Great Smoky Mountains was examined by Neuman (1951) and comprehensively by Neuman and Nelson (1965) as a result

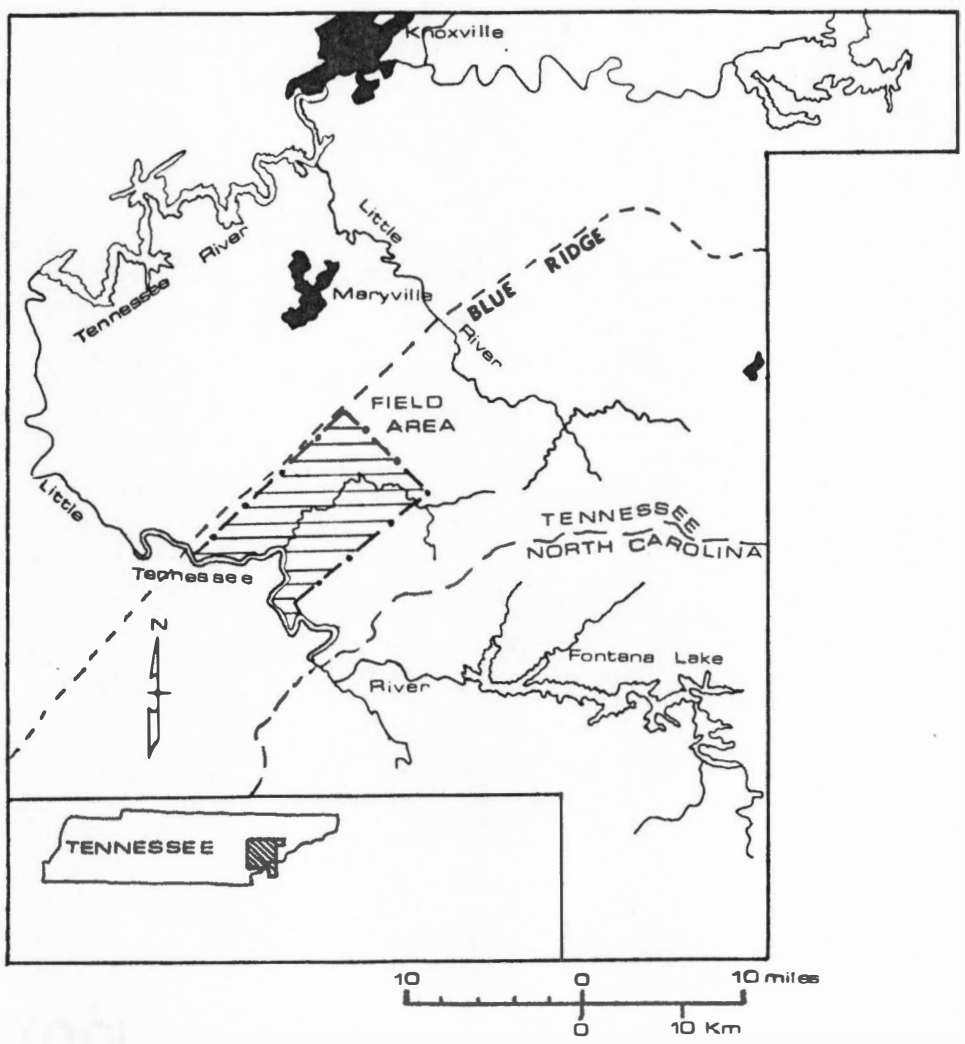

Figure 1. Regional location map showing investigation area for structural analysis.

of their mapping for the U.S. Geological Survey from 1946 through 1954. Structural geology and stratigraphy for the remaining areas of the Great Smoky Mountains are presented in King et al. (1958), Hadley and Goldsmith (1963), and King (1964). The area around Look Rock was mapped and described by Neuman and Wilson (1960). Detailed mapping, measurement of stratigraphic sections, and petrologic examination of carbonate rocks of the Wilhite Formation was undertaken near Chilhowee Lake by Hanselman et al. (1974).

CHAPTER II

STRATIGRAPHY

A. Ocoee Series—Precambrian

Cades Sandstone (Neuman and Nelson, 1965)

The Cades Sandstone (Figure 2) consists of dark-grey sandstone interbedded with dark-grey argillite and siltstone. Sandstones are generally in the medium to coarse grain-size range. Graded beds from one to four feet thick are common, with granule conglomerate at the base grading upward to coarse and medium sandstone to siltstone. The sand fraction is mainly quartz with some feldspar. Minor constituents are fragments of pegmatite, perthite, quartzite, argillite, and siltstone. The micaceous matrix consists of sericite, chlorite, and some biotite.

Wilhite Formation (Neuman and Nelson, 1965)

Located in the Walden Creek Group, the Wilhite Formation is one of the most heterogeneous units in the Ocoee Series. The main body of the formation is calcareous siltstone, which may be as much as 10,000 feet thick in places. Beds of coarse sandstone, pebble conglomerate, and carbonate rocks are found locally.

Quartz pebble conglomerates and quartzose sandstone may be interbedded with the siltstone, or may occur in large,

			FORMATION
MISSISSIPPIAN			Greasy Cove Formation Mgc. Grainger Formation MDgc. Greasy Cove and Grainger Formations (undifferentiated) Mgg. Disconformity
ORDOVICIAN			Bays Formation and Tellico Formation (undifferentiated) Otb. Bays Formation Ob. Tellico Formation Ot. Blockhouse Shale Obl.
		KNOX GROUP	Jonesboro Limestone Oj. (Occurs in Calderwood Window) Sequence broken by Great Smokey Fault
CAMBRIAN		CHILHOWEE GROUP	Helenmode Formation Chm. Hesse Quartzite Ch. Murray Shale Cm. Nebo Quartzite Cne. Nichols Shale Cni. Cochran Formation Cc.
LATE PRECAMBRIAN	OCOEE SERIES	WALDEN CREEK GROUP	Sandsuck Formation pCs. Sequence broken by Miller Cove Fault Wilhite Formation pCw. Sequence broken by Rabbit Creek Fault
			Cades Sandstone pCc

Figure 2. Stratigraphic column of rocks in the vicinity of the field area (Neuman and Nelson, 1965).

separate masses like that next to Chilhowee Dam. Pebbles in the conglomerate are largely rounded quartz, quartzite, and feldspar with angular fragments of dark siltstone. These siltstone blocks range in size from small chips to as much as two feet across, and sometimes show foliation resembling slaty cleavage. Fragments of coarse sandstone, dolomite, and limestone are also found.

Fine-grained rocks include dark-grey, finely laminated slaty siltstone and argillite with thin beds of fine-grained sandstone. Chlorite and sericite occur in equal amounts in the argillite and slate. Most of the siltstone and argillite in the field area show a pervasive foliation resembling slaty cleavage.

Sandsuck Formation (Neuman and Nelson, 1965)

This formation includes grey thin-bedded to fissile siltstone interbedded with feldspathic sandstone and conglomerate. The Sandsuck Formation conformably underlies the Cambrian Cochran Formation in the area of study.

B. Chilhowee Group—Cambrian

Cochran Formation (Neuman and Wilson, 1960)

The Cochran Formation consists of quartzite and feldspathic sandstone. Light-grey, well-sorted medium to coarse-grained vitreous quartzite makes up the uppermost 100 feet. The lower part of the formation is mainly

thick-bedded conglomeratic sandstone, with the proportion of pebbles increasing downward.

Nichols Shale (Neuman and Wilson, 1960)

The Nichols Shale is made up of grey, fissile, argillaceous siltstone, shale, and fine-grained sandstone. Large detrital mica flakes can be found on many bedding surfaces.

Nebo Quartzite (Neuman and Wilson, 1960)

The basal section of the Nebo Quartzite is light olive green fine-grained sandstone. Above this unit is light-grey medium to coarse-grained quartzite. Scolithus tubes are commonly seen on exposed bedding surfaces.

Murray Shale (Neuman and Wilson, 1960)

The Murray Shale is dominantly micaceous, silty shale and argillaceous siltstone. Thin-bedded glauconitic feldspathic fine-grained sandstone occurs in the upper part of the formation.

Hesse Quartzite (Neuman and Wilson, 1960)

This formation consists of light-grey medium to coarse-grained quartzite with well-sorted, well-rounded grains and siliceous cement. Cross-bedding is common and Scolithus tubes are found in some layers.

Helenmode Formation (Neuman and Wilson, 1960)

This formation is exposed north of the study area. It consists of grey, micaceous siltstone and greenish-grey, fine-grained sandstone with abundant glauconitic grains. The argillaceous rocks are interbedded with thin quartzite layers in the lower part of the formation.

C. Rocks Exposed in Calderwood Window

Jonesboro Limestone (Neuman and Nelson, 1965)

The Jonesboro Limestone is in the Lower Ordovician part of the Knox Group. In Calderwood Window, it is probably equivalent to the Mascot Formation and Kingsport Formation. The Jonesboro Limestone is made up mainly of light to medium-grey fine-grained to aphanitic limestone. Less than 10 percent of the formation is dolomite.

D. Other Ordovician Rocks

Blockhouse Shale (Neuman and Wilson, 1960)

This formation is mainly dark-grey, finely laminated calcareous shale with thin beds of dark-grey, very fine-grained limestone in the upper half.

Tellico Formation (Neuman and Wilson, 1960)

The Tellico Formation includes grey calcareous shale with interbedded grey, fine—to medium—grained, feldspathic calcareous sandstone.

Bays Formation (Neuman and Wilson, 1960)

This formation includes red, calcareous mudrock and siltstone with small amounts of grey, feldspathic sandstone.

E. Mississippian Rocks

Grainger Formation (Neuman and Wilson, 1960)

The lower two-thirds of the formation consists of grey and blue-grey noncalcareous siltstone. The upper third includes grey, medium—to coarse—grained, crossbedded calcareous sandstone with layers of pebble conglomerate.

Greasy Cove Formation (Neuman and Wilson, 1960)

This unit consists of interbedded, grey, argillaceous limestone, red shale and fine-grained sandstone, grey shale and siltstone, and grey fine-grained sandstone.

CHAPTER III

STRUCTURAL GEOLOGY

A. Structural Framework

Introduction

The area of the Great Smoky thrust sheet studied in this report is located in the Blue Ridge province of the southern Appalachians, within the Taconic fold belt. Rocks here show some evidence of the Ordovician regional metamorphism and some of the folds observed here are probably Taconic in origin. This area of the Blue Ridge has also been affected by late Paleozoic thrust faulting above the basement at depth, and related folding.

Faults

Major faults in the field area include the Guess Creek fault, the Great Smoky fault, the Miller Cove fault, the Capshaw Branch fault, and the Rabbit Creek fault. These features are shown on the geologic map in Figure 3.

Guess Creek fault. Northwest of Chilhowee Mountain, the Guess Creek fault forms the contact between the highly deformed, undifferentiated rocks of the Middle Ordovician Tellico Formation and Blockhouse Shale above and Mississippian rocks below. The Mississippian rocks are in the

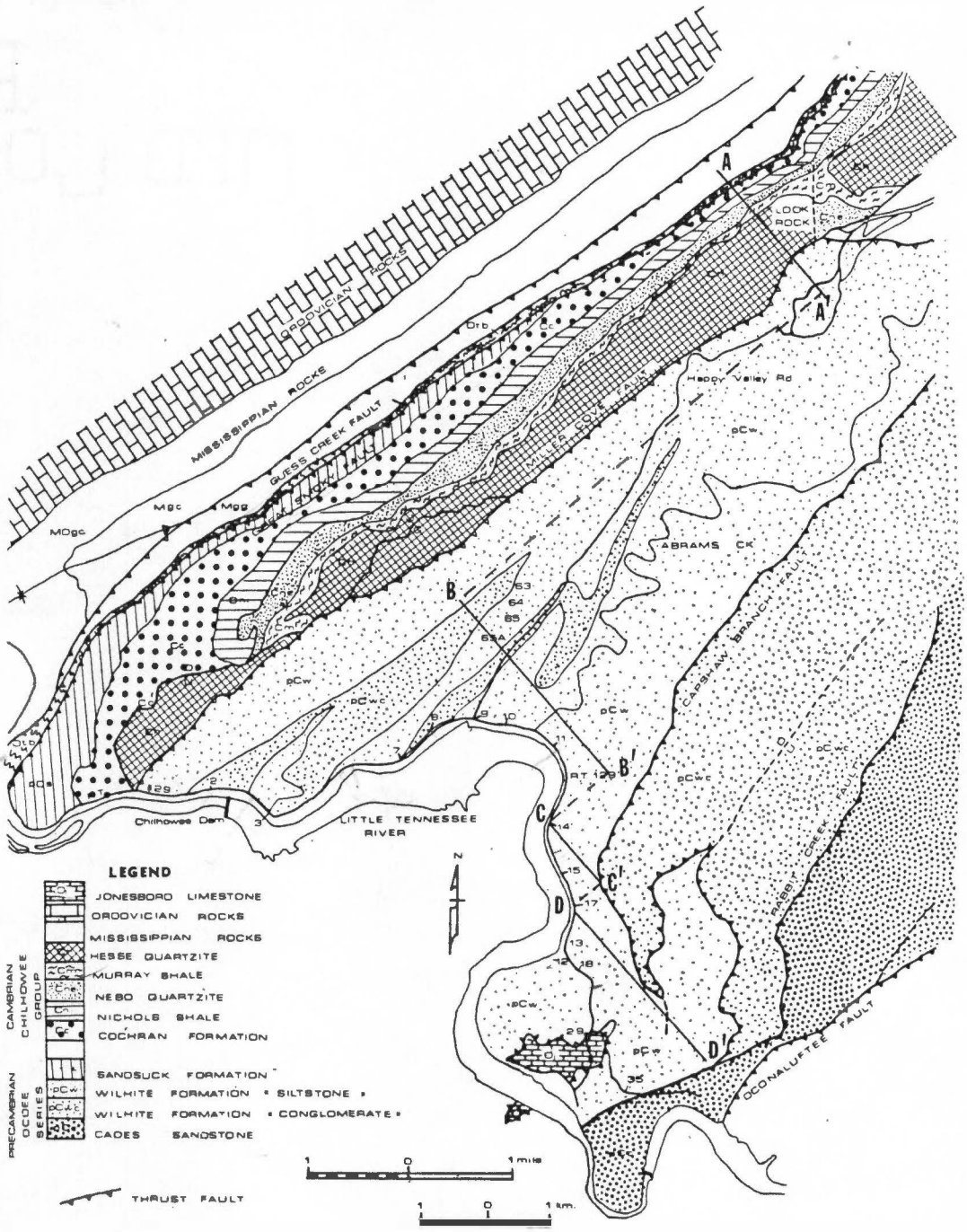

Figure 3. Geologic map of field area (Neuman and Nelson, 1965).

hanging wall of an unnamed reverse fault which attenuates one limb of a large syncline to the northwest. In the Kinzel Springs quadrangle, the Guess Creek fault dips about 60 degrees to the southeast in an exposure. Elsewhere the dips are believed to be between 45 to 60 degrees (Neuman and Nelson, 1965).

Neuman and Nelson (1965) propose two interpretations about the relationship between the Guess Creek and Great Smoky faults. Their preferred hypothesis is that the Guess Creek fault is not parallel to the Great Smoky fault down dip. They base this interpretation on the fact that to the northeast, near the Fair Garden anticline, the traces of the two faults diverge widely. According to this view, the Guess Creek fault is a reverse fault which crosses the Paleozoic sequence to unknown depth, with a displacement of about 2000 feet. The Great Smoky fault followed Middle Ordovician Shale over the Tuckaleechee Cove uplift and then crossed the upturned limbs on the southeastern block of the syncline. It remained in the block uplifted by the Guess Creek fault.

A second interpretation (Neuman and Nelson, 1965) is that the Guess Creek fault is a subsidiary and nearly parallel branch of the Great Smoky fault, formed between strata of contrasting competence within the footwall.

The unnamed reverse fault within the Mississippian rocks marks the base of the disturbed zone. This interpretation is preferred because of its simplicity and because the Great Smoky fault does not cross-cut the Guess Creek fault at any location, despite their close proximity, as might be expected if the Guess Creek fault preceded the Great Smoky thrusting.

Great Smoky fault. The Great Smoky fault outcrops on the northwest side of Chilhowee Mountain and at Calderwood window, in the southern part of the field area. Along the Chilhowee Mountain trace, the Precambrian Ocoee Series and Cambrian Chilhowee Group override Middle Ordovician shales. In a few places, thin slices of Jonesboro Limestone less than half a mile long are found in the footwall. Hanging wall rocks are highly folded and cut into irregular slices by smaller thrust faults. They have been mildly metamorphosed, to the lower part of the chlorite grade (Rodgers, 1970).

Minimum displacement on the Great Smoky fault is believed to be 15 kilometers (Rodgers, 1970). Metamorphic and structural discontinuities across the fault indicate that the slaty cleavage, metamorphic minerals, and many of the folds and faults of the Great Smoky thrust sheet were formed before the thrusting (Neuman and Nelson, 1965).

King (1964) and Neuman and Nelson (1965) believe the Great Smoky fault to be post-Mississippian, and possibly Late Pennsylvanian or Permian in age.

In the study area, the great Smoky fault surface is believed to form a synform southeast of Chilhowee Mountain, while in the vicinity of the Calderwood window it makes an antiform. A structure map of the fault surface based on known outcrops of the fault and constructed structure sections was made by Neuman and Nelson (1965). This configuration is shown on the cross-section in Plate 1. According to this construction, the Great Smoky fault has been thrown only into very broad warps. No other deformations of the fault surface appears in this interpretation. King (1964) stated that this warped nature of the fault is due to the shape of the initial fracture in the Paleozoic rocks. The fault followed the incompetent layers in the sequence for long distances, and ascended abruptly through surrounding more competent strata along inclined planes of shear. King suggests that the Great Smoky fault followed the Blockhouse shale in its long gentle slope northwest of the coves and began its ascent into higher formations in its steeper slope northwest of Chilhowee Mountain. According to this interpretation, the undulations in the fault surface are the result of irregularities in this initial fracture due to the contrasting competency and corresponding variable angle of shear of the involved Paleozoic formations.

The Great Smoky fault was formed after the regional metamorphism of the Blue Ridge province and is discordant with F1 folds and associated axial-plane slaty cleavage.

Miller Cove fault. The Miller Cove fault is the eastern boundary of the Chilhowee Mountain structural block, with the Great Smoky fault forming the northwestern boundary. Rocks in the structural block include the Sandsuck Formation and the Chilhowee Group. Northeast of the Look Rock, the structure of the Chilhowee Mountain block is synclinal, while southwest of Look Rock it is roughly that of a southeast-dipping homocline. This change in structure suggests that the Miller Cove fault cuts across the trough of a previously formed syncline. Another interpretation by King (1964) is that the synclinal structure of the Chilhowee Mountain block results from warping of the overriding strata of the Great Smoky fault. Due to its rise out of the Blockhouse Shale into more competent strata, the fault surface bends abruptly and causes the Chilhowee Mountain syncline.

In the study area, the Miller Cove fault thrusts the Precambrian Wilhite Formation over the Cambrian Chilhowee Group. Neuman and Nelson (1965) and Rodgers (1970) believe the Miller Cove fault to be an imbrication of the Great Smoky fault. The Chilhowee Mountain block

was part of the Great Smoky thrust sheet, picked up late in the fault's development and carried ahead of the main part of the overthrust sheet.

Folds

Four groups of macroscopic and mesoscopic folds and related structures have been determined in the study area. The earliest folds (F1) consist of second-order mesoscopic folds with penetrative slaty cleavage as an axial plane foliation (S1). These occur on the limbs of first-order macroscopic F1 folds which are discordant to the Great Smoky fault. Many of the mesoscopic F1 folds are asymmetric, overturned folds with some degree of hinge thickening and corresponding thinning of fold limbs. Flexural slip and flexural flow are probable mechanisms involved in the F1 fold formation. The geometry of the F1 macroscopic folds is reflected by the associated mesoscopic F1 fold styles.

F1 fold axes trend generally northeast-southwest with gentle plunges to the northeast and southwest. Mesoscopic F1 axial planes northwest of Location 15 dip to the southeast. Southeast of Location 15, the mesoscopic F1 axial planes show a northwest-dipping orientation.

In several places a crenulation cleavage (S2) overprints the S1 slaty cleavage. S2 is characterized by cleavage planes showing preferred mineral orientations separated

by thin slices of rock containing a crenulated cross-lamination. S2 is not penetrative; it forms discrete planar discontinuities which cause localized structural weaknesses within the rock.

In some places, both bedding and S1 are folded into small folds by the crenulation cleavage. These mesoscopic F2 folds generally have an angular zig-zag profile and show attenuation of fold limbs in zones of well-developed foliation. Thin sandstone layers and quartz veins form tight to isoclinal folds. Small-scale boudinage affects some of the fold limbs oriented subparalled to the S2 axial plane foliation.

Macroscopic F3 folds involve the folding of slaty cleavage (S1). An antiformal F3 structure is in the vicinity of Calderwood with an adjacent F3 synform north of the window near Location 15. Smaller F3 folds were found near Location 11 and Location 14. The F3 folds are believed to be related to the deformation of the Great Smoky fault which resulted in its present undulatory nature.

Mesoscopic F4 folds at Location 9 consist of kink bands with reverse fault sense of movement and northwest-dipping axial planes. They are associated with southeast-dipping mesoscopic thrust faults.

Detailed descriptions of the observed folds in the Great Smoky thrust sheet are presented in the following sections. Table 1 is a summary of the structural elements described for the area of investigation. Locations of the folds are shown in Figure 3. The fabric elements used in this structural analysis, terminology adopted in the discussion of fold style, and the conventions used to present the fold orientation data are explained in Appendix A. In the following sections, macroscopic F1 folds will be designated F1(M). Mesoscopic F1 folds will be designated as F1.

B. Mesoscopic F1 Folds and Related Structures

Introduction

The earliest recognized mesoscopic structures in the study area are designated F1 folds. Most other mesoscopic fabric can be found to overprint the F1 folds, and are therefore later in origin. The grouping includes both parallel and congruent fold types with inter limb angles ranging from tight to gentle. Most F1 folds, however, have an associated axial plane foliation which consists of slaty cleavage. Fold symmetry is usually monoclinic. Many of the F1 folds are apparently second-order folds on the limbs of larger structures. Fabric data collected from selected locations (shown in Figure 3, page 13) are

TABLE 1

STRUCTURAL ELEMENTS IN THE GREAT SMOKY THRUST SHEET, ADJACENT TO THE LITTLE TENNESSEE RIVER, TENNESSEE

Folds	Planar Structures
MACROSCOPIC	
F1(M): First-order overturned folds discordant with the Great Smoky fault.	SS: Sedimentary bedding.
F3: Involve folding of S1. An antiformal F3 structure occurs at Calderwood window.	S1: Pervasive axial plane foliation consisting of slaty cleavage. Subparallel to F1 axial planes.
MESOSCOPIC	
F1: Second-order mesoscopic folds occurring on the limbs of F1(M) folds. S1 subparallel to F1 axial planes. F1 fold axes trend northeast-southwest.	
F2: Include angular zig-zag folds and tight to isoclinal folds with boundinage on fold limbs parallel to S2 axial plane foliation.	S2: Slip and crenulation cleavage. Locally transposes S1. Subparallel to F2 axial planes.
F4: Kink-bands with reverse fault sense of movement. Related to southeast-dipping mesoscopic thrust faults.	

discussed below. All structures occur within the Wilhite Formation.

Location 3

Style of folds. Rocks at Location 3 range from medium-bedded (30-120 cm) conglomeratic sandstone, interbedded with shale, to laminated and thin-bedded (6-30 cm) siltstone. Major structures found here are a large (200 meters) doubly-plunging anticline and an adjacent syncline.

The anticline is a parallel-type fold with a gentle interlimb angle and an associated steeply-dipping axial plane slaty cleavage. Quartz-filled fractures perpendicular to bedding surfaces are common. Mineralized and slickensided fault surfaces parallel to bedding are found. These faults, and the abundance of slickensides on bedding surfaces, suggest flexural-slip folding as a mechanism of deformation. Small second-order folds occur on the fold limbs. These have fold axes subparallel to that of the major fold.

Orientation data (Figure 4). Structural fabric data for Location 3 is shown on an equal area diagram in Figure 4. Poles to bedding surfaces (SS) form a distinct girdle, from which an ac-plane of deformation has been constructed. The anticline fold-axis (B1) dips gently

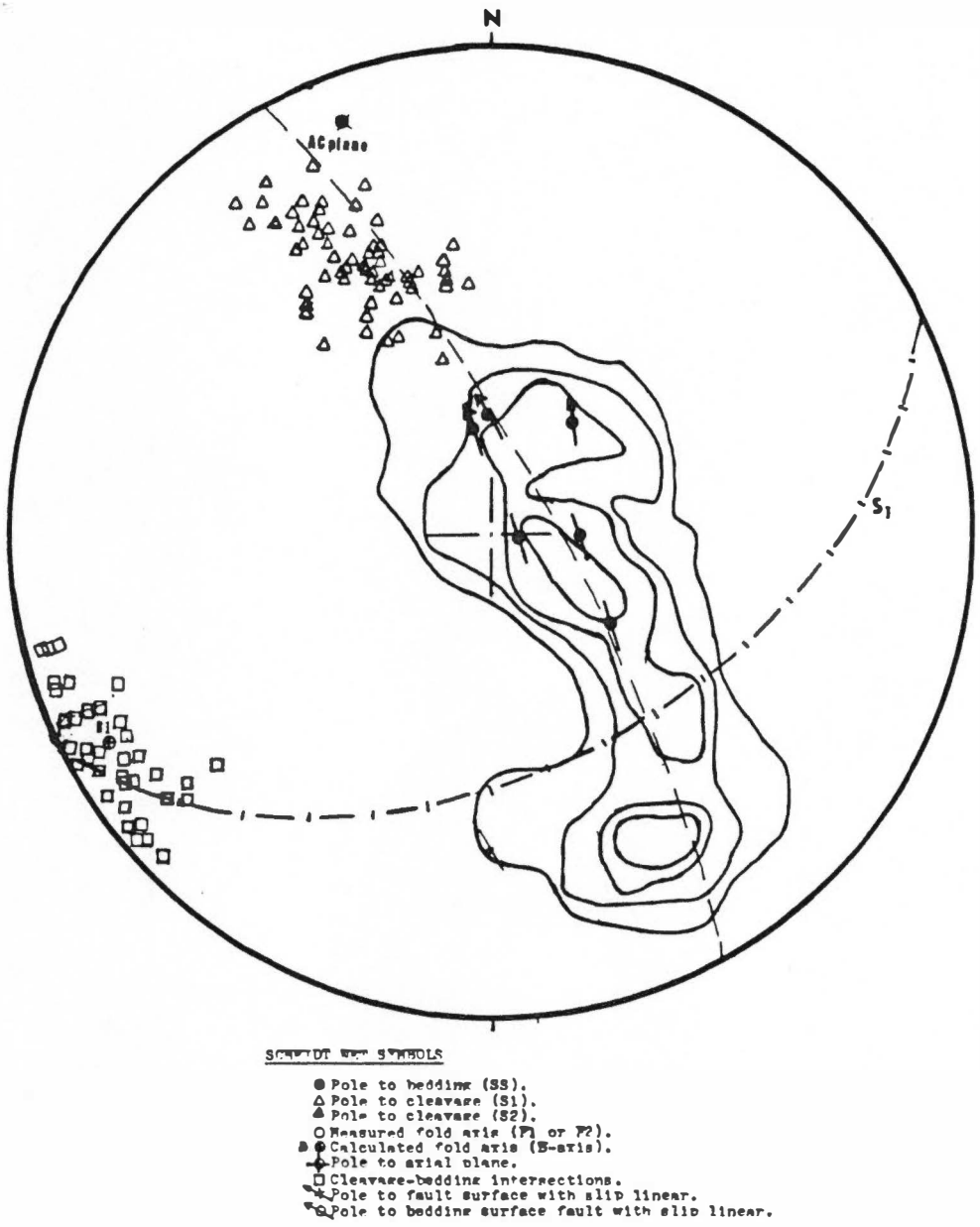

Figure 4. Schmidt net: mesoscopic F1 fold, Location 3. Contours at 2, 4, 8, and 11 percent. Eighty poles to bedding contoured.

to the southwest. Cleavage-bedding intersections are concentrated around the fold axis. Cleavage-poles cluster on the AC-plane, indicated by the bedding-pole distribution. The close proximity between the B1 fold axis and the cleavage-bedding intersections, together with the location of the cleavage-pole cluster on the fold AC-plane suggest that the cleavage is an axial plane foliation and was formed within the same phase of deformation as the fold.

Slip linears in Figure 4 are perpendicular to the fold axis and are parallel with the ac-plane of folding. The relative movement of the bedding-parallel faults on the anticline is apparently that of reverse faults. This is compatable with flexural-slip folding.

Discussion. Evidence of slip along bedding layers, parallel fold shape, and the brittle nature of the rocks, suggested by the fractures perpendicular to bedding, indicate that deformation was probably by a flexural-slip mechanism under conditions of low confining pressure and temperature (Donath and Parker, 1974).

Location 8

Style of folds (Figure 5). Lithologies here are brownish-grey siltstone, sandstone, and limestone conglomerate. For about 200 meters eastward from this

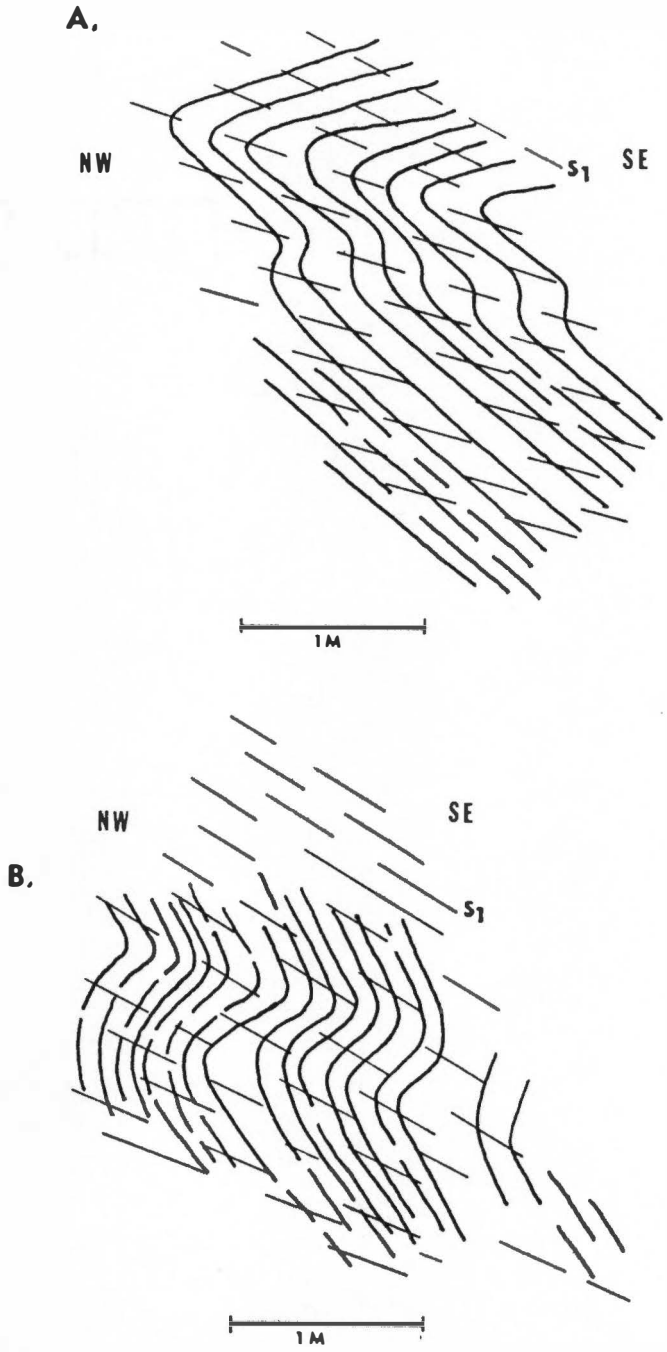

Figure 5. Second-order mesoscopic F1 folds from Location 8 (from photographs).

location, the southeast-dipping beds are overturned. The bedding surfaces show slickensides which indicate normal fault displacement. Bedding dips from forty to fifty degrees southeast, while a poorly developed cleavage dips about fifteen to twenty degrees southeast. These beds are apparently the northern limb of an overturned F1(M) anticline with a northeast-southwest trend.

Farther east, cleavage is better developed and bedding is difficult to distinguish. Rocks in this area have a pervasive slaty cleavage. Mesoscopic folds here (Figure 5) are congruent folds with a close interlimb angle and axial plane slaty cleavage. Fold symmetry is monocline, with long southeast-dipping limbs and short northwest-dipping limbs. These folds are apparently second-order folds on the north limb of the overturned anticline.

Orientation data (Figure 6). The Schmidt net in Figure 6 shows a cluster of cleavage poles in the northwest quadrant. Dashed lines near the net center are ac-planes for second-order folds. Most of the cleavage poles fall on this plane. Measured axial planes of second-order poles coincide with the cleavage cluster. Second-order fold axes plot on the constructed cleavage (S1) plane. Slip linears are parallel to the ac-plane of the second-order fold and show normal fault displacement.

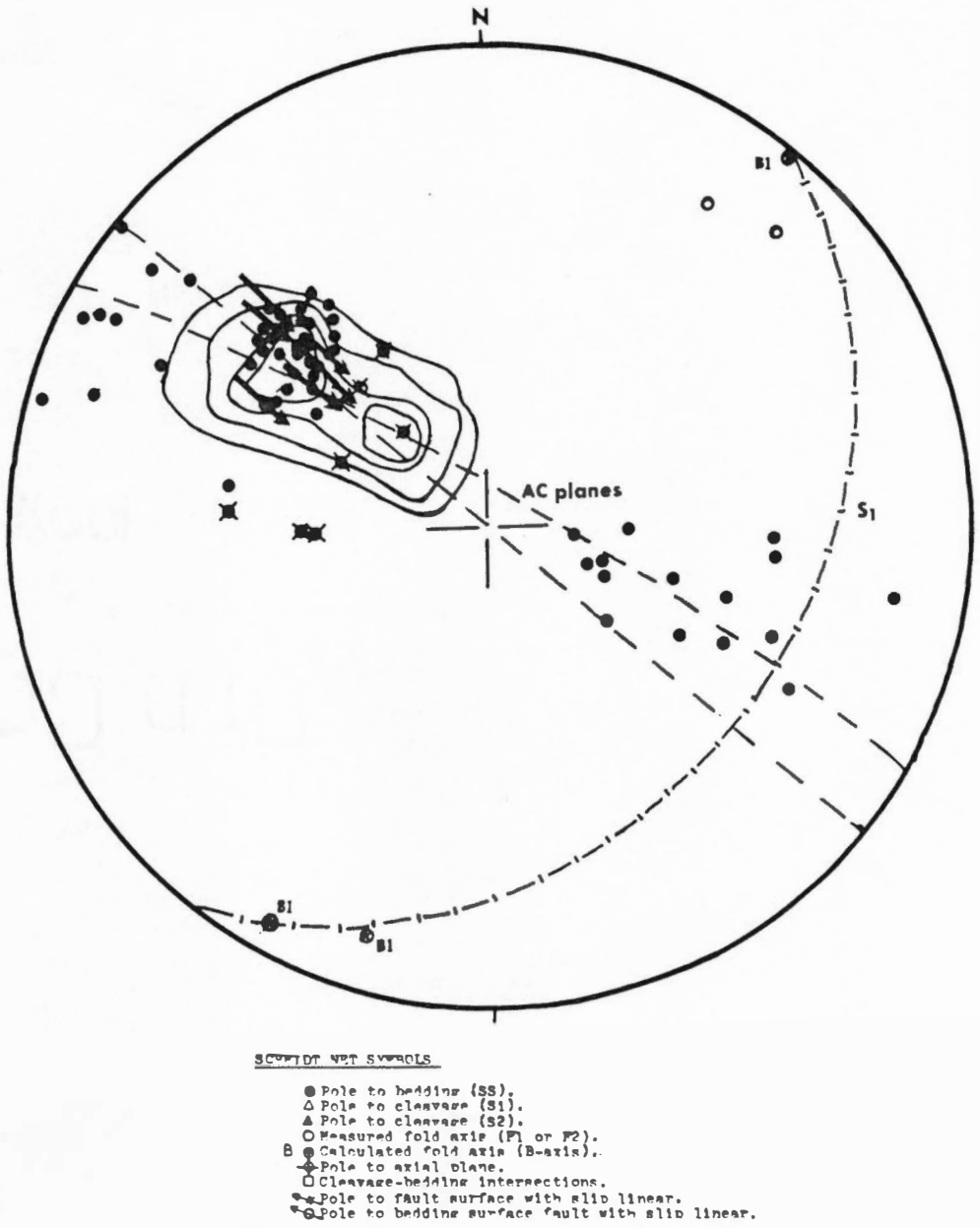

Figure 6. Schmidt net: mesoscopic F1 folds on overturned limb of F1(M) fold. Fifty poles to cleavage contoured. Contours at 4, 11, 18, 25 percent. Location 8.

Discussion. The fact that the small folds are second-order folds on the north limb of an overturned anticline is suggested by the parallelism of their axial planes with the slaty cleavage in the area and also the occurance of their fold axes within the plane of the cleavage. Normal fault displacement for bedding slip is compatible with that expected for the overturned limb of an anticline.

Location 10

Style of folds (Figures 7 and 8). Rocks in this area are thin-bedded (2 to 30 cm) medium-grey siltstone and fine sandstone. From about 250 meters east of Location 10 to Abrams Creek, there is a large, gentle syncline. A large overturned fold, shown in Figure 8, is found 200 meters east of Location 10. A smaller fold with similar style appears in Figure 8A. Both folds are congruent, overturned folds with a close interlimb angle and rounded hinges. Slaty cleavage is subparallel to the fold axial planes. Another congruent fold with axial plane slaty cleavage is in Figure 8B.

Orientation data (Figure 9). A sterogram analysis of structural fabric in Location 10 appears in Figure 9. The bedding pole distribution has been contoured and shows a fairly distinct girdle pattern. Cleavage (S1) poles

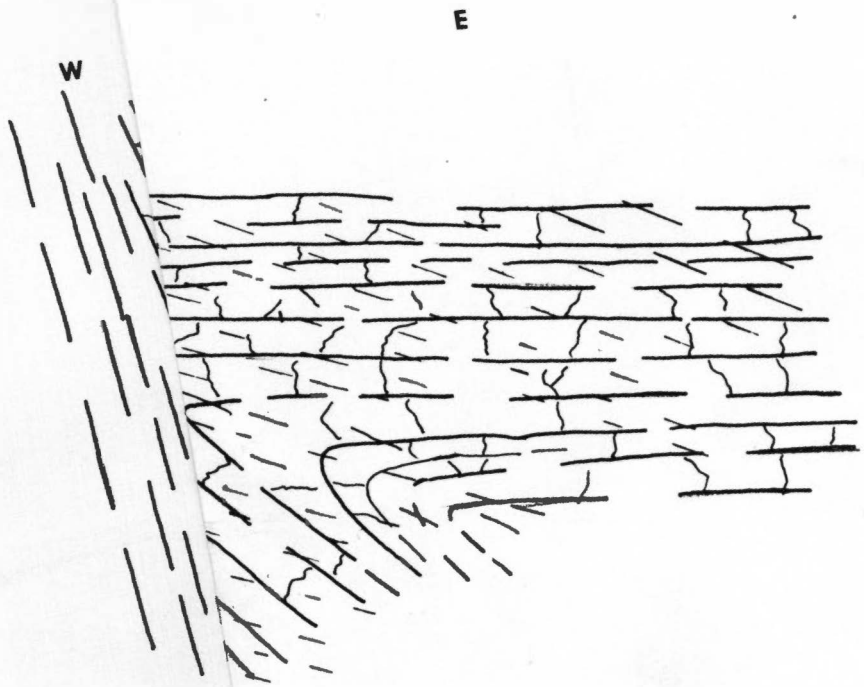

Figure 7. Overturned F1 fold, Location 10 (from photograph).

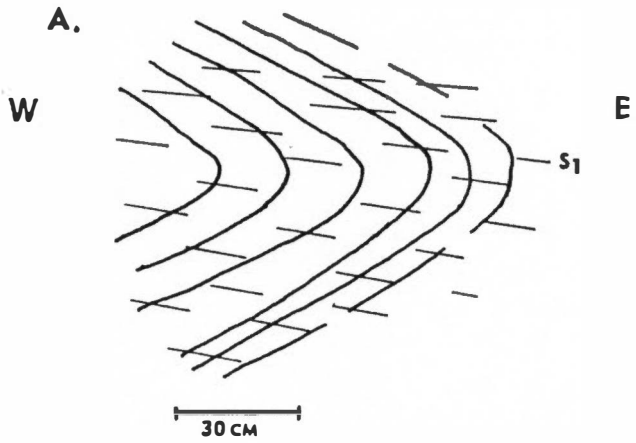

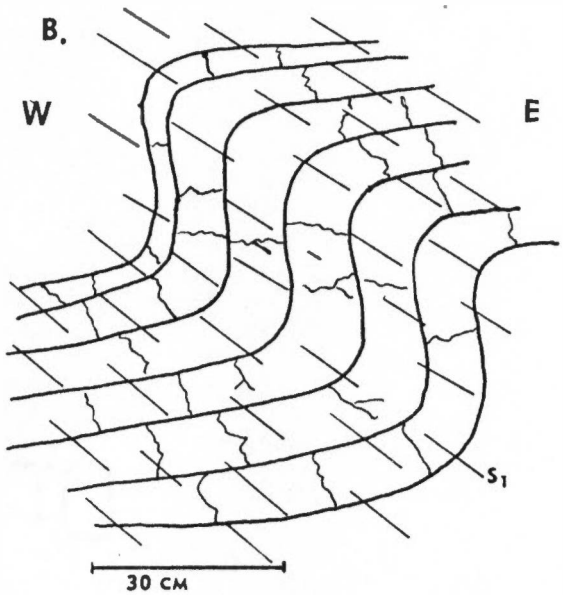

Figure 8. F1 folds, Location 10 (from photographs).

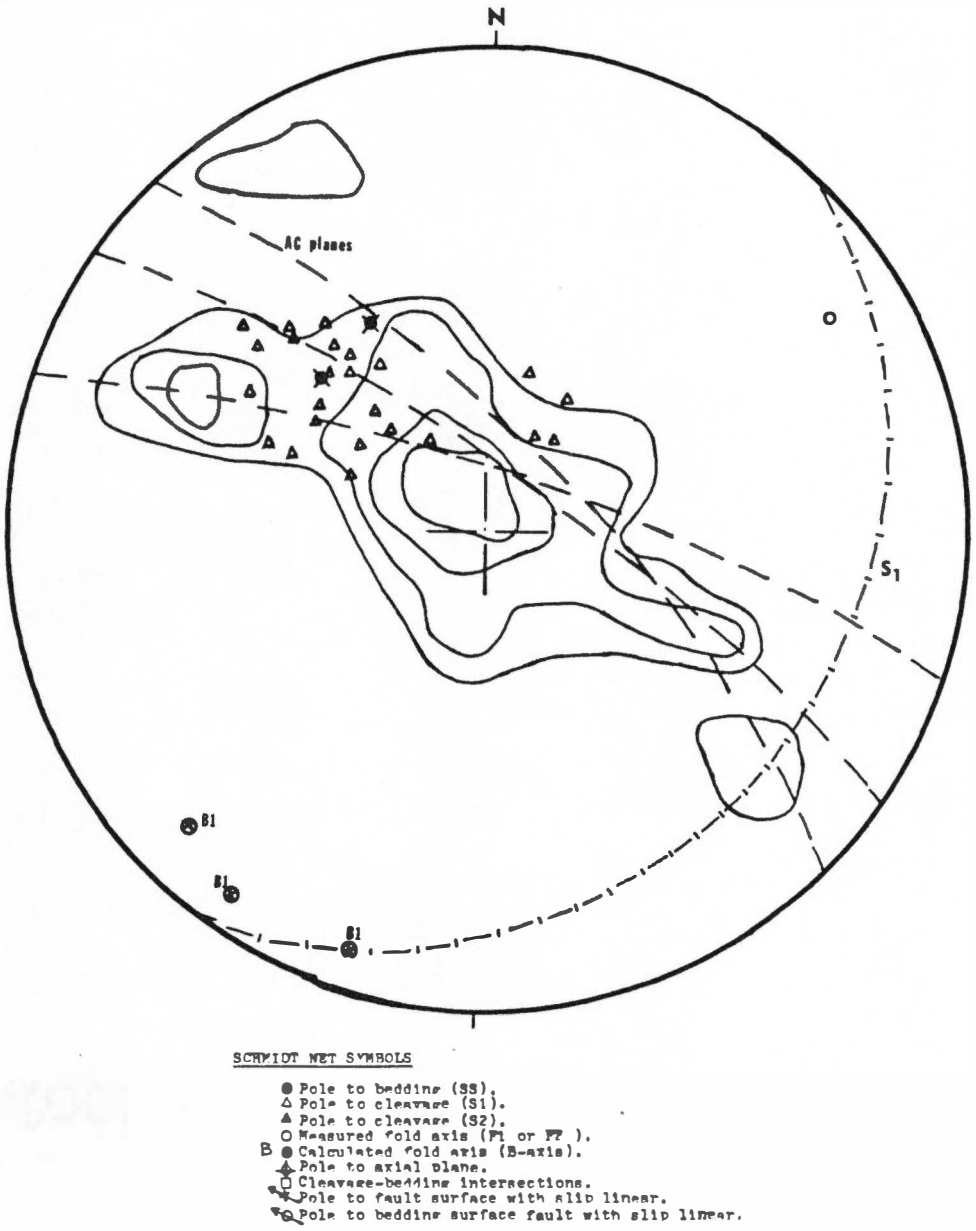

Figure 9. Schmidt net: mesoscopic F1 folds, Location 10. Sixty poles to bedding contoured. Contours at 2, 4, 11 and 18 percent.

form a cluster within this girdle. An approximate S1 plane has been constructed. The constructed fold axes fall very near the cleavage great-circle. Two measured axial plane poles are within the cleavage concentration.

Discussion. The cluster of cleavage on the area ac-plane and the location of fold axes on the S1 great circle support the observation that the slaty cleavage is an axial plane foliation for measured folds. Thickening of the fold hinges and thinning of fold limbs probably indicates that flexural-flow mechanism of folding was at least partly involved in the deformation. Faint slickensides on some bedding surfaces suggests that flexural-slip folding was also involved. This is possible if the folds initially developed as parallel folds and were then modified by superimposed homogeneous strain (Ramsay, 1967, Page 411). Such additional strain would cause thinning of fold limbs and modification of the fold profile.

Location 11

Style of folds (Figures 10 and 11). The lithology in this area ranges from medium-grey siltstone to fine-grained sandstone. One large F1 fold in this area is shown in Figure 10. This is a congruent overturned fold with a tight interlimb angle, rounded hinges, and straight limbs.

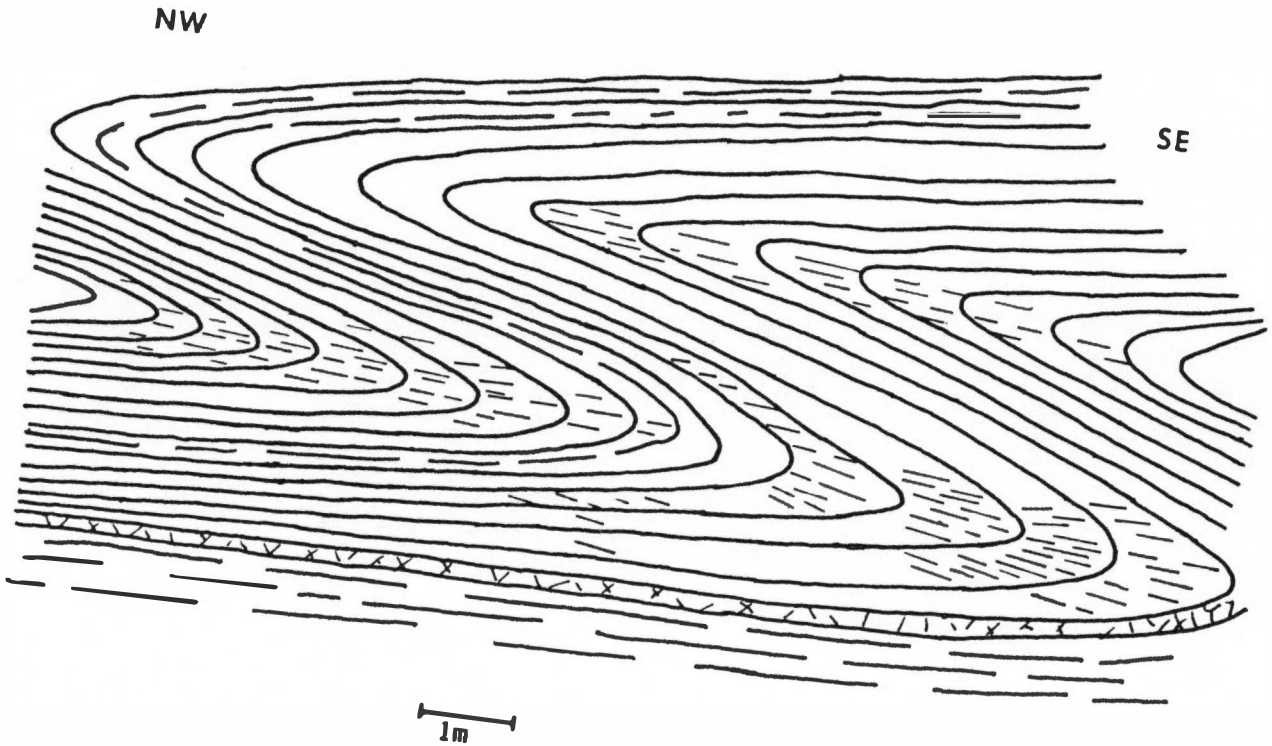

Figure 10. Overturned mesoscopic F1 fold, Location 11 (from photograph).

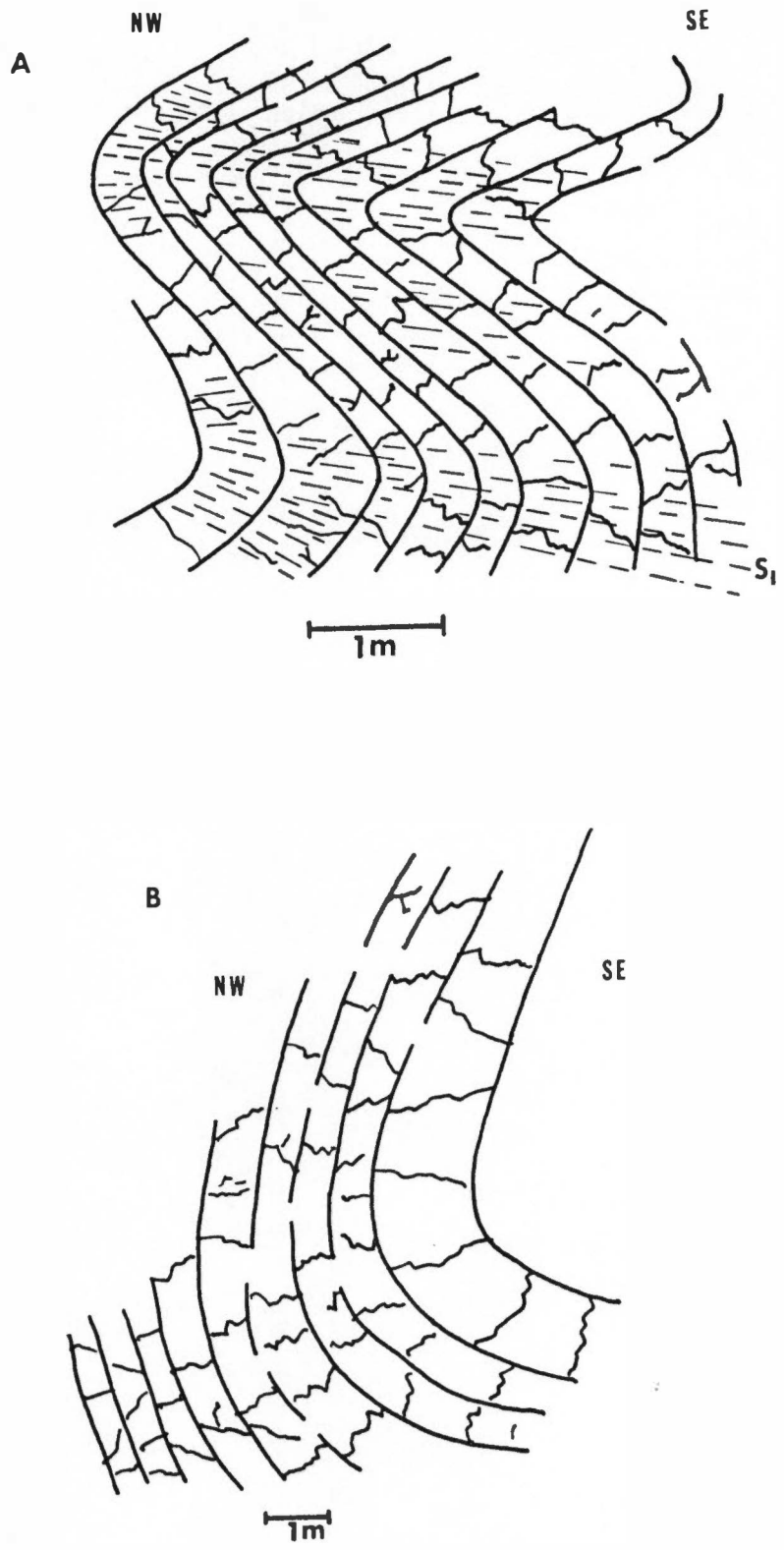

Figure 11. Mesoscopic F1 folds, Location 11 (from photographs).

The hinge area is very small compared to the fold limb length. Pronounced thickening of the hinges can be observed. There is a pervasive axial plane slaty cleavage.

Figure 11A shows another type of F1 fold in this area. It is also a congruent fold-type, but has a close interlimb angle. Some open folds can be found, as in Figure 11B. These approach more closely a parallel fold profile. Folds here show a gradation between the parallel and congruent fold profiles. Generally, the smaller the interlimb angle, the more the fold resembles the congruent fold style. All F1 folds at this location show axial plane slaty cleavage.

Most of the folds in this outcrop region appear to have near-vertical fold envelopes. In the southern part of this area, near Location 14, the fold interlimb angle increases and the folds more nearly approach a concentric fold profile.

Orientation data (Figures 12A and 12B). The bedding (SS) pole distribution is shown by contours in Figure 12A. It shows a crossed girdle, which suggests two different great-circle patterns. Ac-planes have been constructed for three folds. The fold axes show a great variation in strike, but generally dip gently to the northeast.

Figure 12B shows the contoured distribution of cleavage poles. Measured axial planes for the F1 folds

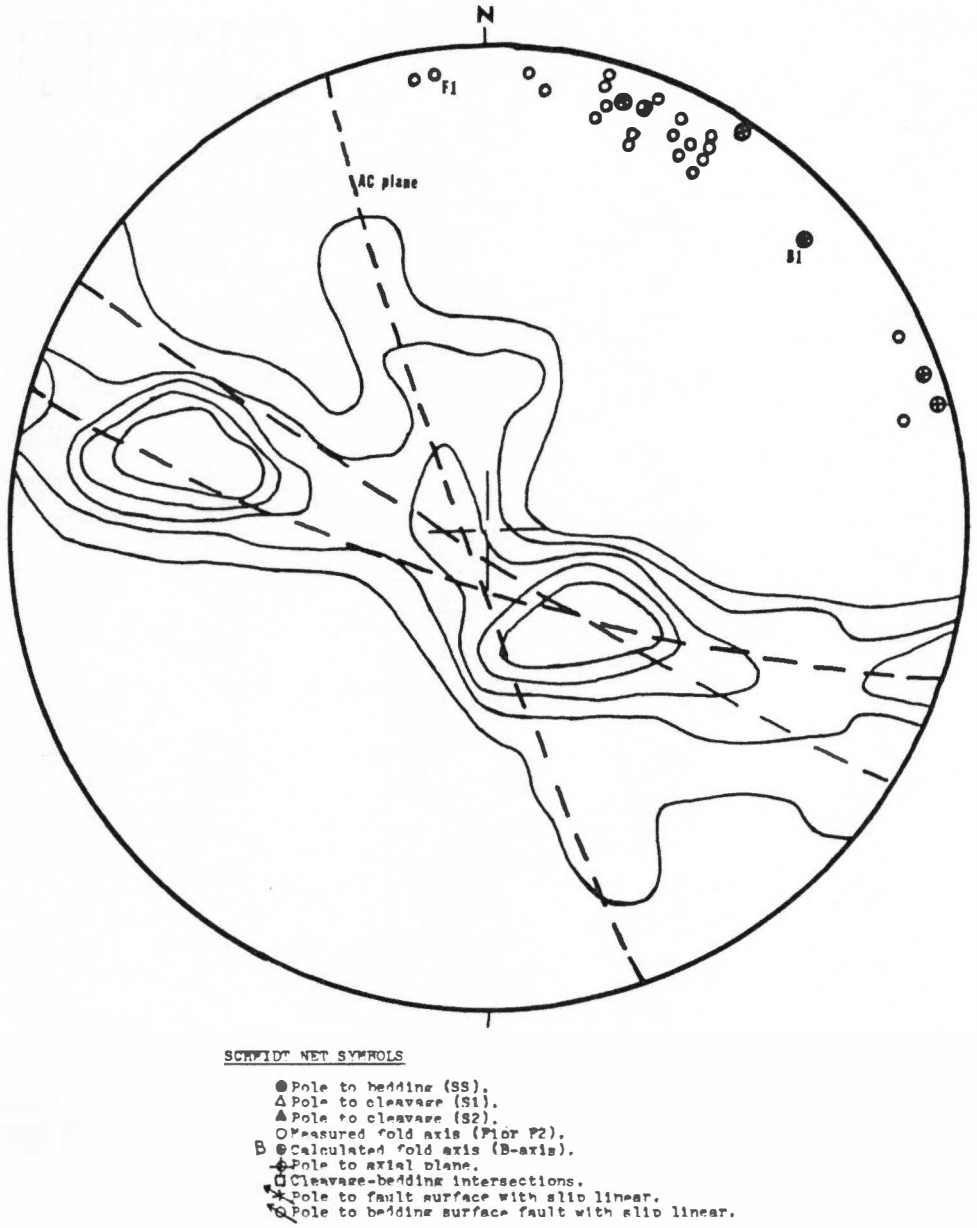

a. Forty-five poles to bedding contoured. Contours at 1, 2, 4, 7, and 11 percent.

Figure 12. Schmidt net: mesoscopic F1 folds, Location 11.

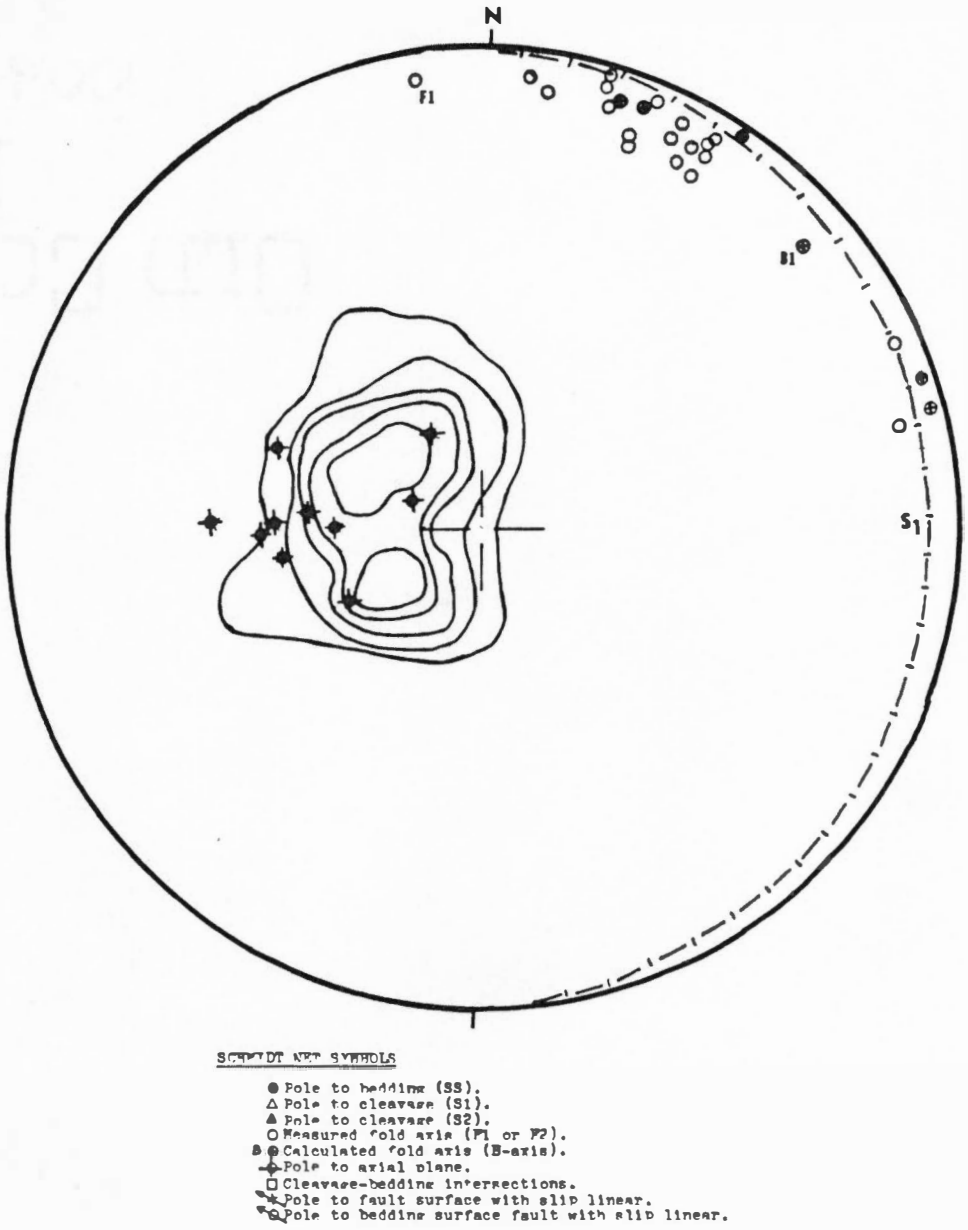

b. Eighty-two poles to S1 cleavage contoured. Contours at 1, 4, 11, 18 and 25 percent.

Figure 12 (continued)

coincide with the cleavage (S1) concentration. A great circle has been drawn which coincides with the average S1 orientation. Most of the fold axes fall very close to this great circle.

Discussion. The bedding-pole crossed-girdle of Figure 12A and the spread of the fold axes suggests that subsequent deformation of the F1 folds has occurred. In Figure 12B, the cleavage pole distribution shows a greater spread than in previously discussed locations.

In outcrop, the slaty cleavage looks parallel to the fold axial planes. The coincidence of the axial plane poles to the cleavage poles in Figure 12B and the fact that all fold axes lie within the plane of the cleavage is further evidence that the slaty cleavage is an axial plane foliation with respect to these F1 folds.

Many of the bedding surfaces show faint slickensides. Although the directions are variable, they appear to be roughly perpendicular to the fold hinge lines. This suggests that flexural-slip has taken place in the fold formation.

Location 12

Style of folds (Figures 13 and 14). Rocks in this location range from thin-bedded (5-31 cm) interbedded siltstone and coarse-graded sandstone to conglomeratic sandstone.

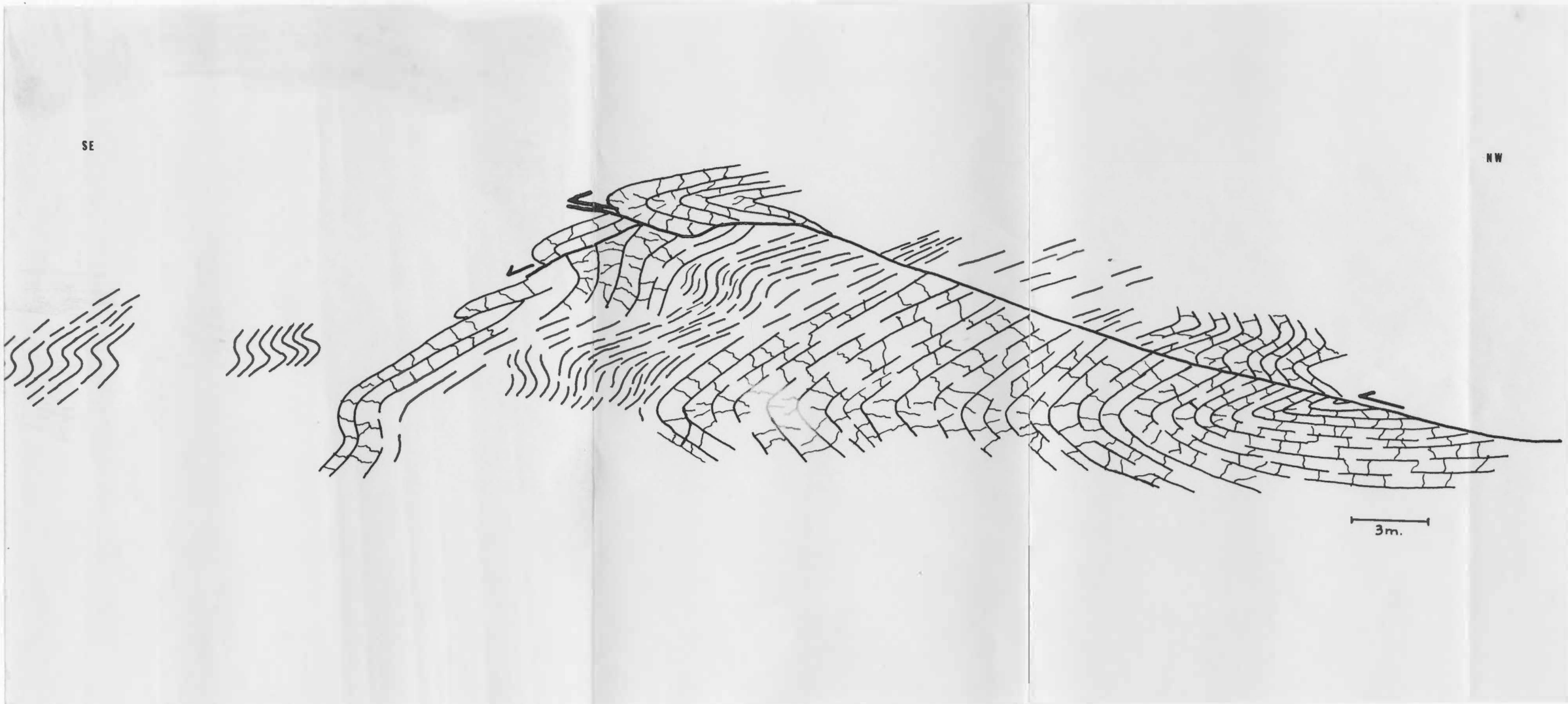

Figure 13. Mesoscopic F1 folds, Location 12 (from photomosaic).

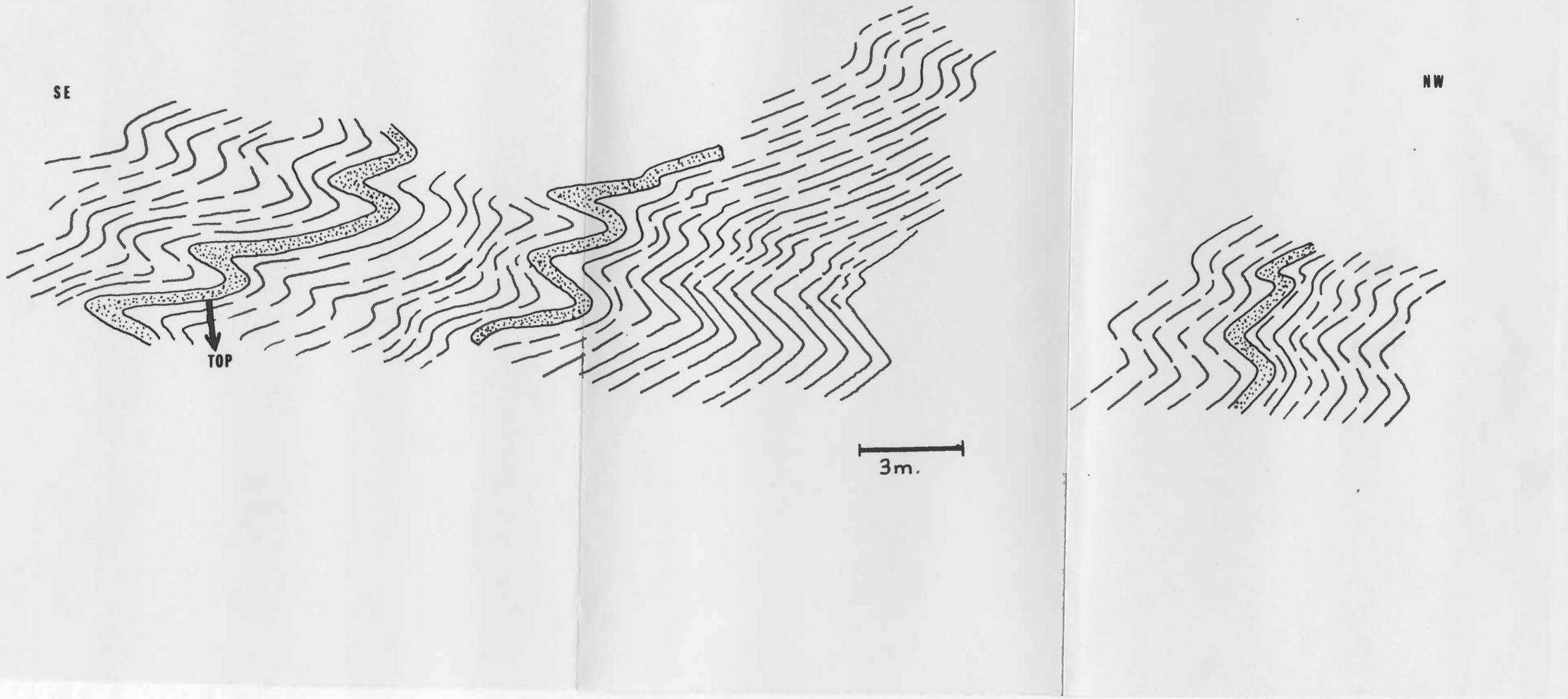

Figure 14. Second-order mesoscopic F1 folds, Location 12 (from photomosaic).

This variability of rock type is responsible for the different F1 fold styles found in this outcrop.

Figures 13 and 14 are diagrams made from a photomosaic of the entire exposure at Location 12. In the right half of Figure 13 is a large parallel fold with a close interlimb angle and rounded hinges. A bedding-parallel thrust fault rises out of the core of the fold and displaces the upper limb.

Figure 14 shows a number of folds with monoclinic symmetry. Bedding is generally overturned, with a northwest direction of younging. Folds found here are probably second-order folds on the northern limb of an overturned anticline. The asymmetry of the folds is compatible with such an interpretation.

Fold style depends on the rock type of the deformed layers. Sandstone beds form parallel folds with rounded hinges and a close interlimb angle. Siltstone interbedded with the sandstones form congruent folds, in some cases approaching the shape of chevron folds. They have thickened, angular hinges and planar limbs which show relative thinning. Slaty cleavage occurs as an axial plane foliation. Faint slickensides, perpendicular to the fold hinge lines, were seen on some bedding surfaces.

Orientation data (Figure 15). Bedding poles for Location 12 (Figure 15) form a distinct girdle, indicating

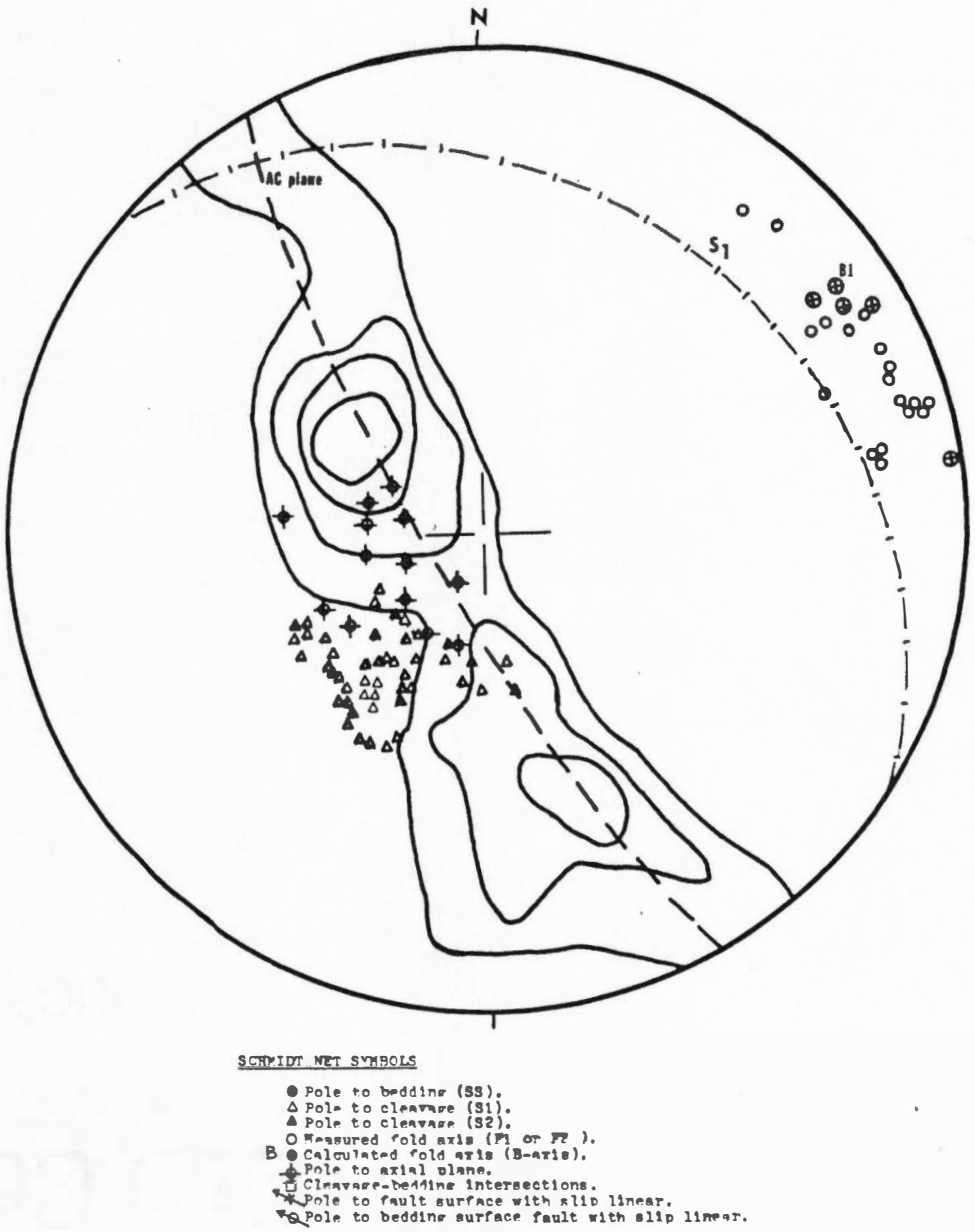

Figure 15. Schmidt net: mesoscopic F1 folds, Location 12. Sixty-seven poles to bedding contoured. Contours at 2, 4, 11, and 18 percent.

a northeast sipping B-axis. This axis lies within the concentration of fold axes. Poles to cleavage are slightly off the ac-plane. Concentrations of cleavage poles and fold axial plane poles are very close. The northeast-dipping fold axes are within about 10 degrees from the northeast-dipping cleavage great circle.

Discussion. Although there is some divergence from the expected pattern, the sterogram analysis suggests that the cleavage is an axial plane foliation. The parallel profile of some folds and slickensides on bedding surfaces are evidence that flexural-slip was a mechanism of folding.

The occurance of chevron folds in regularly-bedded sequences of units with different competence is common. Hinge dilation often accompanies the formation of chevron folds, and may result in the flow of less competent strata into the hinge zone (Ramsey, 1974). Thickening of the hinge zones is a characteristic of the chevron folds in Figure 14, and is evidence that the folds underwent flexural-flow in the late stages of folding.

Location 13

Style of folds (Figure 16). The lithology here is similar to that of Location 12. Graded bedding indicates the beds are overturned, with stratigraphic up-section

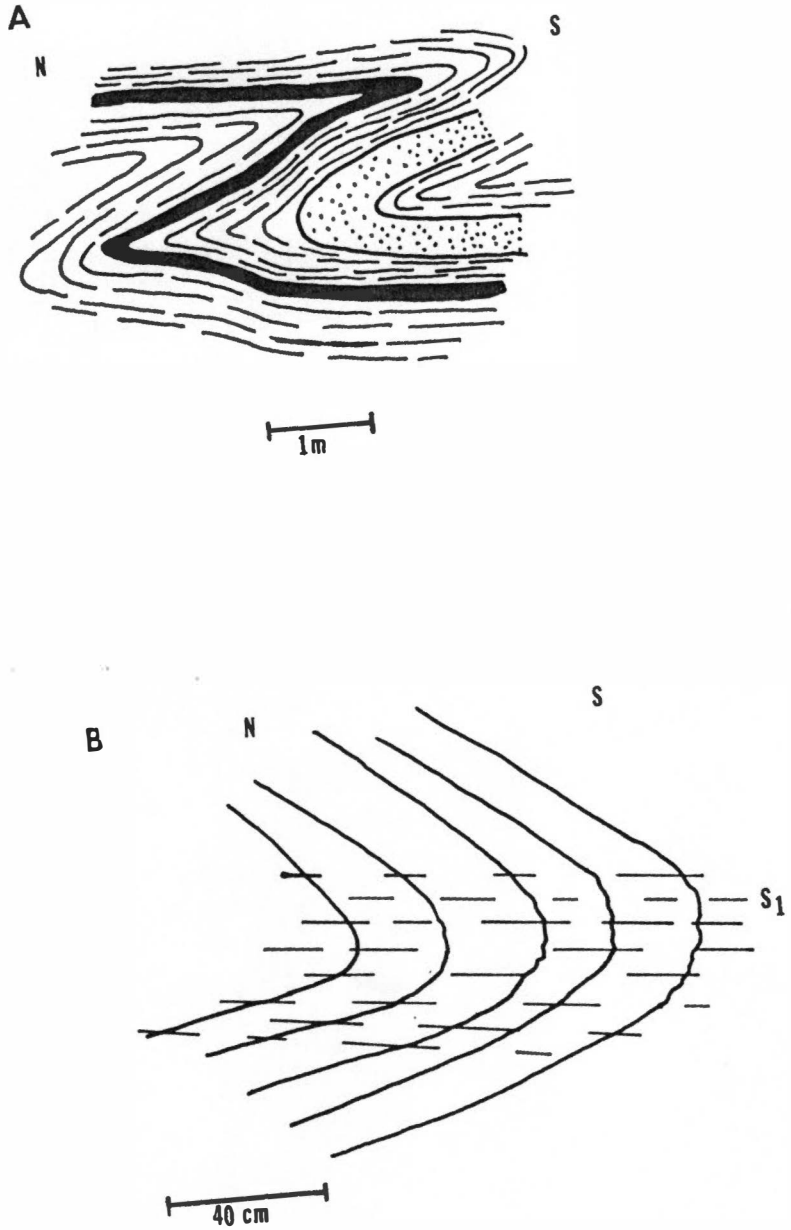

Figure 16. Mesoscopic F1 folds, Location 13 (from photographs).

to the north. Most folds show a monoclinic symmetry and are similar in style to those of Location 12 (Figure 16). They are probably also second-order folds on the north limb of an overturned anticline.

Orientation data (Figure 17). A scatter diagram of bedding poles (Figure 17) shows a great circle girdle with a B-axis near a cluster of measured east-dipping fold axes. Fold axes plot within the plane of the cleavage. S1 dips gently to the northeast. Poles to the cleavage fall near the ac-plane for the folds. Slip linears for faults are shown. They do not appear related to the F1 folds.

Discussion. Figure 16A shows a chevron fold with competent units of different thickness. The chevron fold style is stable when the thickness of the competent units is fairly constant. A single anomalously thick competent layer may be accomodated through the development of bulbous hinges (Ramsay, 1974). The chevron fold of Figure 16A illustrates hinge collapse and the formation of a bulbous hinge by flexural-flow.

The fabric analysis in Figure 17 is consistent with that expected for folds with axial plane cleavage. Faults in this outcrop probably postdate the F1 structures.

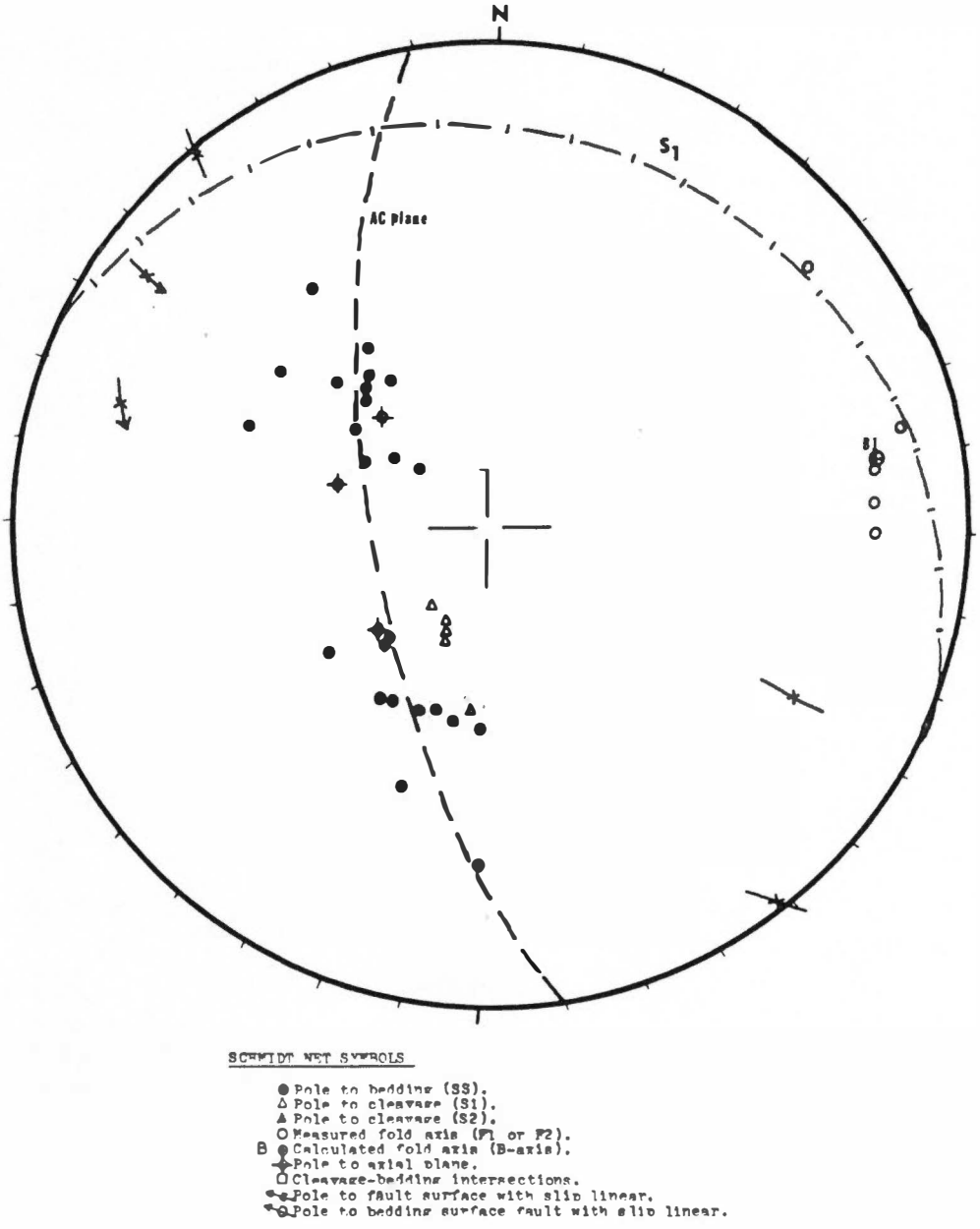

Figure 17. Schmidt net: mesoscopic F1 folds, Location 13.

Location 14

Style of folds (Figures 18, 19, and 20). Rocks between Locations 14 and 15 are mainly laminated to very thin-bedded (up to 5 cm) siltstone with occasional thin beds of fine-grained sandstone. The large fold in Figure 18A is found just north of Location 15. It consists of overturned, congruent folds with small, rounded hinges and long limbs which enclose close interlimb angles. Slaty cleavage is subparallel to the fold axial planes. These folds show monoclinic symmetry.

For about 150 meters south of Location 14, the bedding is apparently subparallel to a well-developed slaty cleavage. Some of the thin sandstone layers have been folded into small, very tight to isoclinal, folds with nearly horizontal fold axes. Other F1 folds between Locations 14 and 15 (Figures 19 and 20) are generally congruent folds with close to open interlimb angles and rounded hinges. All F1 folds in the area have a well-developed axial plane slaty cleavage.

Orientation data (Figures 21A and 21B). A scatter diagram of bedding poles (Figure 21A) shows a concentration of southeast-dipping beds and a diffuse great-circle girdle. Two π-circles (AC planes) from individual folds have been constructed. Cleavage poles for cleavage in the vicinity of these folds are also shown. These poles lie on the

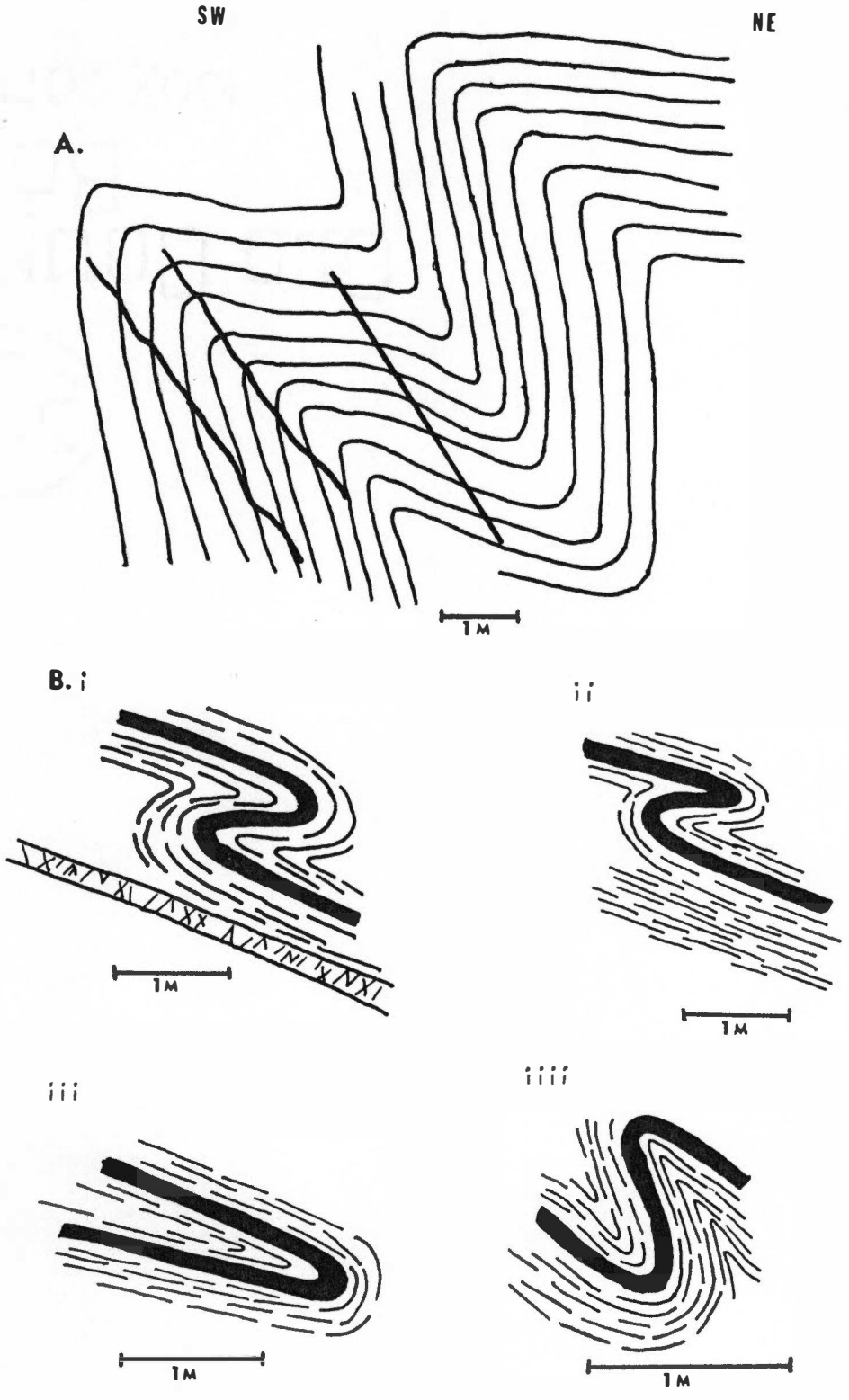

Figure 18. Second-order mesoscopic F1 Folds, Location 14 (from photographs).

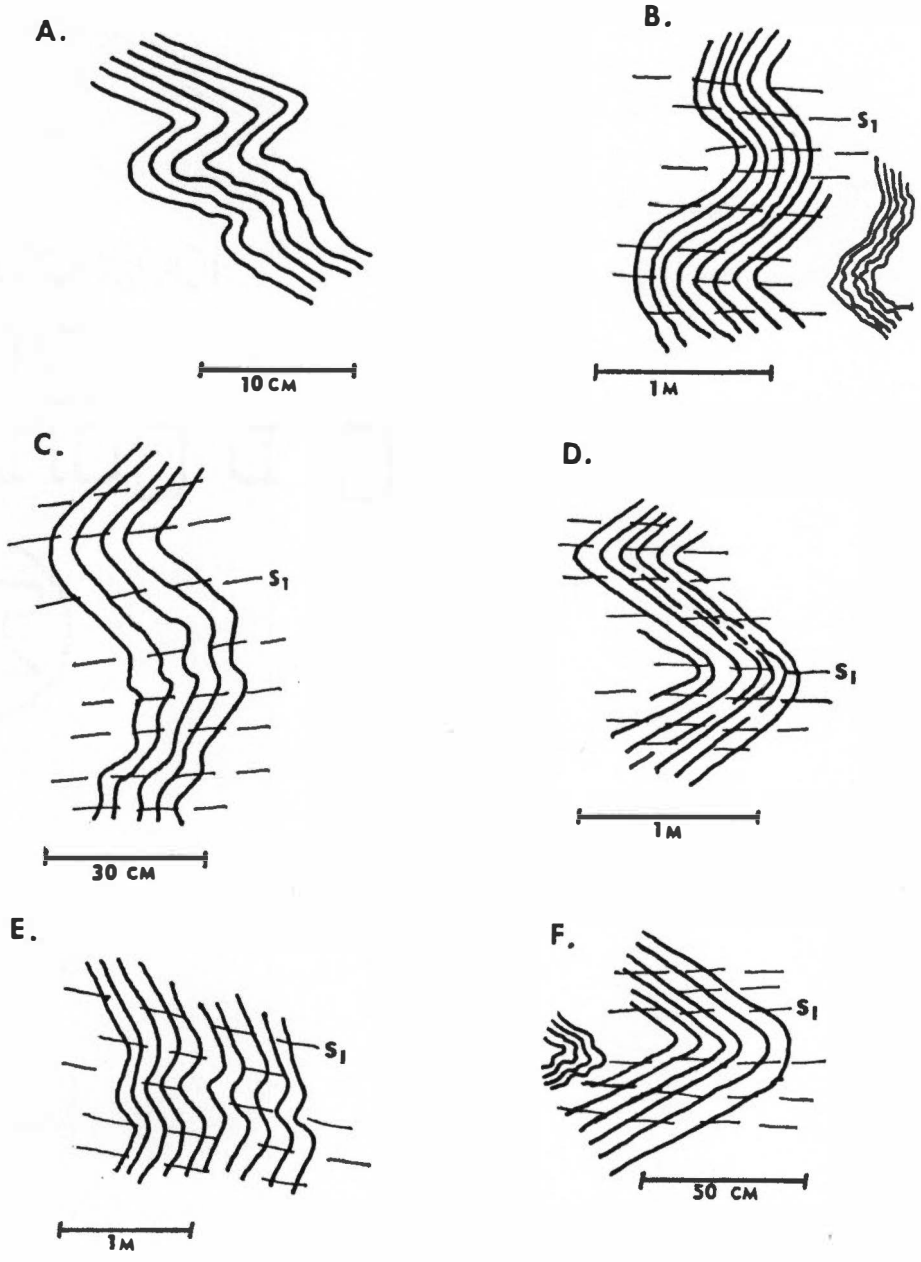

Figure 19. Mesoscopic F1 folds with S1 axial Plane slaty cleavage, Location 14 (from photographs).

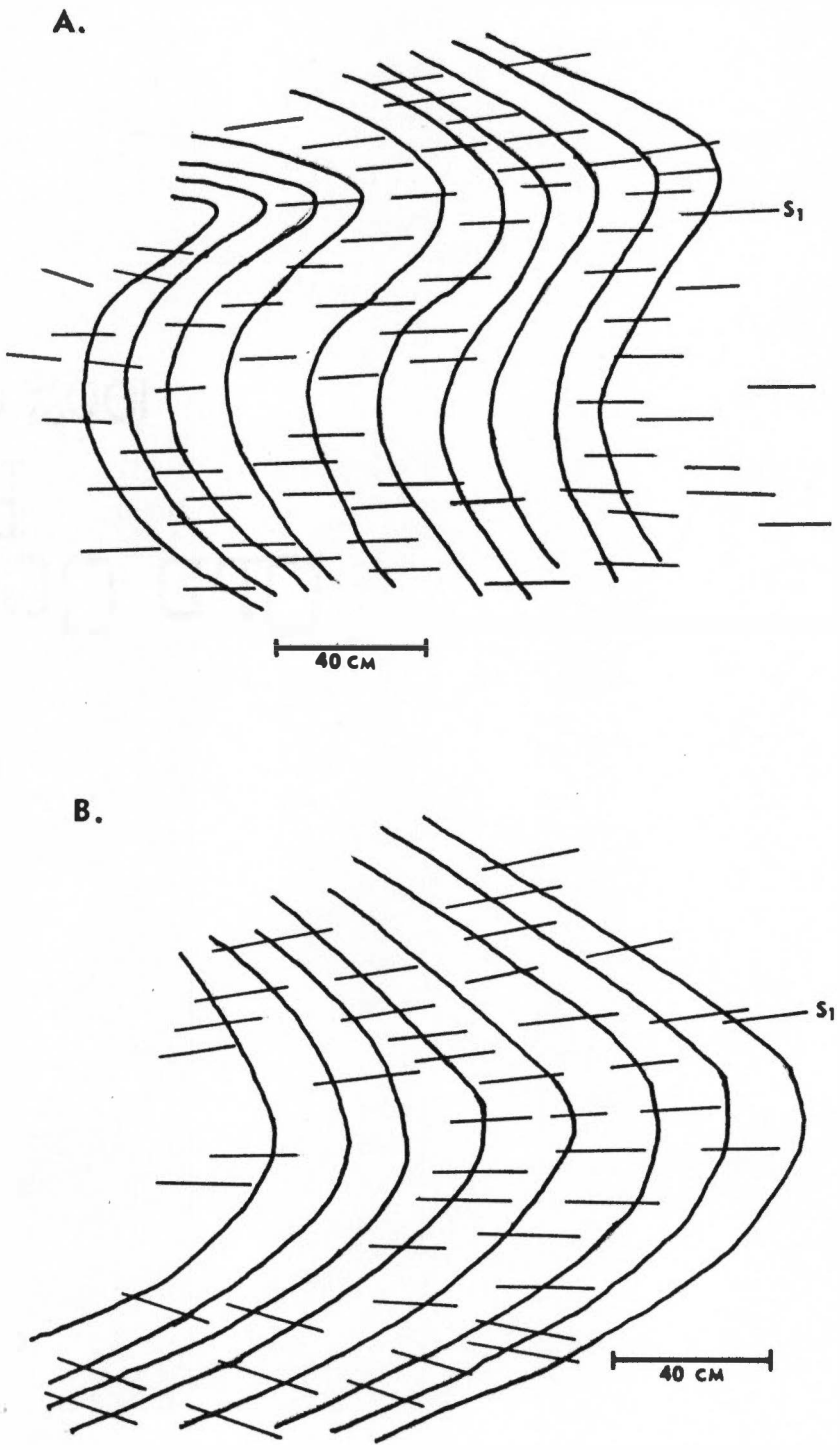

Figure 20. Mesoscopic F1 folds, Location 14 (from photographs).

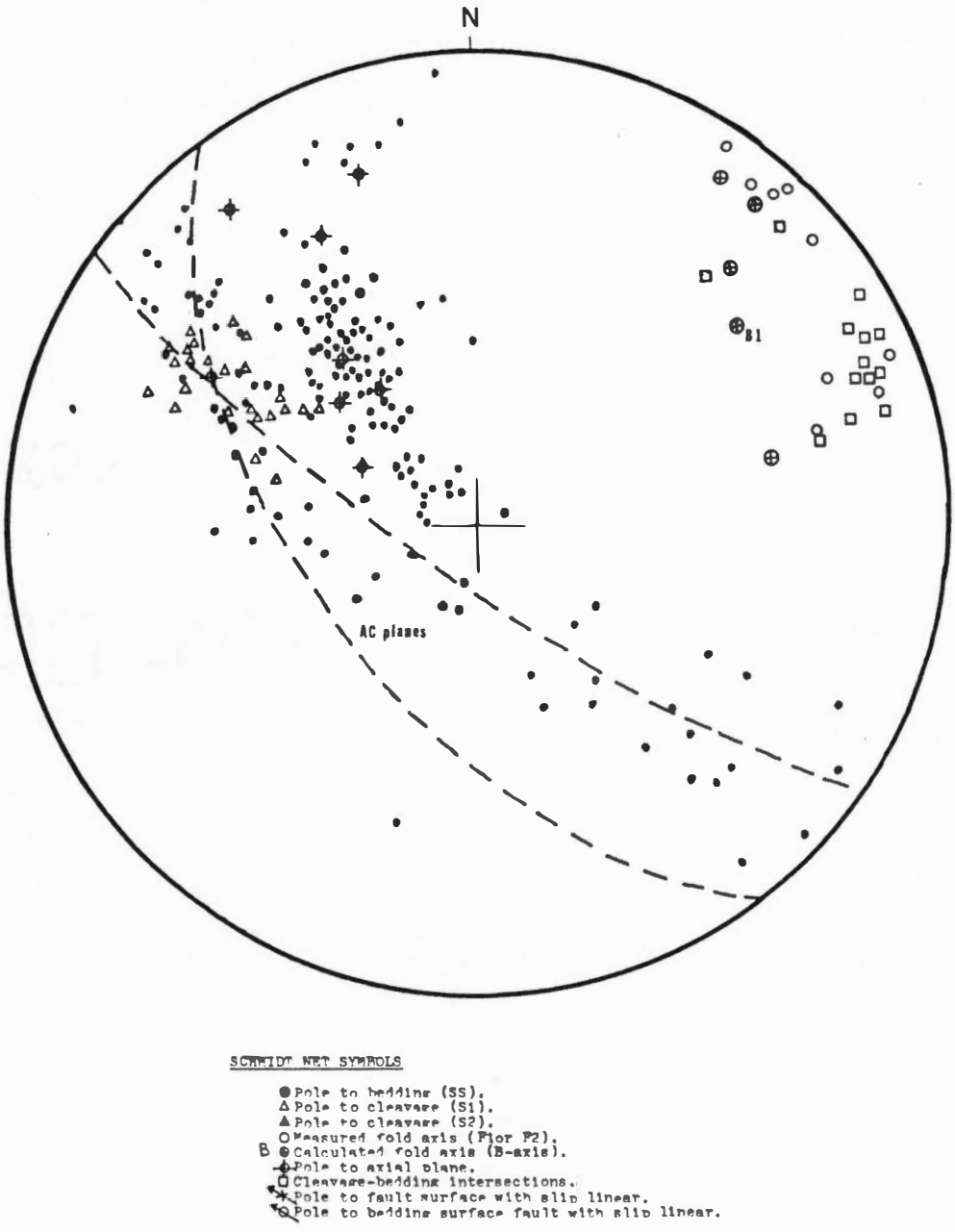

a.

Figure 21. Schmidt net: mesoscopic F1 folds, Location 14.

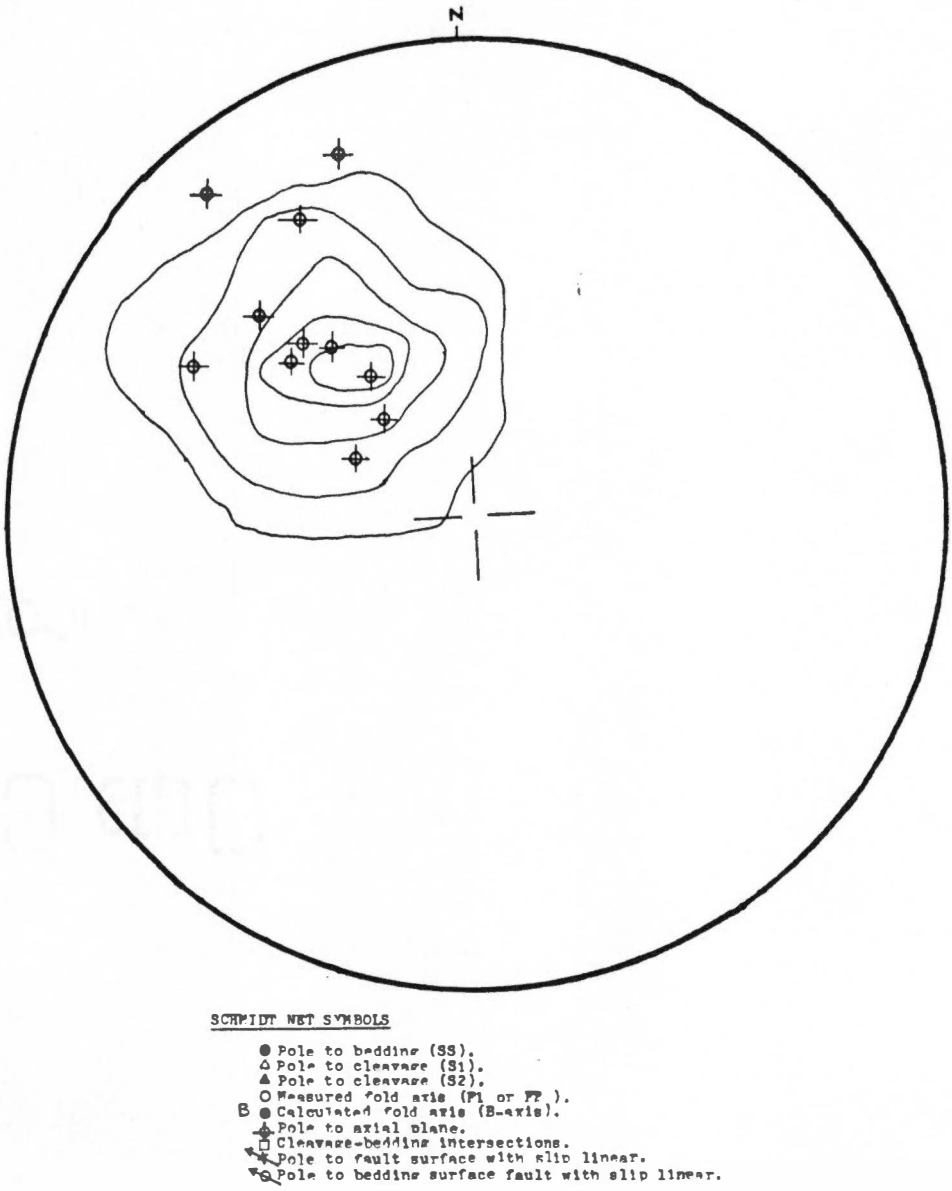

b. Eighty poles to cleavage contoured. Contours at 1, 4, 11, 18, and 25 percent.

Figure 21 (continued)

constructed π- circles. Fold axes and cleavage-bedding intersections make up a loose cluster in the northeast quadrant of the Schmidt net.

The cleavage-pole distribution is shown contoured in Figure 21B. There appears to be a large spread in cleavage orientations for this outcrop. Axial plane poles generally fall within the cleavage distribution.

Discussion. The large spread of cleavage poles in Figure 21B, and the mapped pattern of cleavage in this area, indicates that the slaty cleavage has been folded by post-F1 deformation. This will be examined in more detail in the section on F3 folds. From observation in the field, and from the stereonet analysis in Figures 21A and 21B, cleavage appears to be subparallel to the fold axial planes.

Locations 63, 65, 65A

Style of folds (Figure 22). These locations are on the Foothills Parkway, about 1.5 kilometers north of the Little Tennessee River. Folds discussed in this section are mainly in medium-grey, laminated to thin-bedded (up to 30 cm. thick) calcereous siltstone. F1 folds in these locations are generally modified parallel folds with a close interlimb angle. They have small, angular hinges

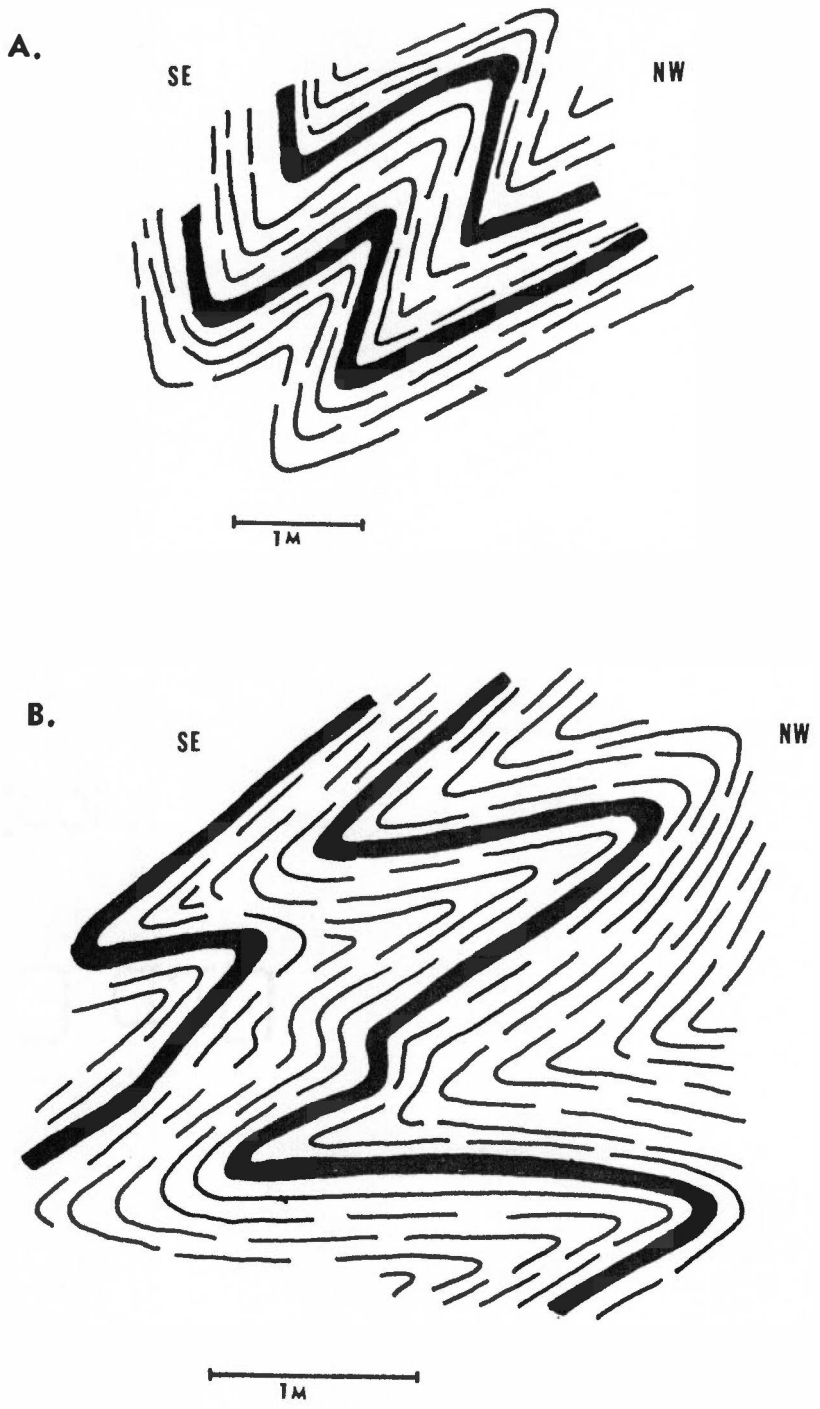

Figure 22. Mesoscopic F1 fold, Location 63 (A) and Location 65 (B)(from photographs).

and long, planar limbs, which in some places (Figures 22A and 22B) approaches a chevron fold style. At Locations 63 and 65, the slaty cleavage was observed to be subparallel to the fold axial planes.

Orientation data (Figures 23, 24, and 25). The stereonet analyses for Locations 63, 65, 65A (Figures 23, 24 and 25) shows bedding poles for small folds in these areas. Ac-planes (π-Circles) for each have been constructed. The fold axes trend northeast-southwest. Cleavage-bedding intersections at Location 63 (Figure 23) cluster around the constructed fold axis (B1). Cleavage-poles for Locations 63 and 65 (Figures 23 and 24) fall very near the ac-planes.

Discussion. These folds are believed to be F1 folds because of the subparallel orientation of the slaty cleavage to the fold axial planes and the absence of any overprinting relationships between successive cleavages. These folds have been differentiated from F2 folds because of the lack of any crenulation cleavage (S2), although the orientations of both F1 and F2 folds in this area are similar.

C. Style and Orientation of Mesoscopic F2 Folds

Introduction

In several locations, a coarse crenulation cleavage (S2) can be observed to overprint the slaty cleavage (S1).

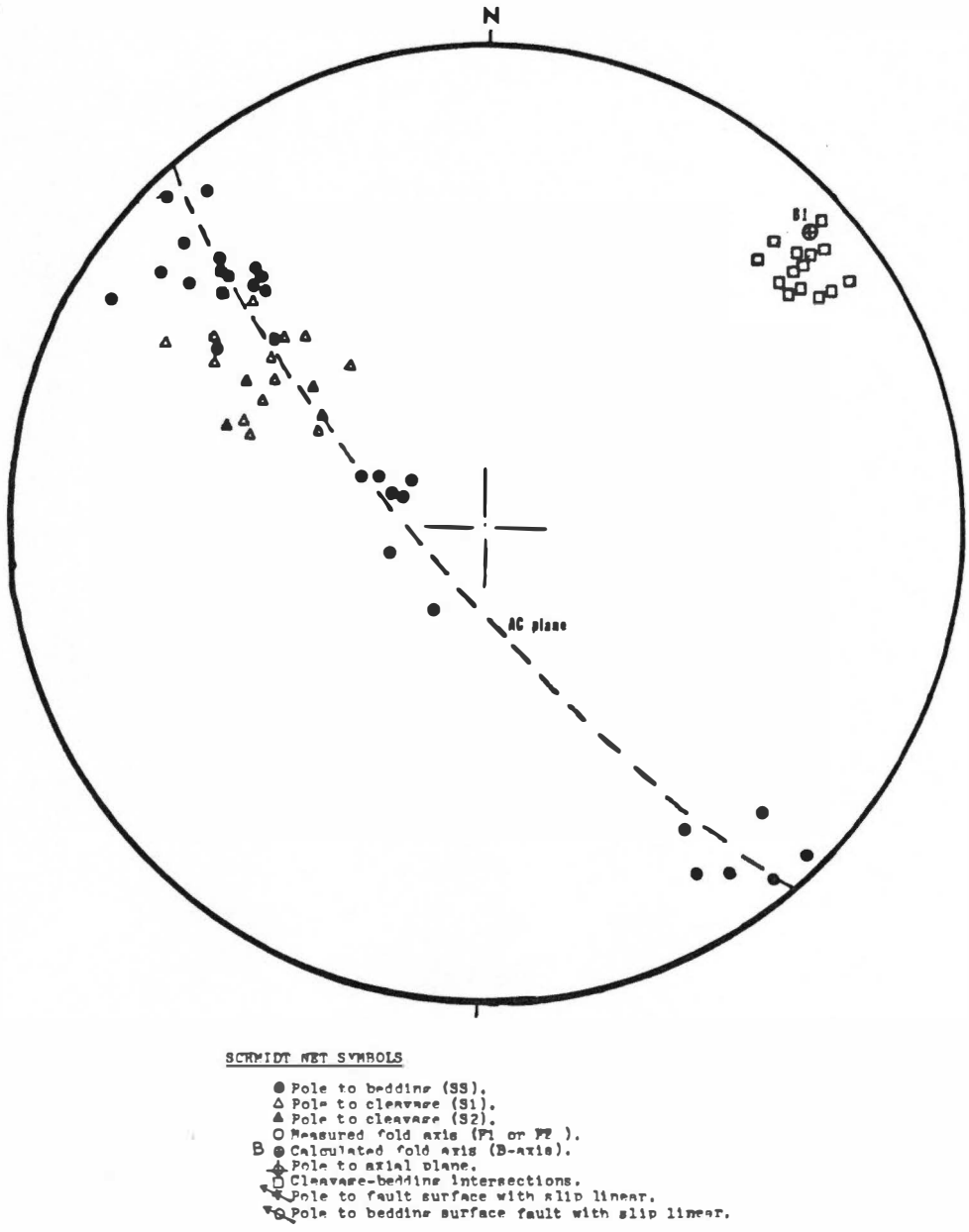

Figure 23. Schmidt net: mesoscopic F1 folds, Location 63.

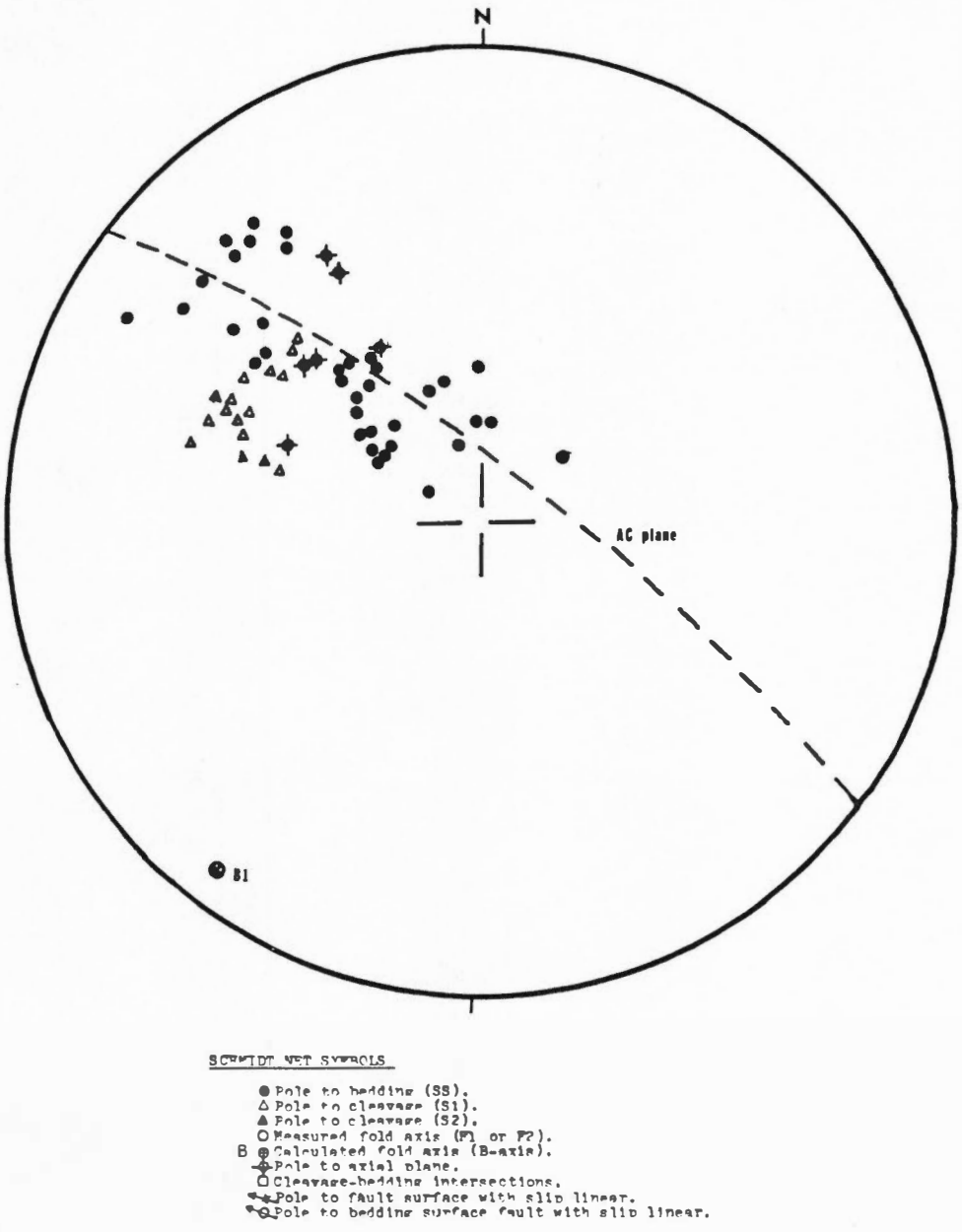

Figure 24. Schmidt net: mesoscopic F1 folds, Location 65.

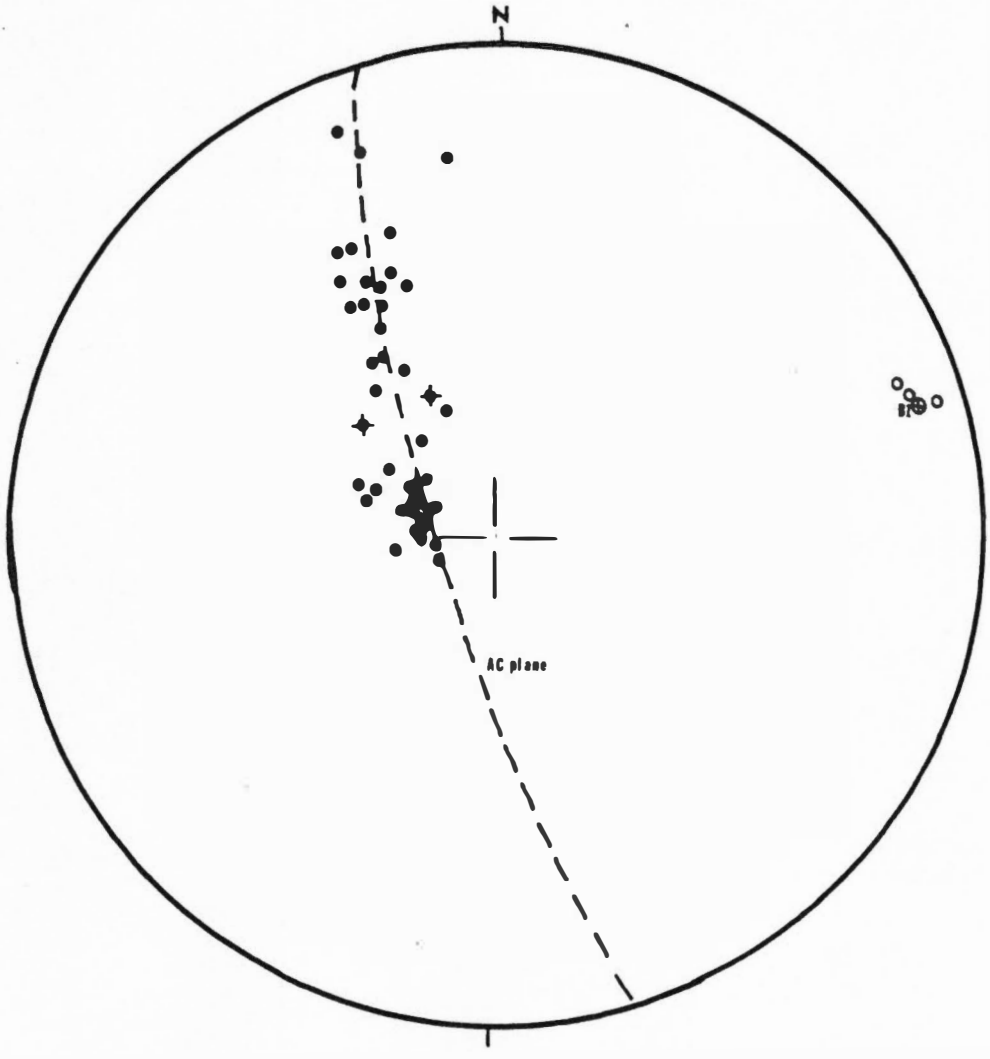

Figure 25. Schmidt net: mesoscopic F1 folds, Location 65A.

Folds in these areas, for which S2 is an axial plane foliation, postdate the F1 folds with their associated S1 axial plane foliation. F2 folds are variable in style. Both bedding and S1 have been deformed into chevron folds up to 10 centimeters in amplitude. Quartz veins and thin sandstone layers form small tight to isoclinal folds with axial planes subparallel to a well-developed foliation. At Location 9, bedding has been deformed into larger, mesoscopic folds which are believed to be F2 folds.

Location 9

Style of folds (Figures 26 to 34). Examples of S2 overprinting S1 are shown in Figures 26 and 27. In Figure 26, A and B, both bedding and an earlier cleavage (S1) have been folded into small folds by a crenulation cleavage. The crenulation cleavage is not penetrative. It occurs in discrete zones, separated by areas where no crenulations can be seen. The discrete zones are characterized by a subparallel orientation of micaceous minerals and by small-scale folding of bedding and slaty cleavage layers. Where S2 overprints S1, S2 is found to dip more steeply to the southeast. Both foliations have approximately the same strike. Faint slickensides appeared on some of the S2 surfaces in Figure 27. Relative movement on S2, as shown by the asymmetric folds of the bedding layers, is consistent throughout the crenulated area (Figures 27 and 28B).

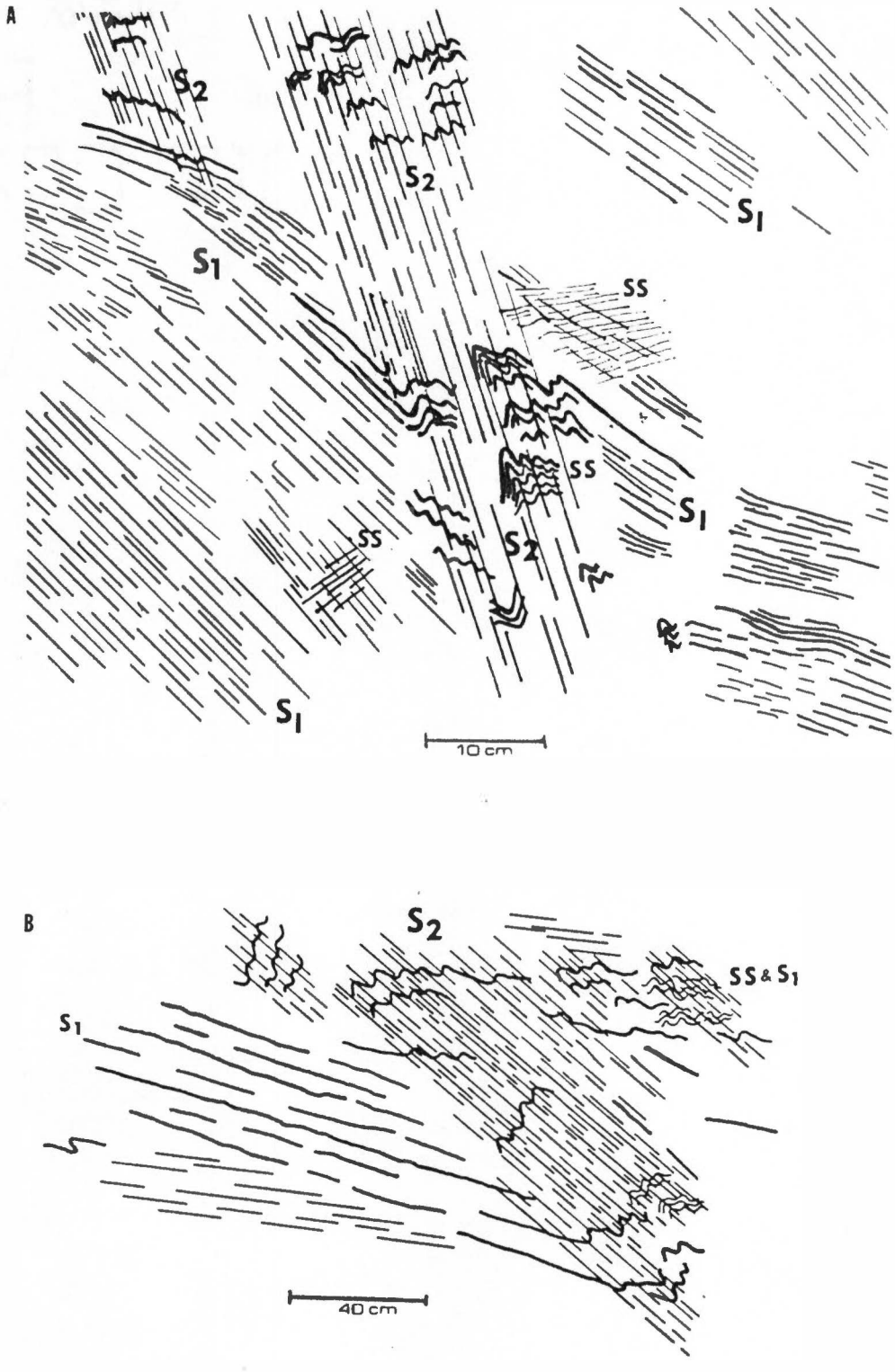

Figure 26. Mesoscopic F2 folds, where S2 crenulation cleavage overprints S1 slaty cleavage, Location 9 (from photographs).

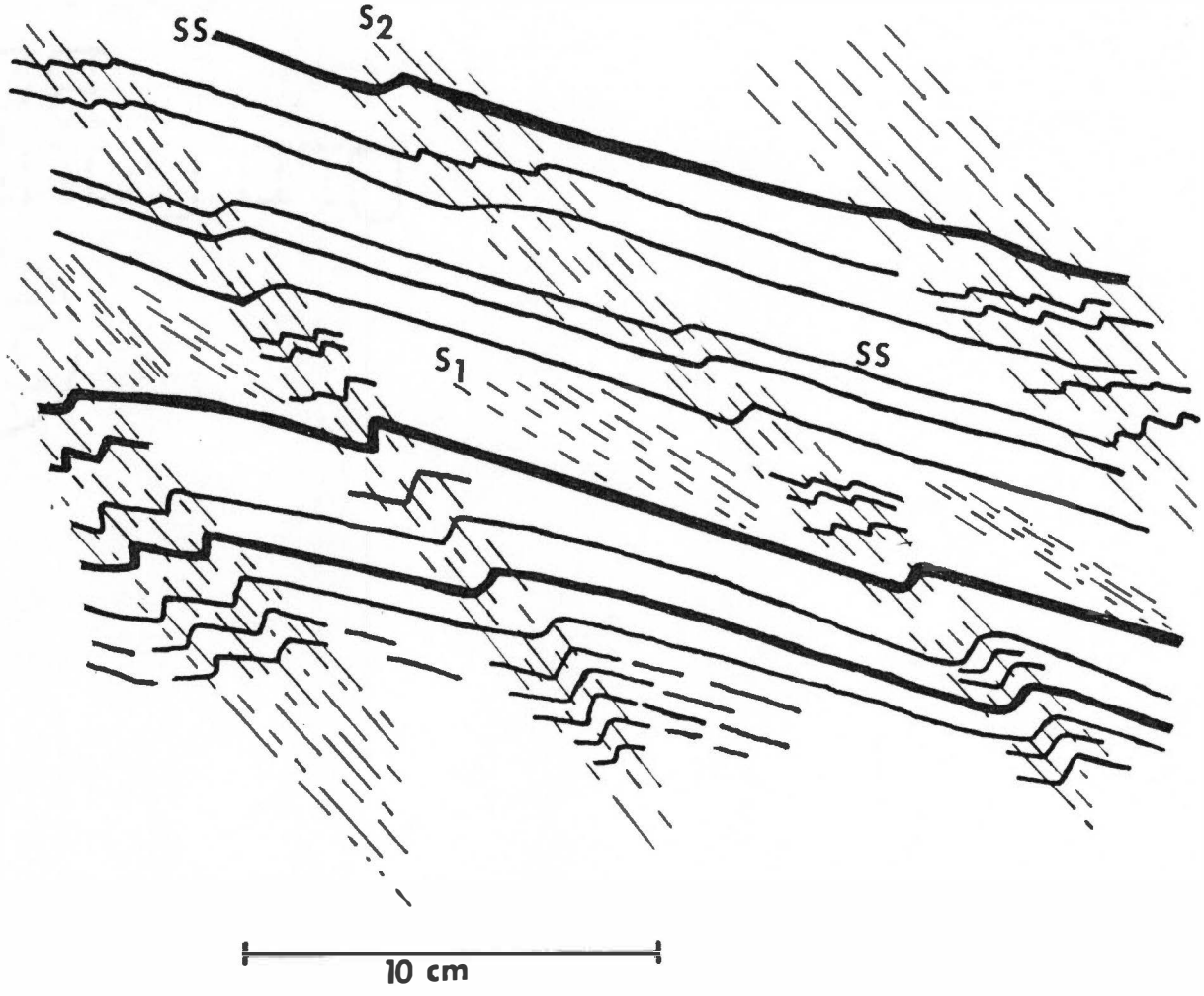

Figure 27. Mesoscopic F2 folds with S2 crenulation cleavage overprinting S1 slaty cleavage, Location 9 (from photograph).

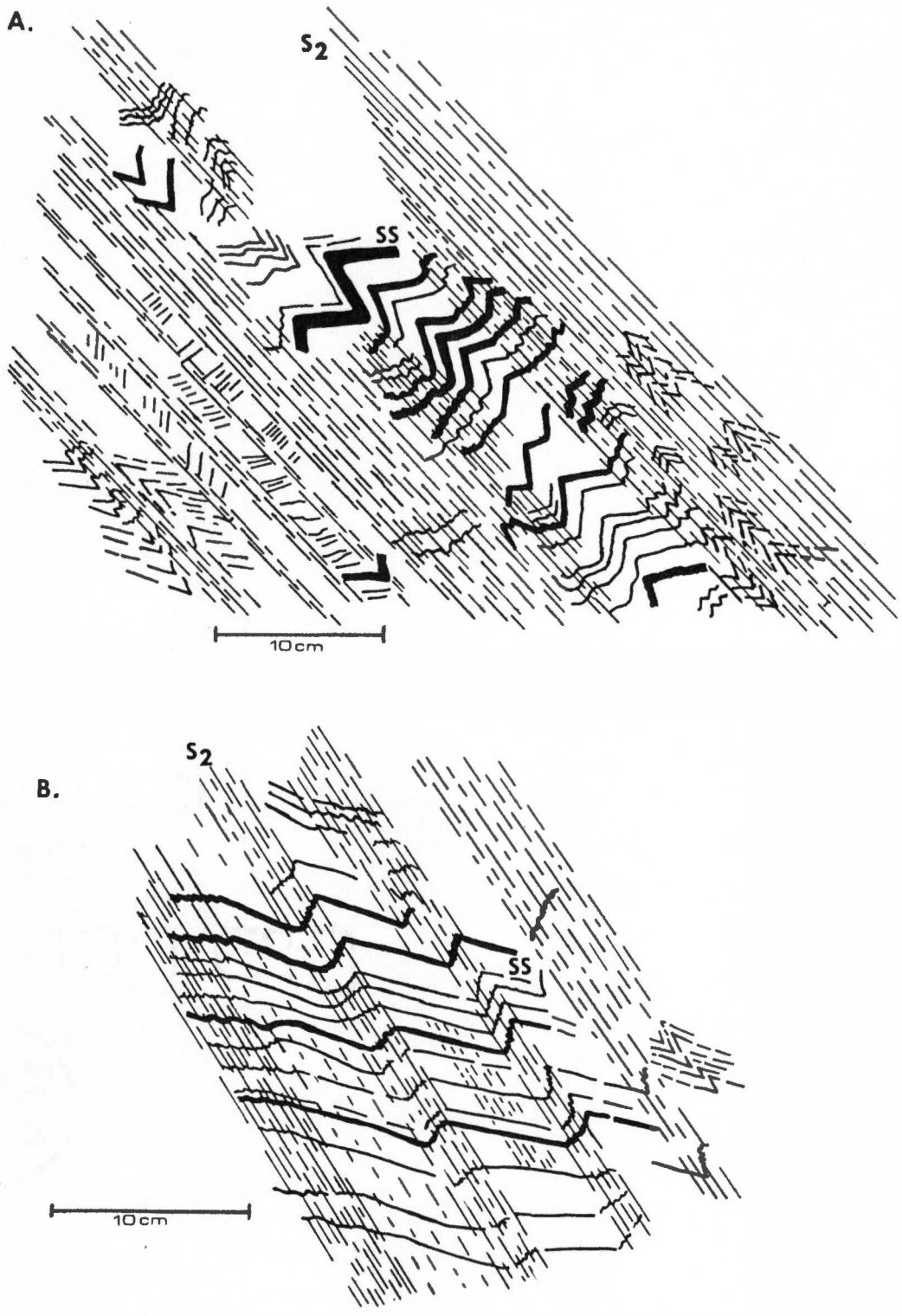

Figure 28. Mesoscopic F2 folds with S2 axial plane crenulation cleavage, Location 9 (from photographs).

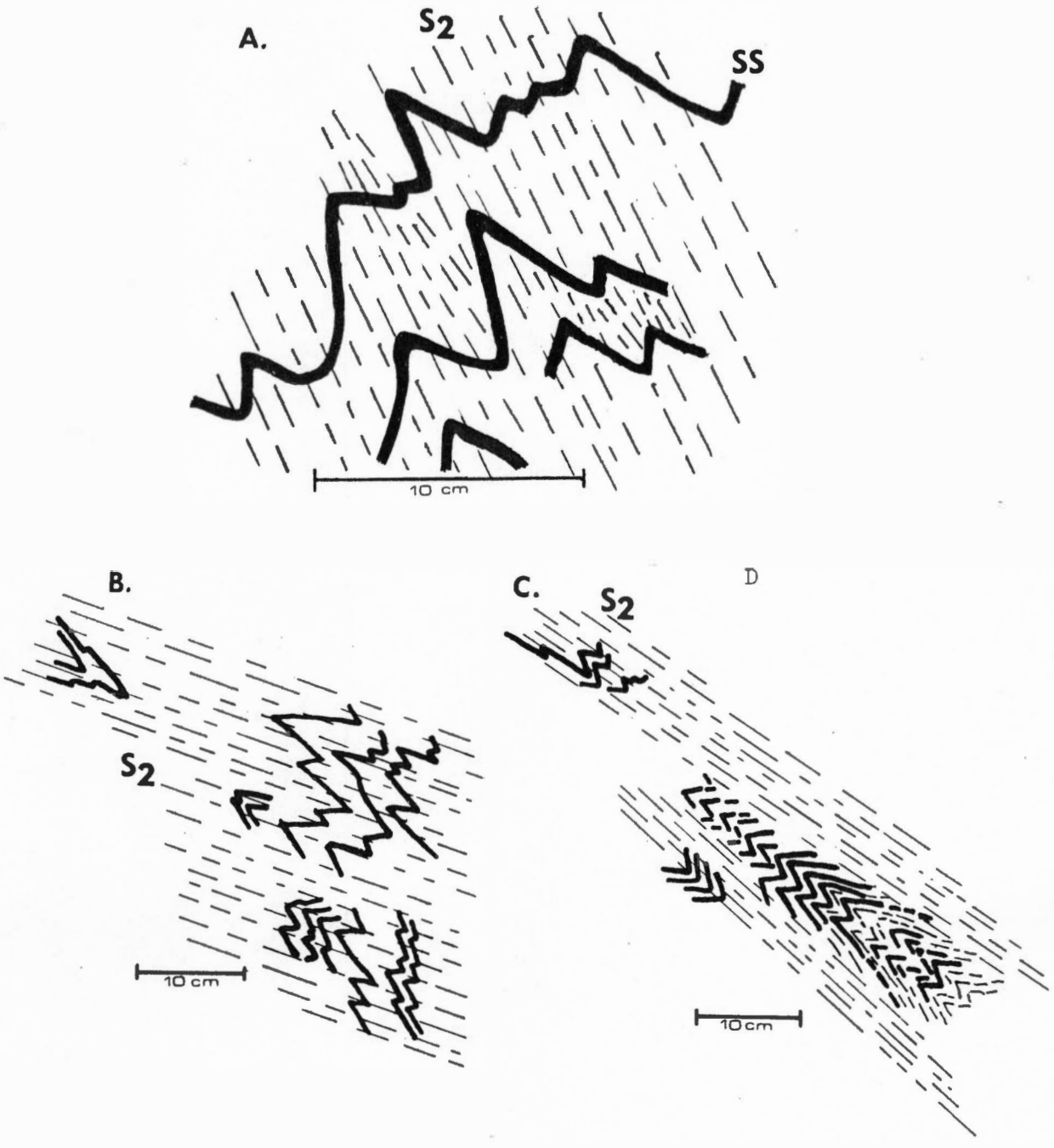

Figure 29. Mesoscopic F2 zig-zag folds with S2 axial plane crenulation cleavage, Location 9 (from photographs).

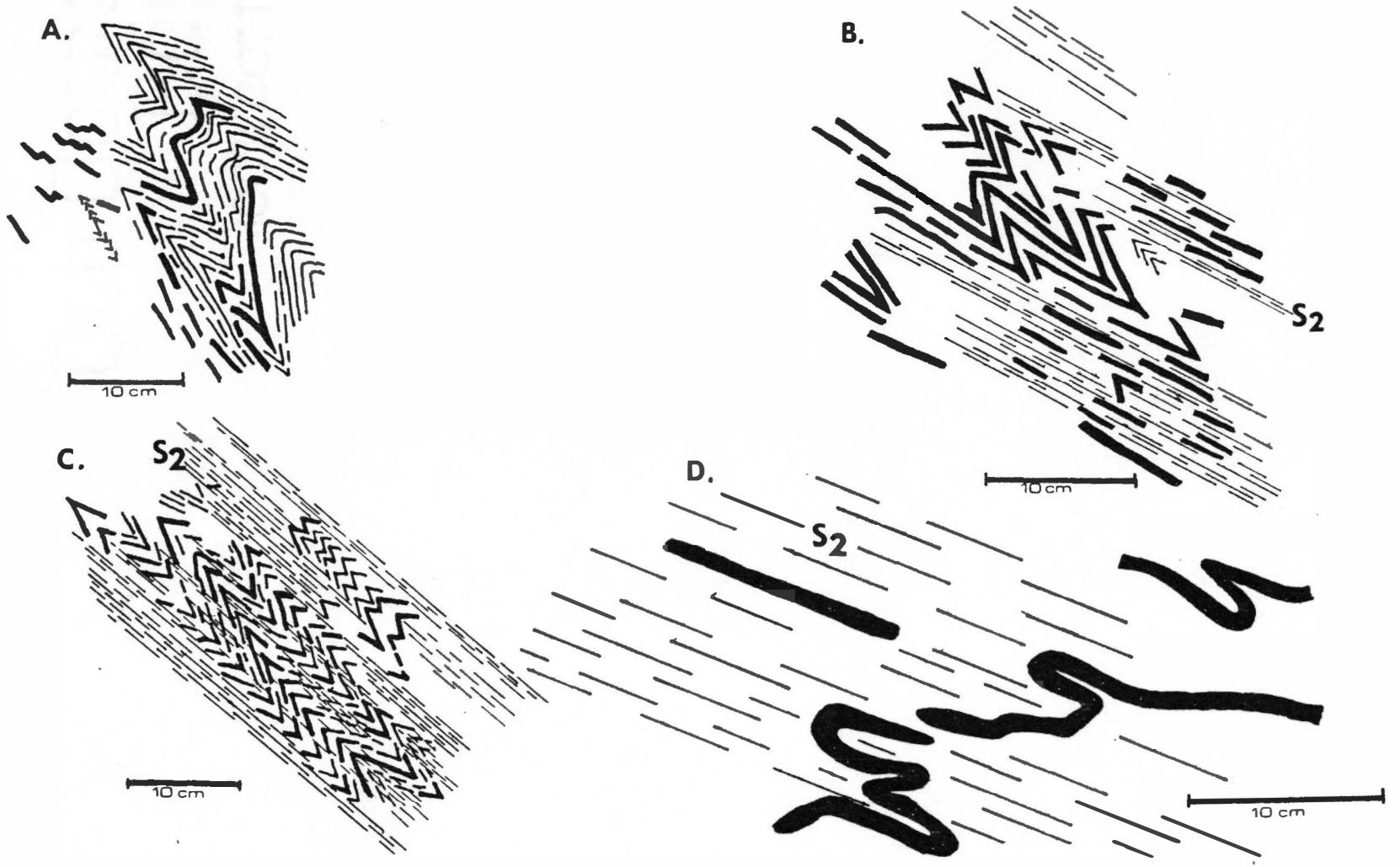

Figure 30. Mesoscopic F2 folds with boudinage of fold limbs subparallel to S2, Location 9 (from photographs).

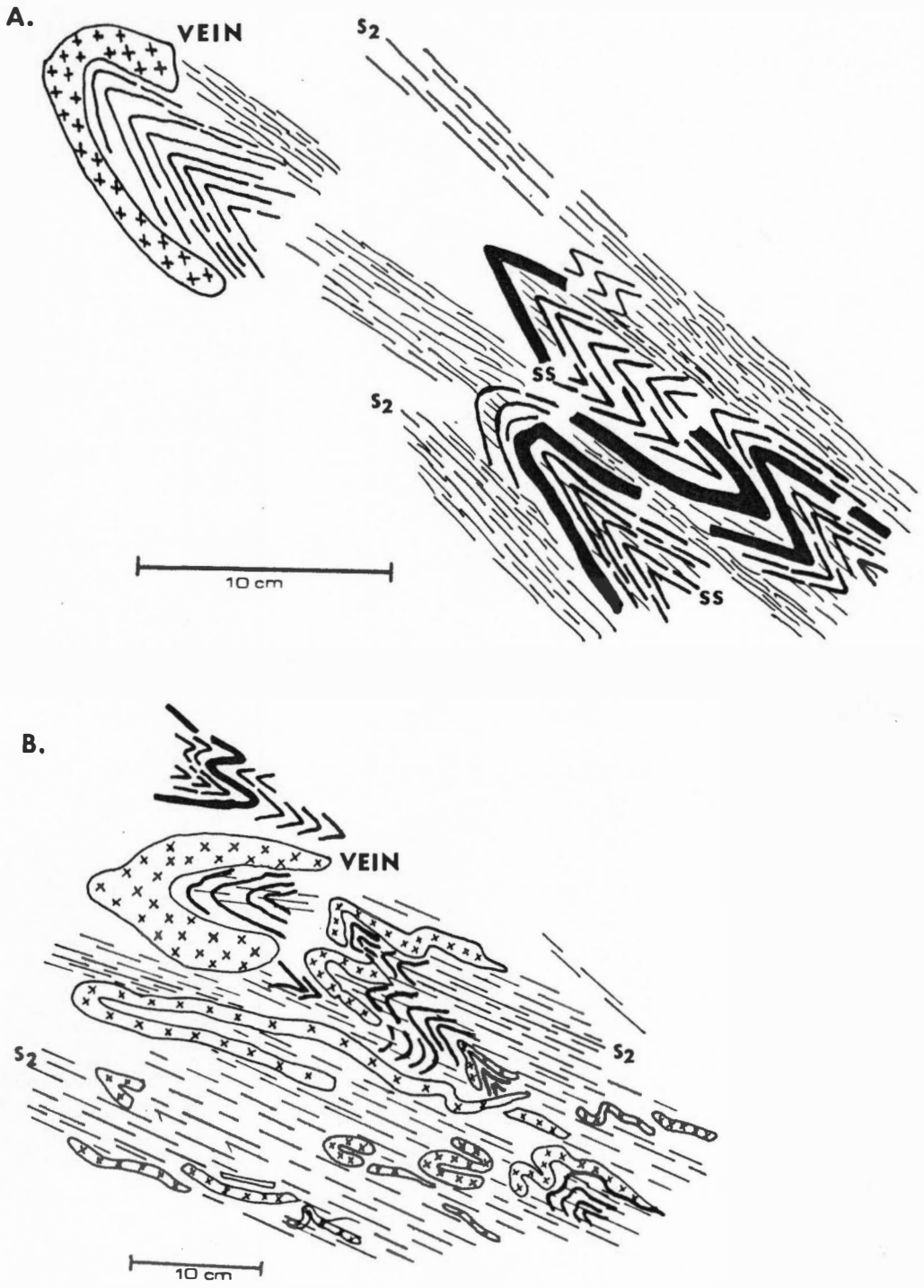

Figure 31. Mesoscopic F2 folds and S2 cleavage, Location 9 (from photographs).

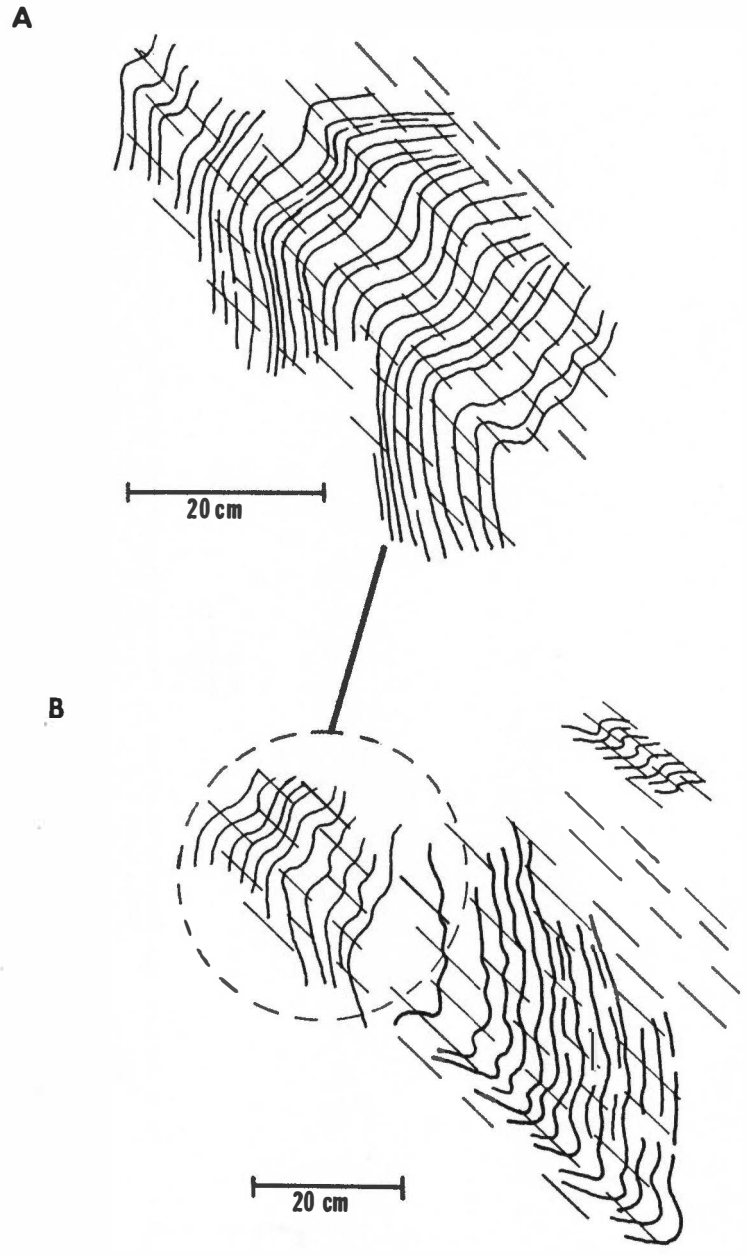

Figure 32. Mesoscopic F2 folds, Location 9, with portion shown enlarged (from photographs).

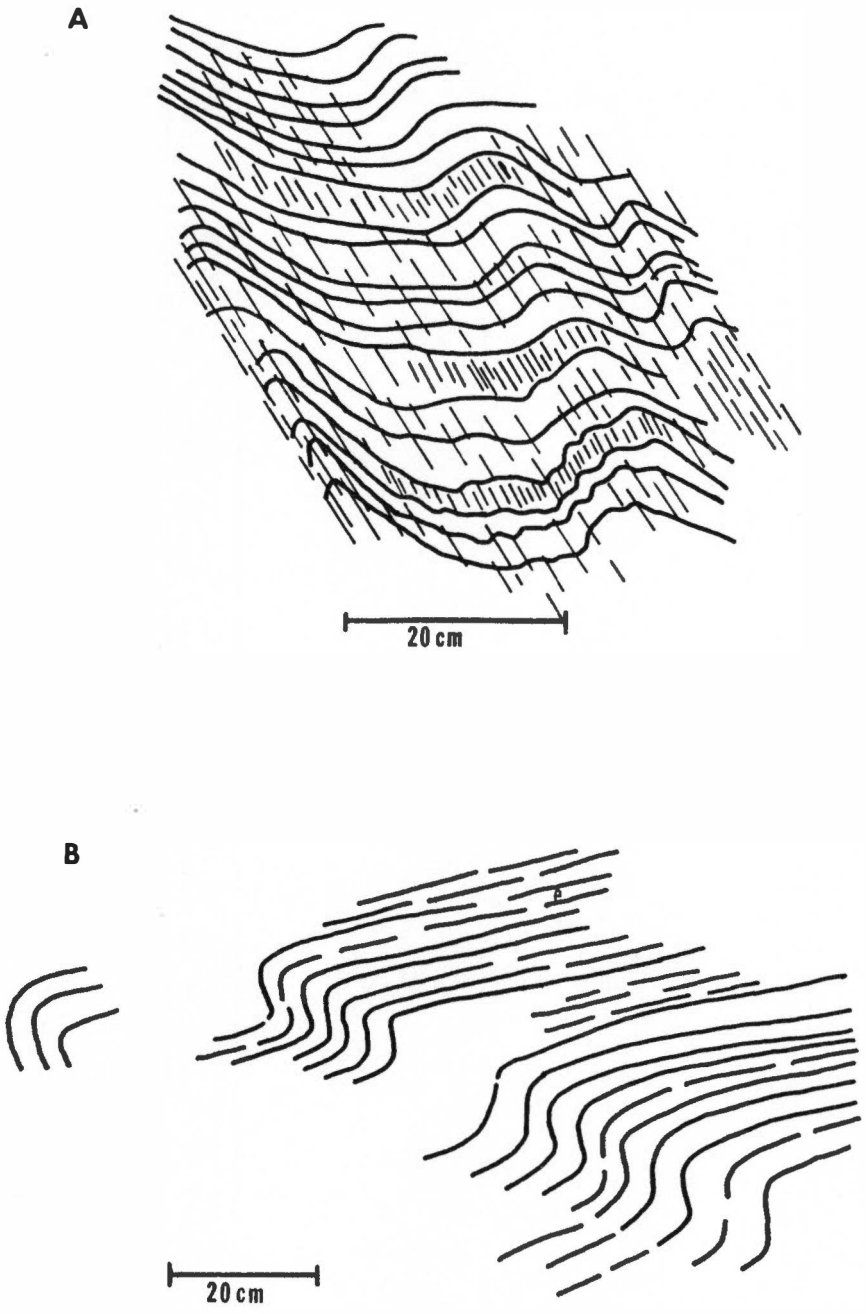

Figure 33. Mesoscopic F2 folds with axial planes sub-parallel to S2, Location 9 (from photographs).

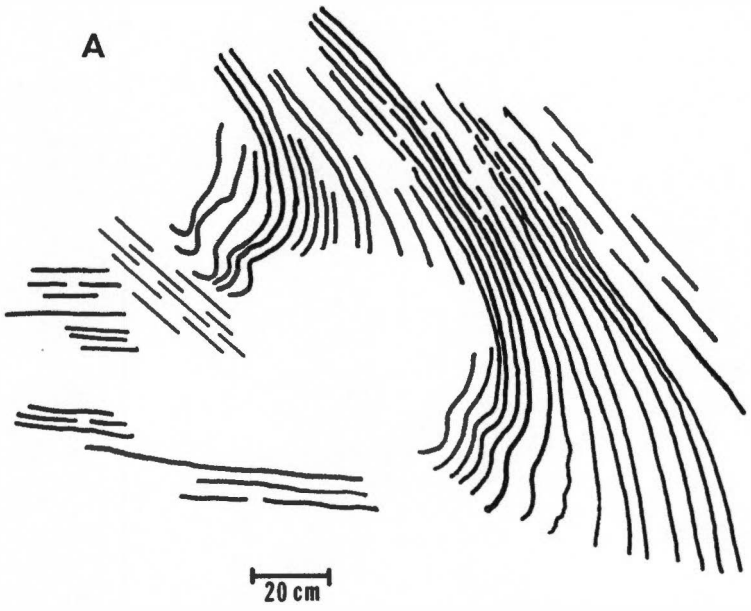

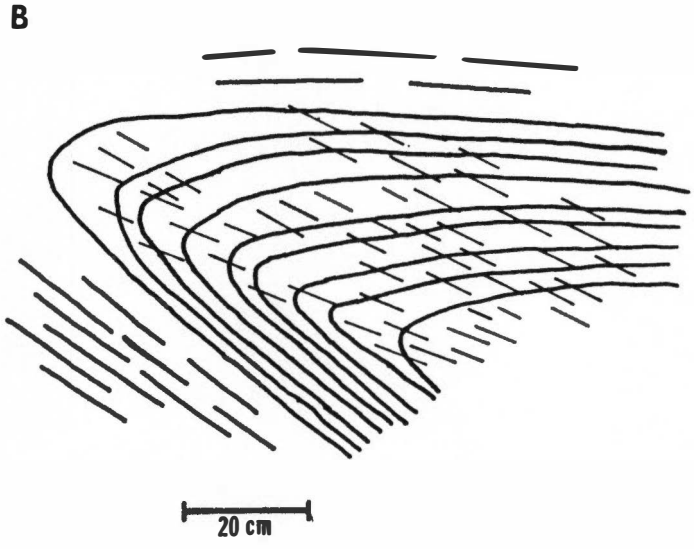

Figure 34. Mesoscopic F2 folds with S2 axial plane cleavage, Location 9 (from photographs).

Throughout most of the exposure at Location 9, the earlier S1 foliation cannot be differentiated from the S2 foliation because of the lack of overprinting evidence. A penetrative foliation defined by a preferred parallel orientation of micaceous minerals is present which is subparallel to the axial planes of mesoscopic folds. In Figures 28A and 28B, layers which are apparently bedding are crenulated in narrow zones defined by subparallel layer silicates. No earlier cleavage can be observed. This foliation, which is believed to be the S2 crenulation cleavage, grades into a parallel penetrative foliation where no crenulation can be observed.

Minor folds associated with an axial plane foliation are shown in Figures 29, 30, and 31. These folds generally have an angular zig-zag profile and show attenuation of fold limbs in zones of well-developed foliation. In some folds (Figures 30A and 30B), the hinges are drawn out in elongated bands parallel to the foliation. Small-scale boudinage occurs on some of the fold limbs, with the segmented layers oriented subparallel to the axial plane foliation.

Thin sandstone layers (Figure 30D) and quartz veins (Figures 31A and 31B) have been folded into tight to isoclinal folds with an associated axial plane foliation. Some of the layers parallel to the foliation show small-scale boudinage.

Larger mesoscopic folds are illustrated in Figures 32, 33 and 34. They are generally congruent folds with an associated axial plane foliation. It cannot be established from outcrop observation whether the foliation is S1 or S2.

Orientation data (Figures 35 to 37). Fold axes for F2 folds, where S2 overprints S1, and S2 cleavage poles are shown in Figure 35. The fold axes and axial planes for the other minor folds described are also shown. All fold axes plot in the same general area (dipping northeast) and lie on or near a great-circle corresponding to the average S2 orientation. The southeast-dipping S2 cleavage poles and fold axial planes also roughly coincide.

Figure 36 shows the contoured distribution of poles to the southeast-dipping axial plane foliation. This diagram involves cleavage where no overprinting information is available.

The orientations of fold axes, cleavage-bedding intersections, axial planes, and associated axial plane foliations for the larger mesoscopic folds are diagramed in Figure 37. Northeast-~~dipping~~ plunging fold axes lie near a great circle which depicts the average axial plane foliation orientation. Both the cleavage pole concentration and axial plane pole concentration coincide.

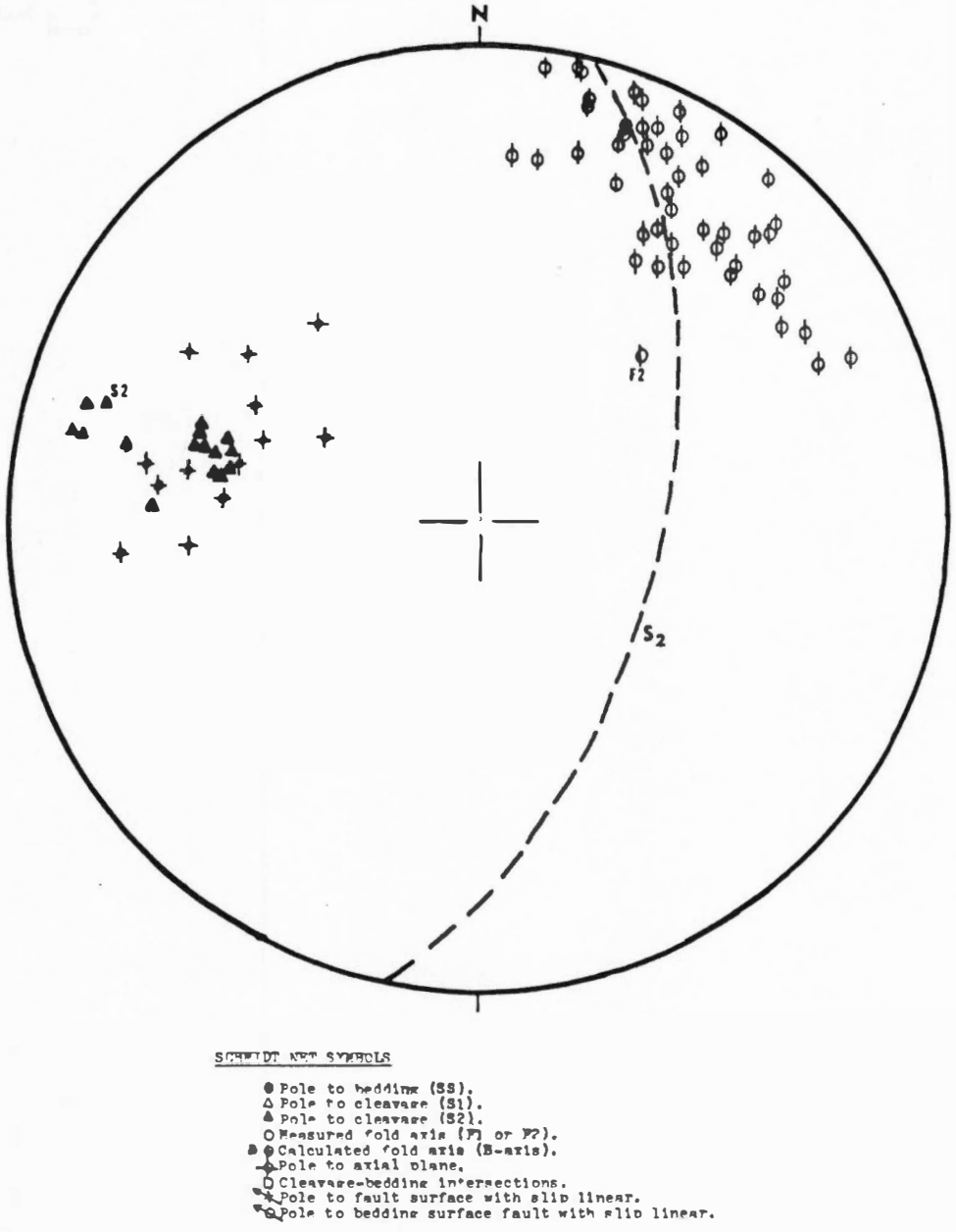

Figure 35. Schmidt net: mesoscopic F2 folds, where S2 can be observed to overprint S1, Location 9.

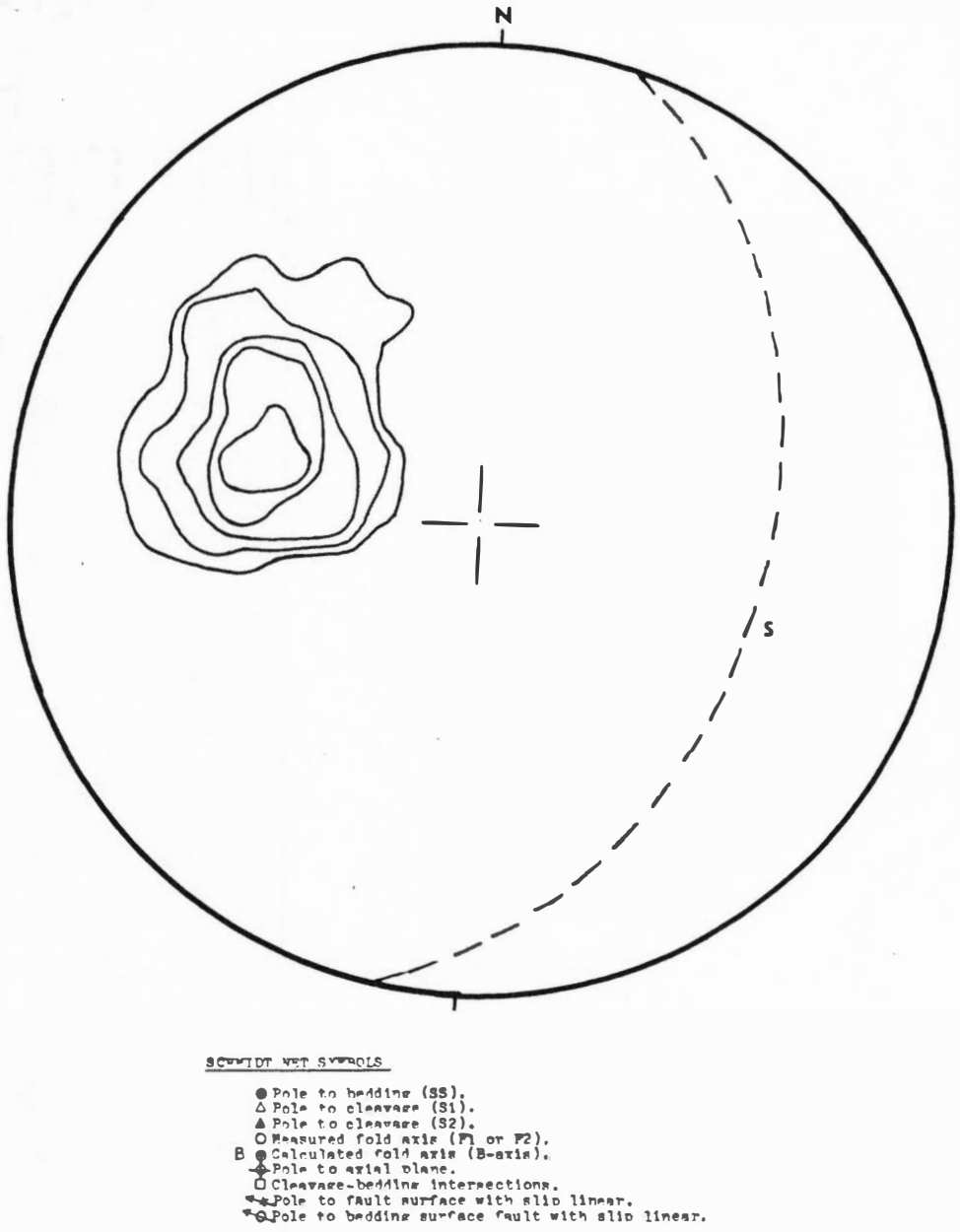

Figure 36. Schmidt net: 106 poles to cleavage contoured, where no overprinting can be observed, Location 9. Contours at 2, 4, 11, 18, and 25 percent.

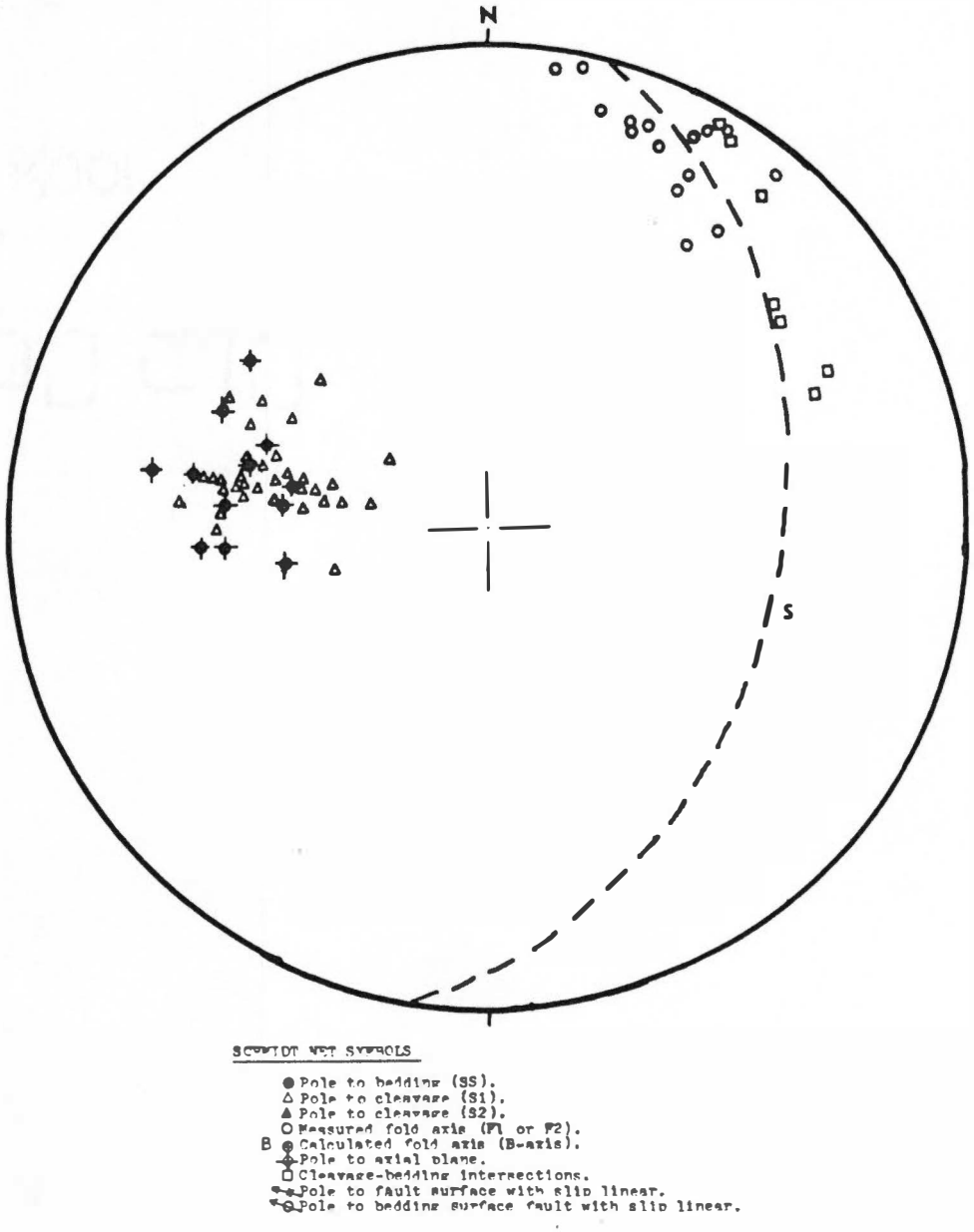

Figure 37. Schmidt net: mesoscopic folds, Location 9.

Discussion. The angular zig-zag folds (minor folds) and the larger mesoscopic folds are believed to be F2 folds with an associated S2 axial plane foliation. In Figure 35, the fold axes of the zig-zag folds are subparallel to those of proven F2 folds and their axial planes are subparallel to proven S2 crenulation cleavage. The lack of an earlier, overprinted S1 foliation could be explained by transposition of S1 into S2. Attenuation of minor fold limbs, tight to isoclinal folds, and boudinage of layers with the segmented layers parallel to the axial plane foliation are evidence that some degree of transposition has taken place (Weiss, 1972, page 9). Figure 38 shows a sequence of events which could lead to the development of transposed layering (S2) and boudinage of bedding (modified from Hobbs, Means, and Williams, 1976, page 262).

The fold axes and axial planes for the larger mesoscopic folds (Figure 37) are subparallel to those of proven F2 folds. The penetrative axial plane foliation of these folds can be seen in some areas to grade into a crenulation cleavage (S2). Rickard (1961) believes crenulation cleavage to be an intermediate stage in the transposition of a schistosity into a new direction. With increasing degree of metamorphism, recrystallization is a dominant factor and mica concentrates in the crenulation axial planes, with quartz migrating to the micro-fold crests. Cosgrove (1976) and Williams (1972)

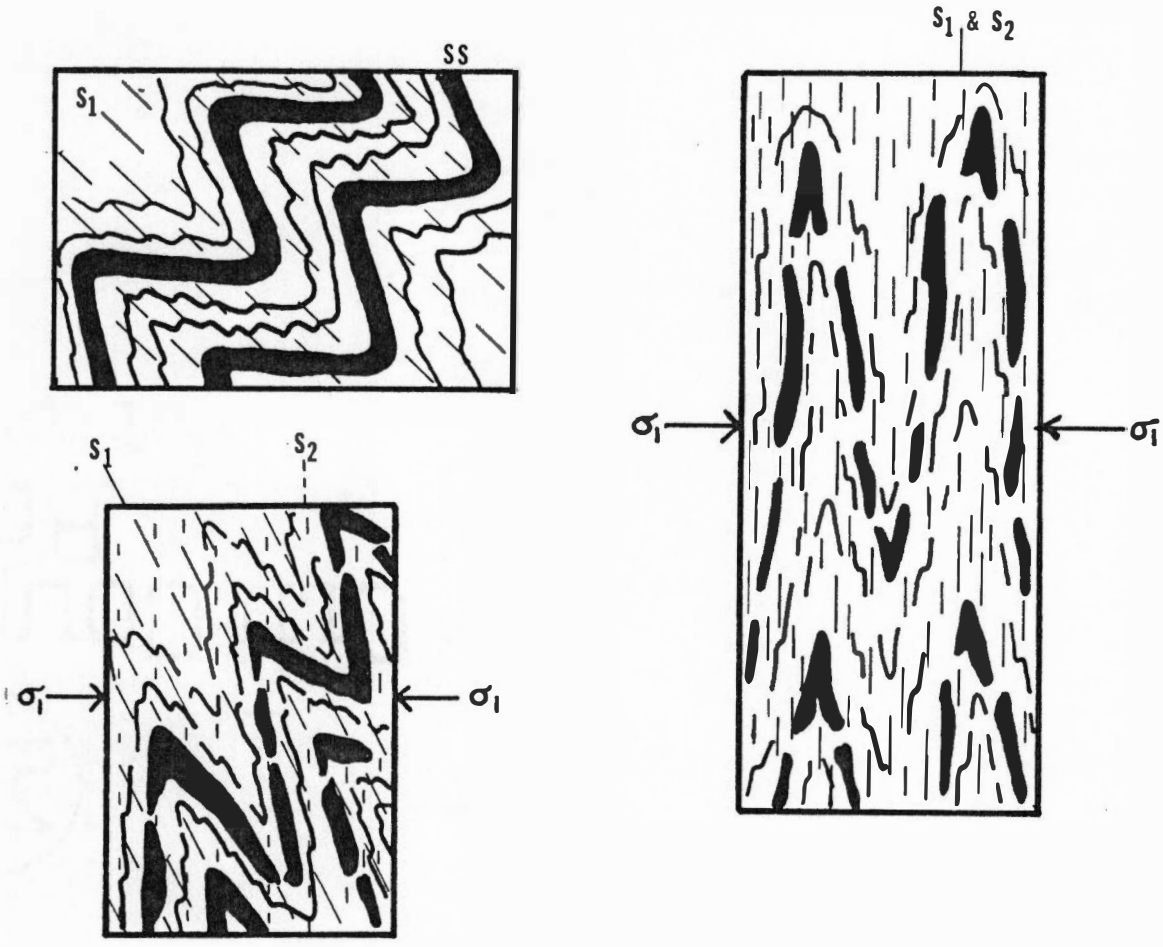

Figure 38. Possible sequence of events in the development of transposed layering (S2) and boudinage of bedding. Compression parallel to σ_1 (modified from Hobbs, Means and Williams, 1976, p. 262).

believe that the process of development of crenulation cleavage involves pressure solution and migration of quartz from the limbs of crenulations to the hinges and the external rotation of layer silicates, resulting in a high degree of preferred orientation. The same processes (selective removal of quartz and rotation) are involved in the development of other foliations, such as slaty cleavage. These foliations can grade into one another. The axial plane foliations of the mesoscopic folds are, therefore, believed to be the result of transposition of an S1 foliation into an S2 foliation and are related to the S2 crenulation cleavage.

Location 64

Fold style (Figure 39). Overprinting of foliations was recognized in a fold in Location 64 (Figure 39). Slaty cleavage, which is parallel to the bedding on one limb of the fold, can be seen refracted across sandstone layers interbedded with siltstone. This early foliation is overprinted by an S2 foliation, which is parallel to the fold axial plane. On the other fold limb, the bedding shows small crenulations.

Orientation data (Figure 40). Figure 40 shows the bedding pole distribution and constructed fold axis (B-axis)

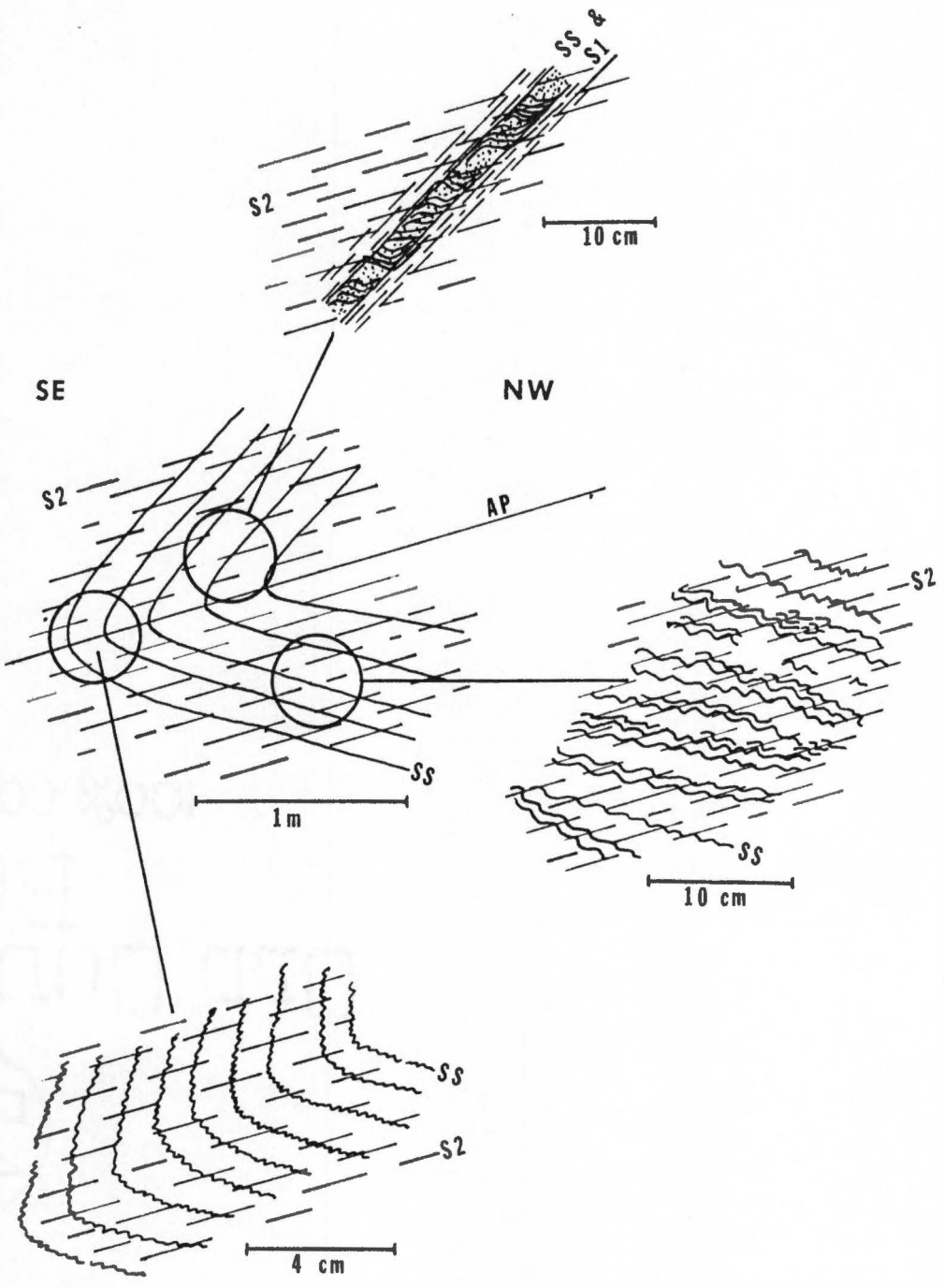

Figure 39. Mesoscopic F2 fold with S2 axial plane crenulation cleavage, Location 64 (from outcrop sketches).

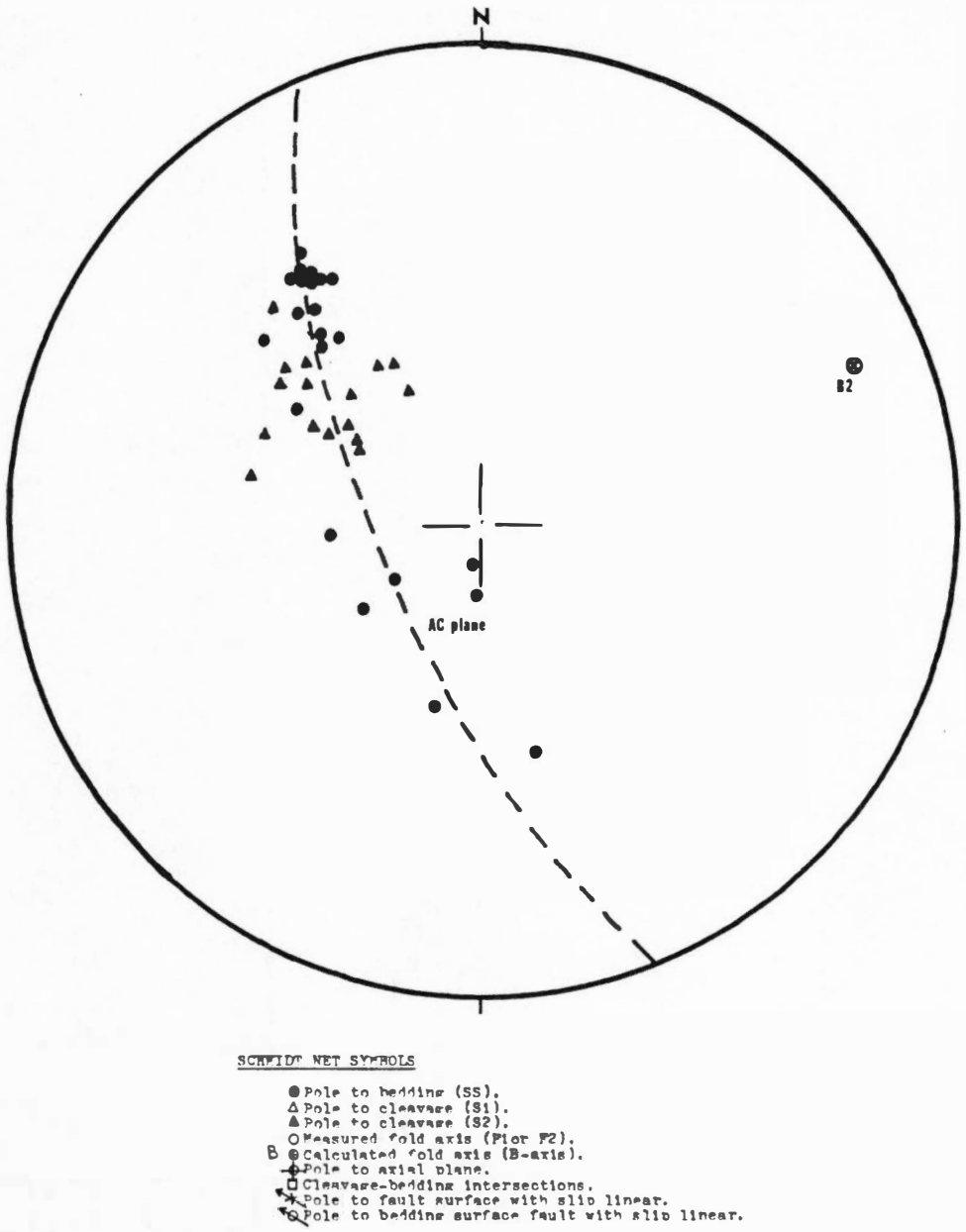

Figure 40. Schmidt net: mesoscopic F2 fold, Location 64.

for the F2 fold. Poles to S2 lie on the ac-plane constructed for the fold. Cleavage (S2) dips to the southeast and strikes northeast-southwest.

D. Macroscopic F3 Folds

Style of Folds (Figure 41)

A form surface map of slaty cleavage (S1) in the southern half of the field area (Figure 4) indicates that S1 was deformed into large folds (F3). The cleavage, which dips predominantly southeast north of Location 15, dips generally northeast from Location 17 to the Calderwood window. South of the window, S1 resumes its southeast-dipping orientation. The F3 folds consist of a synform north of Calderwood window and an antiform in the vicinity of the window.

Orientation Data (Figures 42A and 42B)

The orientations of cleavage from Location 14 to Location 12 were plotted in Figure 42A. There is a wide spread of cleavage poles with two maximums. The distribution suggests a great-circle girdle. A great-circle through the two maxima indicates a northeast-dipping π-axis of folding.

Cleavage orientations from Location 18 to Location 35 are shown in Figure 42B. A great-circle girdle through the

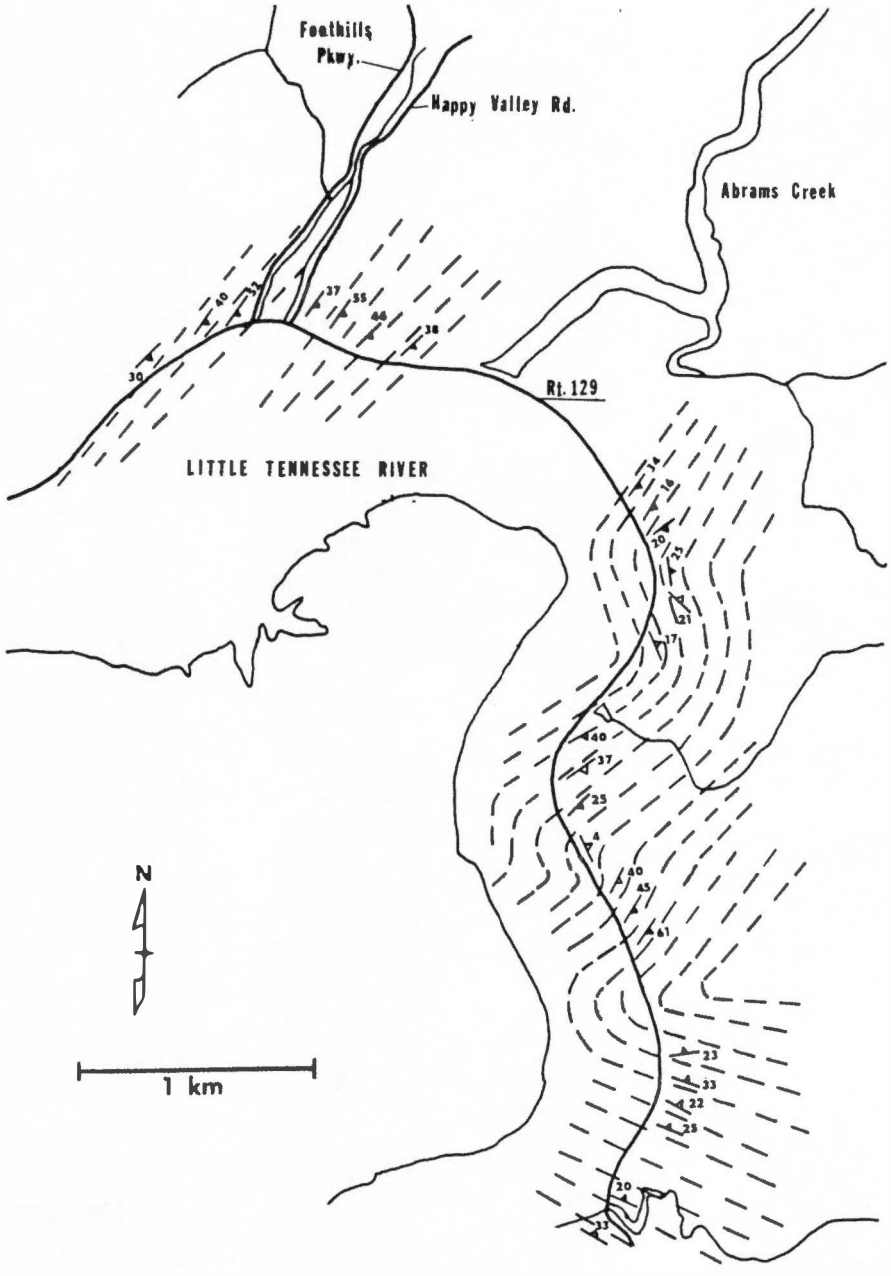

Figure 41. Form surface map of S1 slaty cleavage, showing F3 macroscopic folds.

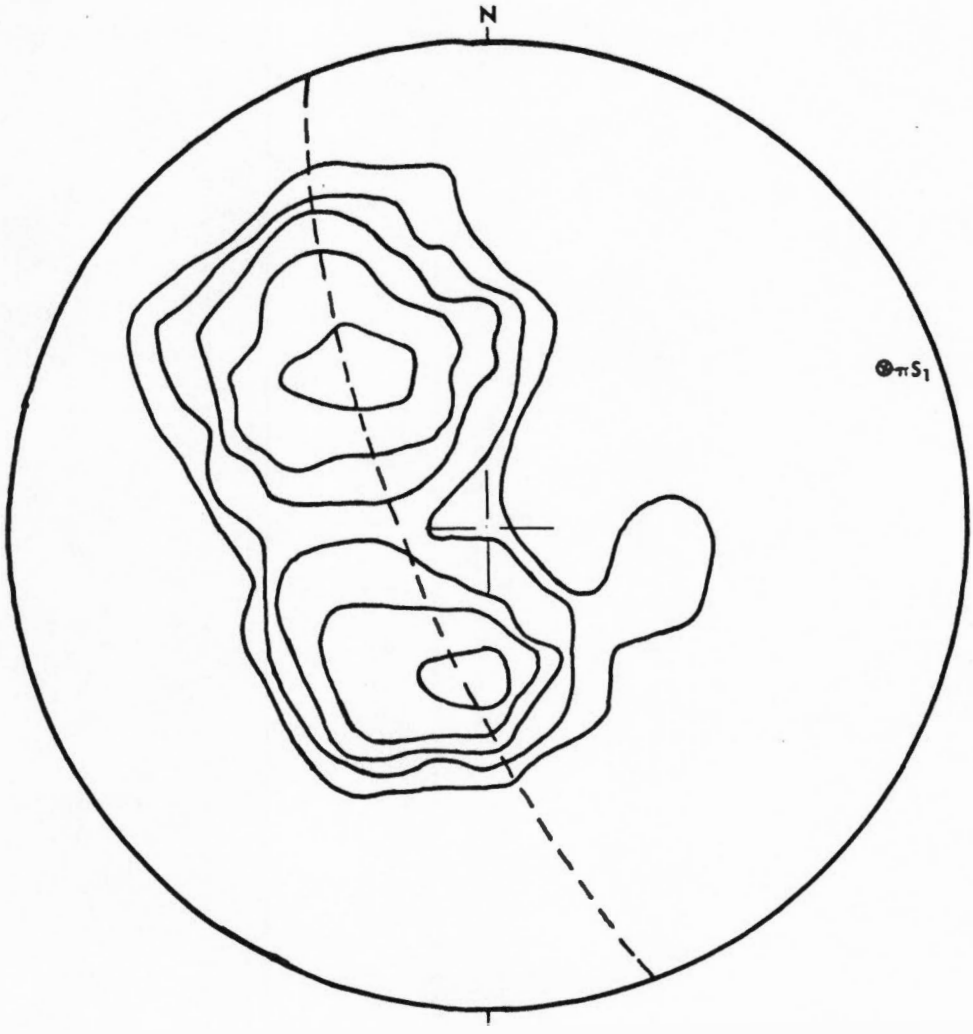

SCHMIDT NET SYMBOLS

- ● Pole to bedding (SS).
- △ Pole to cleavage (S1).
- ▲ Pole to cleavage (S2).
- ○ Measured fold axis (F1 or F2).
- ⊕ Calculated fold axis (B-axis).
- ⊕ Pole to axial plane.
- □ Cleavage-bedding intersections.
- Pole to fault surface with slip linear.
- Pole to bedding surface fault with slip linear.

a. Three hundred nineteen poles to S1 cleavage contoured. Contours at 0.33, 1, 2, 4, and 11 percent.

Figure 42. Schmidt net: macroscopic F3 folds, Locations 14, 17, and 12.

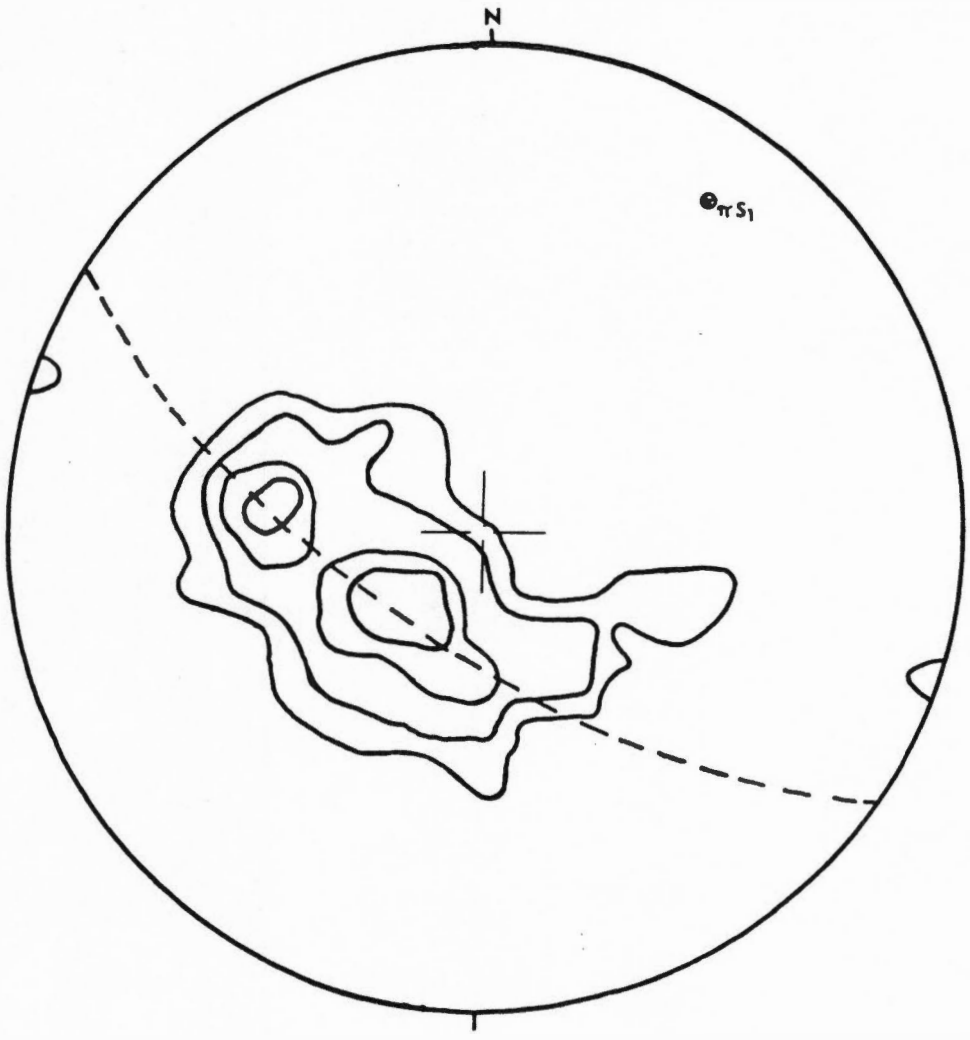

b. One hundred six poles to S1 cleavage plotted, with contours at 2, 4, 11, and 18 percent.

Figure 42 (continued)

distribution would indicate a more northerly-dipping π-axis.

Discussion

The F3 folding of the regional foliation is believed to be related to the folding of the Great Smoky fault surface. Undulations of the fault surface, with its appearance in windows such as Calderwood window, Cades Cove, Wear Cove, and Tuckaleechee Cove, suggest that folding of the fault surface has taken place. DeWindt (1975) states that a high-angle fault belonging to the Gatlinburg fault system offsets the trace of the Great Smoky fault. The F3 folds are believed to be part of this post-Great Smoky fault deformation. This relationship between F3 folding and the Great Smoky fault folding is suggested by the rotation of the S1 regional foliation into an antiformal structure in the vicinity of the Calderwood window. The S1 regional foliation is not present in Ordivician rocks of the Calderwood window or in the rocks northwest of the Great Smoky fault trace on Chilhowee Mountain. S1 is believed to be older than the Great Smoky fault. Other F3 folds suggest further undulations in the thrust fault.

If the regional foliation preceded the Great Smoky fault, then it is possible that in this field area, the

fault surface orientation and the cleavage orientation may have been related by a fairly consistent angle (Neuman and Nelson, 1965). The change in cleavage orientation may then reflect a corresponding subsurface change in the configuration of the Great Smoky fault surface. Such an interpretation has been used in the construction of the Great Smoky fault geometry shown in Plate 1.

E. Mesoscopic F4 Folds and Related Structures

Location (Figures 43 and 44)

F4 folds consists of kinks in the cleavage surfaces. All folds observed (Figures 43 and 44) show right-lateral movement. Orientation data for the F4 folds are shown in Figure 45. Axial planes dip 30-40 degrees northwest. Poles to the cleavage surfaces form a partial girdle, which indicates a northeast-dipping B-axis. Measured fold axes lie near the π-axis for the folds.

Southeast-dipping thrust faults can be observed in this location. Both bedding and cleavage are disrupted in the fault zones with drag of the cleavage surfaces indicating relative movement on the faults (Figure 46A). The thrust faults and F4 kink bands are believed to be related, as shown in Figure 46B. They appear to form a conjugate pair, with antithetic movement on the kink bands and synthetic movement on the thrust faults.

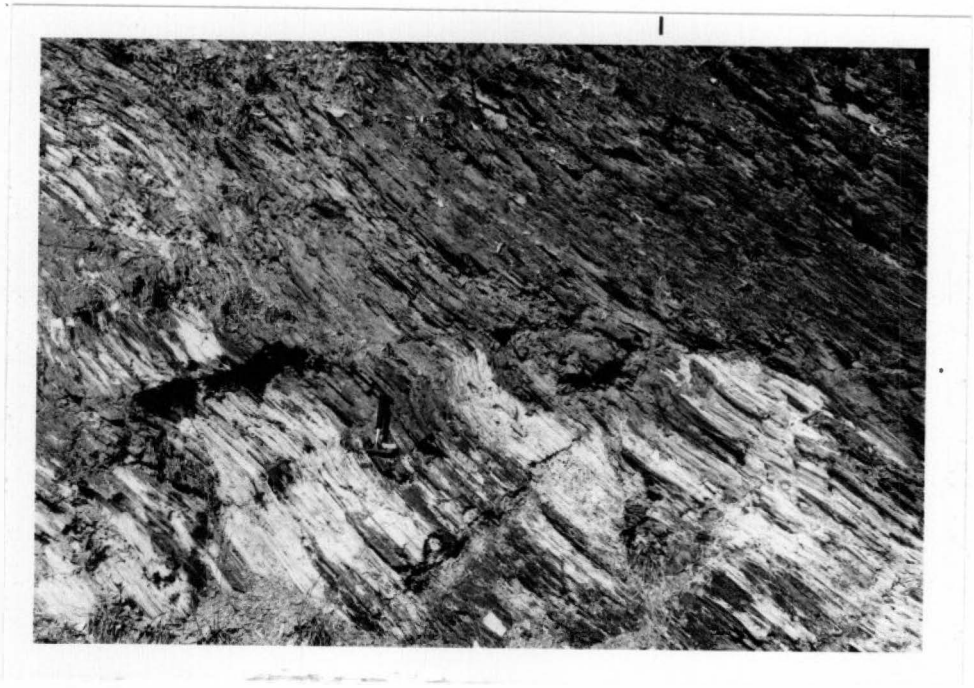

Figure 43. Mesoscopic F4 folds, Location 9. Kink-bands showing right-lateral movement, with NW-dipping axial planes.

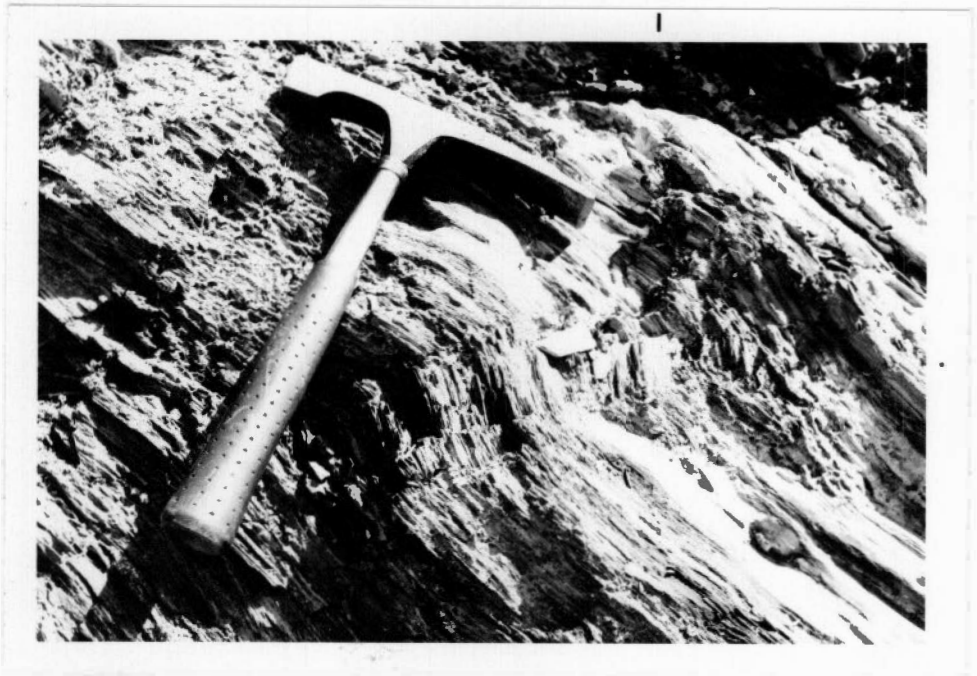

Figure 44. Mesoscopic F4 kink-bands, Location 9.

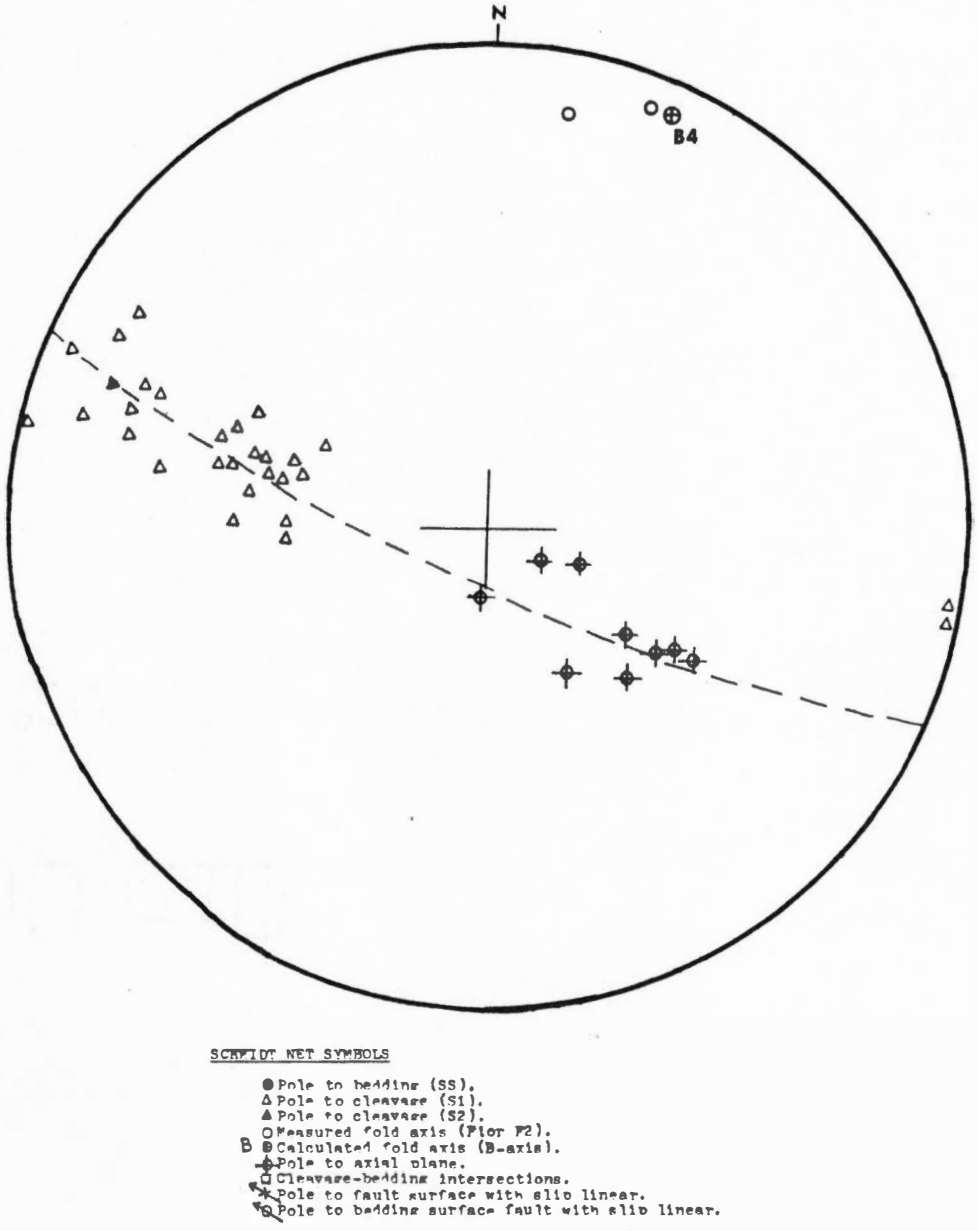

Figure 45. Schmidt net: mesoscopic F4 folds, Location 9.

a. Southeast-dipping thrust faults, Location 9. Scale equals 1 meter.

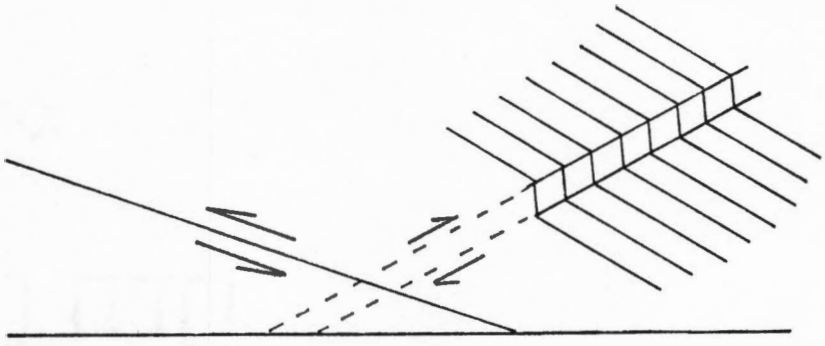

b. Relationship of mesoscopic F4 kink-bands and thrust faults, Location 9.

Figure 46. Mesoscopic F4 folds and thrust faults, Location 9.

F4 folds are believed to post-date F2 folds because they were formed by deformation of the S2 axial plane foliation in Location 9. The relative age between the F3 and F4 folds cannot be determined from direct evidence at Location 9.

CHAPTER IV

STRUCTURAL CHRONOLOGY OF THE SOUTHERN BLUE RIDGE

The Paleozoic metamorphic and tectonic events are dated presently by using the isotopic age dates of metamorphic minerals and examining the stratigraphic record in the rocks northwest of the Blue Ridge (Bryant and Reed, 1970). Close correlation between Paleozoic K/Ar and Rb/Sr ages in Blue Ridge and Piedmont crystalline rocks and the thickness of clastic deposits in the Appalachian basin were found by Hadley (1964). The earliest frequency peak of radiometric ages was about 430 m. y. (Early Silurian). These ages are believed to reflect the last time the rocks cooled below Ar-fixing temperature, rather than the date of metamorphism. This would mean that the zones of regional metamorphism in the Blue Ridge belt were established more than 430 million years ago (Butler, 1973). In a compilation of radiometric age ranges, DeWindt (1975) states that the majority of investigators conclude that the regional metamorphism of the Ocoee Series occurred during Late Ordovician time. A thick wedge (7000 feet) of Middle Ordovician clastic rocks rests disconformably on a Cambrian and Ordovician carbonate sequence. This indicates rapid deposition prior to the recorded thermal event. Roeder and Walker (1975) believe that the estimated rates of subsidence and sedimentation for

this sequence are much greater than those of modern Atlantic-type ocean basins. They suggest that this implies crustal tectonics related to a convergent plate boundary.

In a study of the Spruce Pine area in North Carolina, Butler (1973) described early tight to isoclinal mesoscopic folds which he designated F1. These folds had an axial plane foliation which consisted of a schistosity defined by a subparallel alignment of micas and other platy minerals. Butler stated that the F1 folding began before or during the early stages of regional metamorphism. The climax of regional metamorphism was later than the F1 deformation. A tentative conclusion by Butler was that the F1 isoclinal folding and the later peak of regional metamorphism are both part of the Taconic orogeny, about 430 to 470 m. y. ago. Rb/Sr and K/Ar dates on micas from pegmatites from the Spruce Pine area suggest that no middle-to high-grade metamorphism occurred after about 350-320 million years ago. Butler stated that major thrusting occurred after the main regional metamorphism and pegmatite emplacement. F3 folds in the Spruce Pine area reflect deformation in the pegmatite bodies. F3 folds in the pegmatites and in metasandstone and schist have a slip cleavage or crenulation cleavage parallel to axial surfaces. Butler speculated that F3 folding is related to emplacement of the Blue Ridge thrust sheets in Late Paleozoic time.

In a summary of structural elements in Blue Ridge rocks south of the Great Smoky Mountains, Kish et al. (1975) state that the earliest stage of folding (F1) in post-Grenville rocks consist of east-west trending, subvertical to recumbent similar folds with an axial plane cleavage or schistosity. In rocks below garnet grade, this consists of slaty cleavage. The S1 foliation dips to the southeast. F1 folds preceded the Greenbrier fault. Since metamorphic isograds cross the fault without offset, it appears that major movement on the Greenbrier fault ceased before the peak of metamorphism (King, 1964; DeWindt, 1975).

Second generation (F2) folds are open, asymmetric folds with a north-northeast trend. An S2 axial plane foliation consists of slip and crenulation cleavage. Most metamorphic porphyroblasts, including metamorphic index minerals, grew after the development of S1 schistosity but before the development of S2 slip cleavage. Two further generations of slip cleavage also postdate the peak of metamorphism.

In his study of the central Great Smoky Mountains, King (1964) described a first-generation foliation in the Ocoee Series as slaty cleavage, produced by the recrystallization of micaceous minerals. This slaty cleavage is an axial plane foliation to folds in the Walden Creek Group. King believed that the first-generation foliation and related folds were accompanied by the regional metamorphism. They would then

be Taconic structures. Metamorphic and structural discontinuities across the Great Smoky fault indicate that it postdates the regional metamorphism (King, 1964; Neuman and Nelson, 1965). Rodgers (1970) believes the Great Smoky fault, Gatlinburg and related faults are late Carboniferous or Permian.

This review of structural events in some areas of the southern Appalachians shows that at least two major episodes of deformation can be found. The first recognizable episode involves the formation of early "similar"-type folds with slaty cleavage as an axial plane foliation, regional metamorphism, and thrusting on the Greenbrier fault. This early deformation is believed to be representative of the Taconic orogeny (430 to 470 m.y. ago).

A second episode of deformation involved the formation of folds with a crenulation or slip cleavage axial plane foliation, emplacement of the Great Smoky and Blue Ridge thrust sheets, and faulting of the Gatlinburg fault system.

This sequence of structural elements in the southern Appalachians can be adapted to the area of this report (Table 2). Early Fl folds with a slaty cleavage axial plane foliation (Sl) are overprinted by F2 folds with a crenulation cleavage axial plane foliation (S2). The Fl folds are believed to belong to the early period of deformation and the regional metamorphism of Taconic age. The F2 folds

probably belong to the second episode of deformation and are related to the Late Paleozoic thrust faulting. F3 and F4 folds postdate the Great Smoky fault, but may still belong to this second period of deformation.

TABLE 2

CHRONOLOGICAL SEQUENCE OF STRUCTURAL ELEMENTS

Taconic Orogeny (Middle to Late Ordovician)	
	Greenbrier fault thrusting. Regional metamorphism. F1 folds with slaty cleavage axial plane foliation.
Allegheny Orogeny (Late Carboniferous to Permian)	
	Great Smoky fault thrusting with associated Miller Cove fault and other splays. F2 folds with crenulation cleavage axial plane foliation.
	Macroscopic F3 folds.
	Mesoscopic F4 folds and related thrust faults.

CHAPTER V

DISCUSSION OF CROSS-SECTION

Plate 1 is a northwest-southeast cross-section through the field area. The lack of key beds and an accurate stratigraphy of the Wilhite Formation makes determination of the macroscopic structures difficult. Macroscopic F1 fold styles are believed to be reflected by the mesoscopic F1 fold styles, however, and this interpretation was used in the construction of the cross-section. Many of the mesoscopic F1 folds are overturned folds. This mesoscopic geometry and overturned strata at Locations 12, 15, and 8 suggests the existence of macroscopic overturned folds. The greater variability of bedding orientations over shorter intervals in the northern half of the cross-section suggests folds of smaller amplitude than those south of Location 15.

The orientations of the macroscopic F1 folds are believed to change going northwest from the Calderwood window uplift. Nearly recumbent macroscopic F1 folds on the northwest flank of the uplift are rotated so that their axial planes dip more steeply northwest around Location 17. Figure 47 is a stereonet of bedding from Locations 15, 16 and 17. A great circle through the bedding pole distribution indicates a northeast-dipping fold axis. Cleavage poles from Location 17 fall on this great circle, suggesting that the

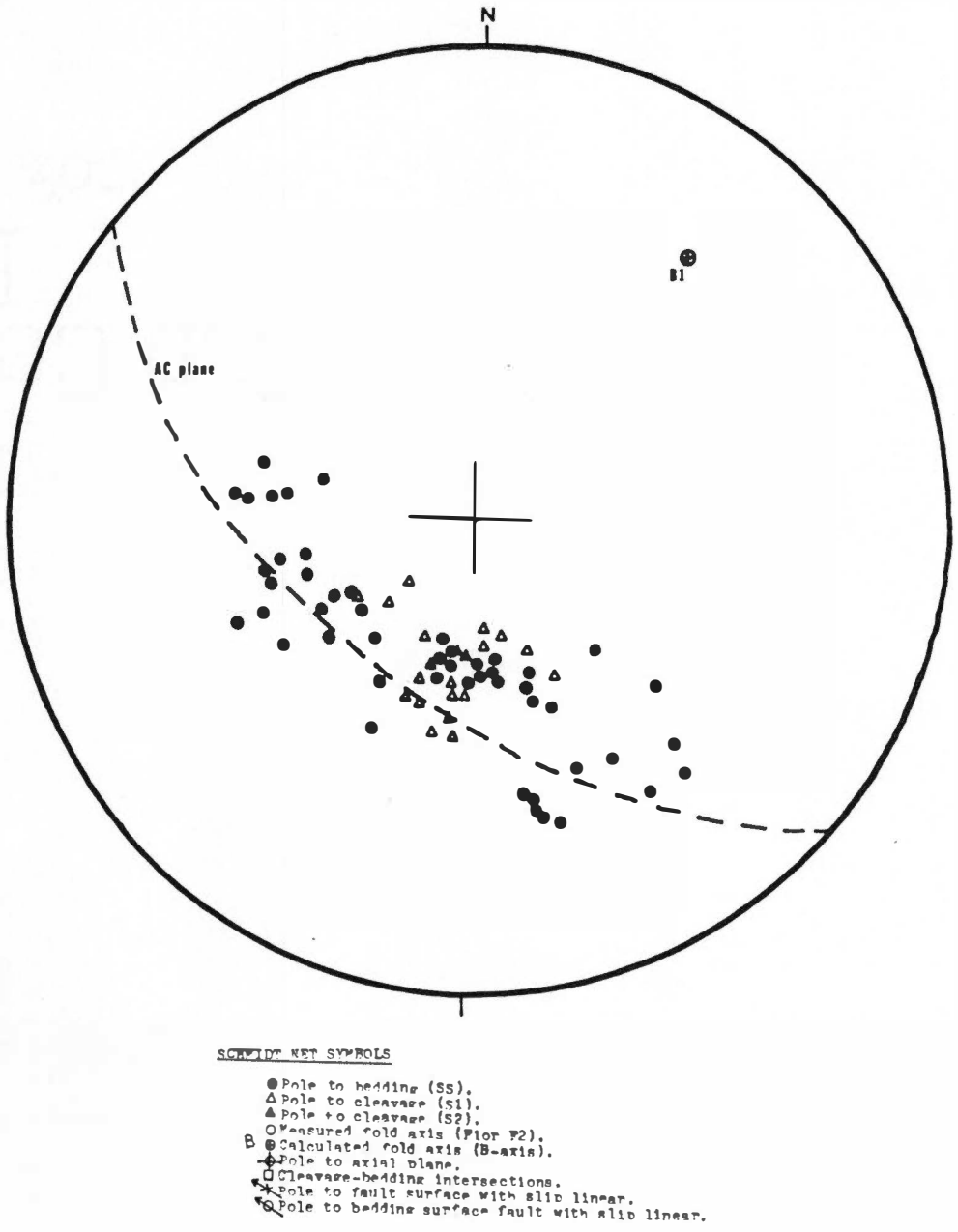

Figure 47. Schmidt net: macroscopic F1 folds, Locations 15, 16, and 17.

cleavage is an axial plane foliation for this macroscopic fold. Farther northwest, the F1 fold axial planes dip southeast. Macroscopic F1 folds are believed to be older than the Great Smoky fault and would therefore be discordant with the thrust fault.

Siltstones adjacent to the conglomeratic units northwest of Location 63 dip steeply to the northwest. Gentle northwest dips were found in sandstones in the conglomeratic units, suggesting a fold in the conglomerate body with dips steeply to the northwest in the subsurface. Folds in Locations 63 and 65 approach a chevron fold style and appear to have northwest-dipping fold envelopes. F1 axial planes here dip about forty degrees southeast.

The orientations of the S1 foliation are shown as dashed lines in Plate 1. Slaty cleavage forms an F3 antiform in the vicinity of the Calderwood window uplife and a F3 synform north of this area. Other F3 folds are located northwest and southeast of Location 14. These F3 folds are believed to be reflections of warps in the Great Smoky fault surface. A consistent angle between the slaty cleavage and fault surface is probable and an angle of 15 degrees was chosen for the construction. This gave a fault configuration which best fit the constraints provided by known outcrops of the thrust fault. The warped nature of the Great Smoky fault due to F3 folds becomes apparent in this construction. For

comparison, the heavy dashed line represents the Great Smoky fault surface based on data from a structure map of the thrust surface made by Neuman and Nelson (1965).

The Chilhowee Mountain structural block syncline is believed to be discordant with the Great Smoky fault, with the thrust fault cutting across the axis of the fold. The Miller Cove fault is depicted as a splay of the Great Smoky fault.

CHAPTER VI

SUMMARY AND CONCLUSIONS

Four groups of folds and related structures have been determined in the study area. F1 folds with S1 slaty cleavage as an axial plane foliation are overprinted by F2 folds with a S2 crenulation cleavage axial plane foliation. Both S1 and S2 have been deformed by the F4 kink folds and related thrust faults. Macroscopic F3 folds have deformed the slaty cleavage, and are younger than the F1 folds. There is no direct evidence to prove the relative age of the F3 folds with respect to the F2 and F4 folds.

The F1 folds are believed to be the same as the first-generation folds described by King (1964) in the central Great Smoky Mountains. Both groups of folds have slaty cleavage as an axial plane foliation (the first-generation foliation of King). F1 folds in this report area are also tentatively correlated with the F1 folds found in the Spruce Pine area (Butler, 1973) and the F1 folds described by Kish et al. (1975). They are believed to be Taconic structures and were formed in the Late Ordovician during the time of regional metamorphism. These F1 folds, therefore, are older than the Great Smoky fault.

F2 folds in the study area have a crenulation cleavage axial plane foliation like those described by Butler (1973)

as F3 folds, which were formed in Late Paleozoic time. F2 folds described by Kish et al. (1975) also have a crenulation cleavage axial plane foliation. These folds postdate the time of regional metamorphism. The F2 folds in the study beleived to have been formed after the Late Ordovician regional metamorphism, probably during the time of thrusting on the Great Smoky fault in Late Carboniferous or Permian.

The deformation of slaty cleavage into F3 folds near the Calderwood window is believed to postdate the Great Smoky faulting. Warping of the thrust fault caused the cleavage to be rotated over the Calderwood window uplift and formed the F3 folds. F4 folds are believed to be late structures formed either during or after the broad warping which deformed the Great Smoky fault.

REFERENCES

REFERENCES

Billings, M. P. (1972) Structural Geology: 3rd ed., Prentice-Hall, Inc., Englewood Cliffs, New Jersey, 606p.

Butler, J. R. (1973) Paleozoic deformation and metamorphism in the Blue Ridge thrust sheet, North Carolina: Am. Jour. Sci., v.273-A, p. 72-88.

Bryant, B., and Reed, J. C., Jr. (1970) Structural and metamorphic history of the southern Blue Ridge: p. 213-225 in: Fisher, G. W. et al. (eds), Studies of Appalachian geology—central and southern: Wiley-Interscience, New York, 460p.

Carpenter, R. H. (1970) Metamorphic history of the Blue Ridge province of Tennessee and North Carolina, G. S. A. Bull, v.81, p. 749-762.

Cosgrove, J. W. (1976) The formation of crenulation cleavage: J. Geol. Soc. Lond., v.132, p. 155-178.

DeWindt, J. T. (1975) Geology of the Great Smoky Mountains, Tennessee and North Carolina: The Compass of Sigma Gamma Epsilon, v.52, p. 73-129.

Dieterich, J. H. (1969) Origin of cleavage in folded rocks: Am. J. Sci., 267, p. 155-165.

Donath, F. A., and Parker, R. B. (1964) Folds and folding: Geol. Soc. Am. Bull., v.75, p. 45-62.

Fleuty, M. J. (1964) The description of folds: Geol. Assoc. Proc., v.75, pt.4, p. 461-489.

Hadley, J. B., and Goldsmith, R. (1963) Geology of the eastern Great Smoky Mountains, North Carolina and Tennessee: U.S. Geol. Surv. Prof. Paper 349-B, 118p.

Hatcher, R. D., Jr. (1972) Developmental model for the Southern Appalachians: Geol. Soc. Amer. Bull., v.83, p. 2735-2760.

Hobbs, B. E., Means, W. D., and Williams, P. F. (1976) An outline of structural geology: John Wiley and Sons, Inc., New York, 571p.

King, P. B. (1964) Geology of the central Great Smoky Mountains Tennessee: U.S. Geol. Surv. Prof. Paper 349-C, 148p.

King, P. B., Neuman, R. B., and Hadley, J. B. (1968) Geology of the Great Smoky Mountains National Park, Tennessee and North Carolina: U.S. Geol. Surv. Prof. Paper 587, 23p.

Kish, S. A., Merschat, C. E., Mohr, D. W., and Wiener, L. S. (1975) Guide to the geology of the Blue Ridge south of the Great Smoky Mountains, North Carolina: Carolina Geological Society Field Trip Guidebook, p. 6-9.

Knill, J. L. (1960) A classification of cleavages, with special references to the Craignish district of Scottish highlands: 21st Int. Geol. Cong. Report, pt. 18, p. 317-325.

Neuman, R. B. and Nelson, W. H. (1965) Geology of the western Great Smoky Mountinas, Tennessee: U.S.G.S. Prof. Paper 349-D, 81p.

Neuman, R. B., and Wilson, R. L. (1960) Geology of the Blockhouse quadrangle, Tennessee: U.S. Geol. Surv. Geologic Quadrangle Map GQ-131.

Ramsay, J. G. (1962) The geometry and mechanics of formation of "similar" type folds: J. Geol., v.60, p. 466-481.

Ramsay, J. G. (1967) Folding and Fracturing of Rocks: McGraw-Hill, New York, 568p.

Ramsay, J. G. (1974) Development of chevron folds: Geol. Soc. of Am. Bull., v.85, p. 1741-1754.

Rickard, M. J. (1961) A note on cleavages in crenulated rocks: Geol. Mag., 98 (4), p. 324-332.

Rodgers, J. (1970) The tectonics of the Appalachians: Wiley-Interscience, New York, 271p.

Roeder and Walker (1975) The Tellico-Sevier shale belt in East Tennessee—an early Paleozoic backarc basin (abs.): Geol. Soc. America Abs. with Programs, v.7, p. 528.

Turner, F. J., and Weiss, L. E. (1963) Structural analysis of metamorphic tectonites: McGraw-Hill, New York, 545p.

Weiss, L. E. (1972) The minor structures of deformed rocks, Springer-Verlag, New York, 431p.

Williams, P. F. (1972) Development of metamorphic layering and cleavage in low-grade metamorphic rocks at Bermagui, Australia, Amer. J. Sci., 272, p. 1-47.

APPENDIX

METHODS AND CONVENTIONS

A. Fabric Elements Used—Planar Structures

Bedding. Bedding in the field area is usually recognizable, although in some places it has been nearly obliterated by well-developed cleavage. Primary structures such as load casts and graded bedding have been used for determining the younging direction of units. Sedimentary bedding is used as an internal marker whose geometric configuration indicates the nature and magnitude of deformation (Turner and Weiss, 1963).

Axial planes of folds. The orientation of axial planes of mesoscopic folds was recorded wherever possible. A fold axial surface is the surface connecting the hinge lines in adjacent fold surfaces.

Cleavage. A general definition of cleavage, given by Billings (1972), is the property of rocks to break along parallel surfaces of secondary origin. Classification of cleavages is difficult, because there seems to be a continuous morphological gradation between cleavage types. Four end members which have been defined include slaty cleavage, fracture cleavage, pressure solution cleavage, and crenulation cleavage (Cosgrove, 1976). Slaty cleavage and crenulation cleavage occur as axial plane foliations in

the field area. Axial plane foliations are those inclined to the folded surface which are approximately parallel to the axial surface of the fold in the hinge area.

Slaty cleavage in this report is designated S1. Hand lens examination of rocks with slaty cleavage shows they are characterized by a highly developed planar preferred orientation of layer silicates. The fabric is uniformly developed (penetrative), on the visible scale, throughout the rock material. Slaty cleavage is believed to be oriented perpendicular to the direction of maximum finite shortening (Ramsay, 1967; Dieterich, 1969).

Crenulation cleavage, designated S2, involves a parallel mineral orientation resulting from the refolding of a preexisting secondary foliation (Knill, 1960). It consists of cleavage planes, whether micaceous layers or sharp breaks, which are separated by thin slices of rock containing a crenulated cross-lamination (Rickard, 1961). Preferred mineral orientation develops along the cleavage planes. Crenulation cleavage is not penetrative; it forms discrete planar discontinuities which cause localized structural weaknesses within the rock. A rock showing crenulation cleavage will break only along discrete planes, while a rock with a slaty cleavage will break along any surface parallel to the cleavage.

B. Fabric Elements Used—Linear Structures

Fold axes. The fold hinge line is the locus of points of minimum radius of curvature of the folded surface. In cylindrical folds, the folded surface can be outlined by moving a straight line parallel to itself. This line is called the fold axis. Since folds in the field area are believed to be approximately cylindrical, fold axis and hinge line will be interchangeable. The fold axes of minor folds were measured where possible. In some cases, the fold axes were defined statistically as the pole to the great circle that best fits the distribution of poles to the folded surface (π-poles) on an equal-area net (Schmidt net).

Cleavage-bedding intersections. The lineation defined by the intersection of bedding and cleavage surfaces was measured in several areas. For folds with an associated axial plane foliation, the cleavage-bedding intersections should be statistically subparallel to the fold axes.

C. Other Structural Elements

Fault surfaces and slickenside striae are not considered fabric because they are usually not penetrative. Surfaces showing the relative movement of beds or slickensided mineral-coatings were measured. In some cases, relative movement

was estimated by the direction of mineral growth-fiber thickening on the slickensided surfaces.

D. Fold Style

Fold style includes all the morphological features of a folded surface. It involves the shape of the fold in profile, the presence of an axial plane foliation, the type of axial plane foliation, and whether the fold is cylindrical or not. Although there are many transitional forms between ideal fold types, end members adopted in this report include parallel, concentric, and congruent folds. For parallel and concentric folds, the thicknesses of beds measured normal to bedding surfaces are consistent throughout the folds. Cylindrical folds are those with near-circular layers. In congruent, or "similar-type" folds, the thickness of beds measured at right angles to bedding is variable, while the thicknesses measured in directions parallel to the axial plane are consistent. Folds in the field area were classified according to which ideal fold type they more closely resembled.

The area of a fold with a small radius of curvature is called the fold closure or hinge. This area may be rounded or angular. Adjacent to the fold hinge are two areas of larger radius of curvature called the fold limbs. The interlimb angle of a fold is defined as the minimum angle between the limbs, as measured in the profile plane. Terms

used in this report to describe the interlimb angle, adopted from Fleuty (1964), are shown in Table 3.

TABLE 3

TERMS USED TO DESCRIBE TIGHTNESS OF A FOLD

Description of Fold	Interlimb Angle-Degrees
Isoclinal	0
Tight	Less than 30
Close	30-70
Open	70-120
Gentle	120-180

A surface that is tangential to the hinges of folds in a given surface is called the enveloping surface. If the axial planes of a group of folds are perpendicular to their enveloping surface, they are considered symmetric (orthorhombic symmetry). If the axial planes are not perpendicular, the folds are considered asymmetric (monoclinic symmetry), with uneven limb length and dip. Folds in which one limb is stratigraphically inverted are called overturned folds.

E. Orientation Data

The structural elements in a given area are analyzed by plotting their orientations on a lower hemisphere equal-area projection called a Schmidt net (stereonet or stereogram). Symbols used for the various elements are listed in Table 4.

Patterns of preferred orientation of structures on an equal-area net are of three general types (Turner and Weiss, 1963). A maximum is a single area of high concentration. A great-circle girdle is an arcuate maximum which coincides with a great circle of the net. The pole of the great circle is called the B-axis. A small-circle girdle, or cleft girdle, is an annular maximum which occupies a small circle of the net. Where large number of bedding or cleavage orientations were measured, the distribution was contoured using density contours.

TABLE 4

SYMBOLS USED ON SCHMIDT NETS

● Pole to bedding (SS)
△ Pole to cleavage (S1)
▲ Pole to cleavage (S2)
○ Measured fold axis
⊕ Calculated fold axis (B-axis)
⊕ Pole to axial plane
□ Cleavage-bedding intersections
↖ Pole to fault surface with slip linear

VITA

John Edward Livingston was born in Wilmington, Delaware, on November 14, 1952. He attended elementary schools in Swarthmore, Pennsylvania, and Sewell, New Jersey, and graduated from Clearview Regional High School in June 1970. September 1970 he entered the University of Notre Dame and received a Bachelor of Science degree in Geology in May 1974.

He entered the University of Tennessee Graduate School on a graduate assistantship in September 1974, to begin work on a Master of Science degree in Geology. At the University of Tennessee he was a member of Sigma Gamma Epsilon. Presently the author is employed as a production geologist for the Gulf Oil Exploration and Production Company in Oklahoma City.

Mr. Livingston is married to the former Sandra Scheuneman of Knoxville, Tennessee.

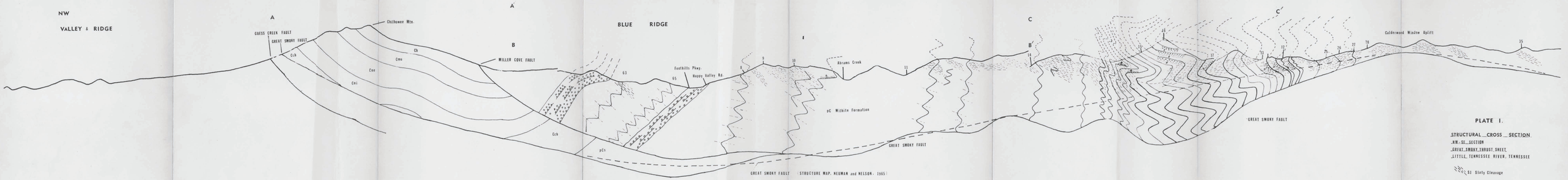

(STRUCTURE MAP, NEWMAN and NELSON, 1965)

PLATE I.

STRUCTURAL CROSS SECTION
NW-SE SECTION
GREAT SMOKY THRUST SHEET,
LITTLE TENNESSEE RIVER, TENNESSEE

St Slaty Cleavage

SCALE:
1: 6000
0 100 m